ROLE OF THE ARYL HYDROCARBON RECEPTOR ACTIVITY IN INTESTINAL EPITHELIAL CELLS IN THE FORMATION OF COLONIC TERTIARY LYMPHOID TISSUE AND COLORECTAL CANCER DEVELOPMENT

A Dissertation

by

ERIKA LEONOR GARCIA VILLATORO

Submitted to the Graduate and Professional School of
Texas A&M University
in partial fulfillment of the requirements for the degree of

DOCTOR OF PHILOSOPHY

Chair of Committee,	Clinton D. Allred
Committee Members,	Robert S. Chapkin
	Yuxiang Sun
	Arul Jayaraman
Head of Department,	David Threadgill

August 2021

Major Subject: Nutrition

ABSTRACT

Functioning as both a boundary and gatekeepers between the external environment and internal tissues, intestinal epithelial cells (IECs) play a significant role in overall gut homeostasis. Dysfunction of the colonic mucosal epithelial barrier allows intestinal bacteria to gain access to gut immune cells, thereby contributing to intestinal inflammation and colorectal cancer (CRC). It has been demonstrated that Aryl hydrocarbon receptor (AhR) activation with xenobiotics, dietary, and microbial-derived ligands can decrease inflammation in the gut via immune-mediated pathways and maintain gut-barrier function. As an environmental sensor, the AhR is a ligand-activated transcription factor implicated in maintaining gut homeostasis. However, the interaction between dietary fat and diet-derived ligands with the activity of the AhR in terms of CRC and the development of tertiary lymphoid tissues (TLTs) remains unclear.

In the present work, we first examined the effects of a high-fat diet on IEC-specific AhR knockout mice during sporadic CRC. Loss of AhR activity in IECs and a high-fat diet significantly increased the development of premalignant lesions through increased cell proliferation and altered expression of pro-inflammatory and pro-carcinogenic genes while modifying the microbial communities and their production of AhR metabolites. Moreover, the loss of AhR in IECs resulted in fewer TLTs. As organized structures that develop at sites of inflammation or infection in the colon, TLTs serve as localized centers of adaptive immune responses, and their presence has been associated with the resolution of inflammation and tumorigenesis. Using a model of acute colitis in conditionally IEC-

specific AhR knockout mice, we determined that the formation and composition of TLTs was dependent on both AhR activity on IECs and sex. Furthermore, AhR activation in IECs by 3,3′-diindolylmethane (DIM) promoted intestinal barrier integrity through the upregulation of various tight junction (TJ) genes and genes and downstream signaling required for the formation of TLTs after an inflammatory event in a sex-dependent manner.

Taken together, the present study demonstrates the modifying effects of the diet and AhR deletion on IECs in gut-associated lymphoid tissue development, tumor initiation and progression and adds to the growing body of literature indicating that AhR activation in IECs modulates gut homeostasis.

ACKNOWLEDGEMENTS

There are many who helped me along the way on this journey. I want to take a moment to thank them. First, I would like to extend my deepest gratitude to my committee chair, Dr. Clinton Allred, for taking a chance with me and making me part of his lab family, and for his guidance through each stage of the process. The competition of this body of research and my dissertation would not have been possible without the support and nurturing of my committee members, Dr. Robert Chapkin, Dr. Yuxiang Sun, and Dr. Arul Jayaraman; thank you for your valuable advice and profound belief in my work and abilities.

Thank you also to my friends, colleagues, teachers, the Nutritional Science Graduate Association, and staff at the Department of Nutrition for making my time at Texas A&M University a great experience. A special thank you to Dr. Jennifer DeLuca and Mrs. Kimberly F. Allred for their helpful advice, guidance, and support throughout these projects and for being by my side through this stage of my life.

Finally, thanks to my family for their encouragement and my husband for his patience, support, and encouragement throughout this journey.

CONTRIBUTORS AND FUNDING SOURCES

Contributors

This work was supervised by a dissertation committee consisting of Dr. Clinton D. Allred [advisor], and my committee members, Dr. Robert Chapkin, and Dr. Yuxian Sun of the Department of Nutrition and Dr. Arul Jayaraman of the Artie McFerrin Department of Chemical Engineering.

The animal model verification and the colon cancer initiation experiment in Chapter 2 was conducted and provided by Evelyn Callaway of the Artie McFerrin Department of Chemical Engineering and was published in 2020. The RNA sequencing in Chapter 2 was conducted by Jennifer Goldsby of the Department of Nutrition and was published in 2020. The quantification of targeted metabolites from fecal aromatic amino acids presented in Chapter 2 was conducted by Dr. Rani Menon of the Artie McFerrin Department of Chemical Engineering. The histological identification of premalignant colon lesions for Chapter 3 was performed by veterinary pathologist Dr. Martha Hensel of the Department of Veterinary Pathobiology. 16S rRNA and gene expression data presented in Chapter 3 was analyzed by Dr. Rani Menon of the Artie McFerrin Department of Chemical Engineering. Lastly, special thanks to Kerstin Landrock who bred and genotyped all mice used in Chapter 4.

All other work conducted for the dissertation was completed by the student independently.

Funding Sources

Graduate study was supported by the scholarship for graduate studies abroad from the National Council on Science and Technology of Mexico (CONACyT) and graduate teaching assistantships from Texas A&M University (Department of Nutrition).

Research conducted in this body of work was made possible by the National Cancer Institute (RO1-CA202697, R35-CA197707) of the National Institutes of Health, the National Institute of Environmental Health Sciences (RO1-ES025713) of the National Institutes of Health, and by the Cancer Prevention and Research Institute of Texas (RP160589) and funds from the Allen Endowed Chair in Nutrition & Chronic Disease Prevention and the Syd Kyle Chair.

Its contents are solely the responsibility of the authors and do not necessarily represent the official views of any funding sources.

TABLE OF CONTENTS

Page

LIST OF FIGURES

Page

LIST OF TABLES

Page

CHAPTER I

INTRODUCTION

Colon anatomy and physiology

Structure and function of the colon

The colon is the terminal part of the gastrointestinal (GI) tract which primary functions involve the final absorption of nutrients, water, the synthesis of vitamins, and the formation and elimination of feces.[1] The large intestine is divided into four main regions, including the cecum, the colon, the rectum, and the anus. As in other GI tract segments, the large intestinal wall is divided into four layers: the mucosa, the submucosa, the muscularis propria, and the serosa.[2] However, structurally and functionally, the mucosa is the most complex and relevant section in the colon and consists of three layers. First, the layer facing the lumen entails of a single layer of specialized intestinal epithelial cells (IEC) that constitute a barrier that separates the host from the external environment. These cells are attached to a basement membrane over the second layer, the lamina propria, containing subepithelial connective tissue, stromal, hematopoietic cells, and lymphatic nodules.[3] Underneath, the third layer is called muscularis mucosae, consisting of a smooth muscle layer.[2] Furthermore, the submucosa contains a myriad of inflammatory cells, lymphoid tissue, nerve fibers, arteries, and venous channels that further spread throughout the muscularis propria (parallel arrays of smooth muscle cells that follow peristaltic contractions) to the serosa (a sheet of squamous epithelial cells).[1,2]

In contrast with the small intestine organization and structure, the colon's mucosa has fewer enzyme-secreting cells and does not contain villi but its organized in deep tubular pits (crypts) predominantly made of IECs and Goblet cells that deepen and extend toward the muscularis mucosae.[1]

The gut microbiome

Composed by various bacteria, archaea, viruses, and eukaryotic microbes, the human microbiome has a significant impact on various physiological functions in the body, including regulating the metabolism and protection against pathogens and the education of the immune system. Specifically, the gut microbiota comprises over 100 trillion bacterial species predominantly from the *Firmicutes, Bacteriodetes, Proteobacteria, Verrucomicrobia,* and *Actinobacteria* phyla, with the first two representing 90% of the gut microbiota.[4] The gut microbiome is integral to the host digestion and nutrition since it can produce a series of compounds (microbial-derived compounds) from the anaerobic carbohydrate fermentation through the production of CO_2, H_2, CH_4, and short-chain fatty acids (SCFA) from indigestible fibers such as xyloglucans.[5,6] From indigested proteins, the gut microbiota can produce shorter peptides and amino acids, short and branched-chain amino acids, and gases.[7] The gut microbiome can also convert aromatic amino acids (AAAs) to a collection of signaling metabolites that impact the host as well as the microbiome.[8] Additionally, the synthesis of Vitamin K and B group vitamins (biotin, cobalamin, folates, nicotinic acids, pantothenic acid, pyridoxine, riboflavin, and thiamine) by the gut microbiota has been long-established in numerous studies using both rodent

and human subjects.[7] The colonic microbiota can modify the structure and function of bile acids, which in turn can affect the host metabolism and downstream signaling functions locally (in the colon), or they can be reabsorbed to the enterohepatic circulation.[6,7] Lastly, polyphenols and phytochemicals from fruits and vegetables are significantly modified by the colonic microbiota, impacting their bioavailability, metabolism, and bioactivity.[6,7]

Aside from its metabolic functions, the gut microbiota and the host interact in a complex and bidirectional manner. Specifically, the immune system progressively learns to tolerate commensal microbiota while responding appropriately to pathogens by promoting anti-inflammatory regulatory T cells (Treg).[5] Hence, changes in the microbiome associated with diseased states (dysbiosis) have been widely studied in the context of colorectal cancer,[9] obesity, cardiovascular disease, diabetes, and other inflammatory bowel diseases.[56] However, these interactions are difficult to investigate since not only the microbiota can influence the host, but the underlying diseased state can alter the microbiome in return. It is critical to note that the microbiome of an individual is stable over time, but significant variations between sex and age exist. Diet and other environmental factors can also significantly affect the composition of the microbiome.

Intestinal epithelial cells

Intestinal epithelial cells (IECs) play essential anatomical and physiological roles to promote homeostasis in the body.[3] Fundamentally, IECs act as a biochemical and physical barrier between the body and foreign particles and microorganisms abiding within the lumen. The challenge in this endeavor occurs due to their additional physiological role in

nutrient absorption to the bloodstream. Functioning as both a boundary and gatekeeper ("segregation"), the integrity of this single layer of cells is commonly assessed to ensure the adequate containment of undesirable luminal contents within the intestine, such as pathogens while preserving the ability to absorb nutrients and water efficiently. IECs are capable of maintaining this selective barrier function through the regulation of the spacing (gap) between adjacent cells that are linked by protein complexes (tight-junction proteins) and the coordination of appropriate immune responses ("mediation") to aid the development and homeostasis of mucosal immune cells in the lamina propria.[3] Taken together, the barrier and immunoregulatory functions of the IECs demonstrate that these cells have a more significant role in overall gut homeostasis that it was previously considered.

As previously mentioned, the intestinal epithelium is organized as crypts in the colon. Pluripotent intestinal stem cells located at the base of the crypt continuously divide to generate differentiated IECs, such as absorptive enterocytes and secretory goblet cells, which migrate towards the top of the crypt. To fulfill its "segregation" functions, goblet cells secrete mucus that protects the colon from the effects of commensal bacteria-derived products and pathogens.[10] Compared to the small intestine, the colon has a significantly higher number of mucus-producing goblet cells. Consequently, the colon's mucus layer is thick, and it is composed of an inner (firm) and an outer (loose) mucus layer.[11] In addition to the secretion of mucus, the release of anti-microbial peptides (i.e., the C-type lectin regenerating islet-derived protein IIIγ-REGIIIγ) by IECs allows the establishment of a biochemical barrier between the luminal contents of the intestine (i.e., pathogenic bacteria)

and the underlying immune cells.[3] Besides these biochemical defenses, the epithelium forms a physical barrier on its own, in which the tight and adhesion junction proteins (occludins, claudins, zonula occludens) liking IECs obstruct the paracellular passage of microorganisms.[11] Gut immune cells can also influence the mucosal barrier by producing various cytokines such as interleukin 17 (IL-17) and interleukin 22 (IL-22) produced by Th17 cells or type 3 innate lymphoid cells (ILC3), respectively.[12,13] These cytokines, in turn, upregulate the secretion of antimicrobial peptides or promote colonic wound healing through the promotion of IECs proliferation.[11,12]

IECs can be stimulated by environmental factors, such as the gut microbiome, and interact with the host immune cells to create a host-commensal microbial relationship and finally sustain overall gut homeostasis. The "mediation" functions of IECs are associated to their production of various and diverse cytokines (TNF-α and IL-6) and chemokines (IL-8, CXCL-1/2/5) that regulate chemotaxis of immune cells such as neutrophils, macrophages, basophils, and T-cells.[10] Furthermore, the colonic epithelium coordinates immune responses through recognizing microbial and endogenous patterns as pathogen-associated molecular patterns (PAMPs) through pattern recognition receptors (PRRs), including nod-like receptor (NLR) and toll-like receptor (TLR) innate signaling pathways.[3] In the presence of commensal bacterial (such as segmented filamentous bacteria), IECs secrete humoral factors such as serum amyloid A that further initiate the production of IL-22 by activated ILC3. However, in the presence of pathogenic bacteria, the IECs upregulates the expression of genes involved in the production of reactive oxygen species (*Nos2, Duoxa2,* and *Duox2*) and pro-inflammatory enzymes such as the inducible

nitric oxide (iNOS) and cyclooxygenase-2 (COX-2), that facilitates the differentiation of Th17 and consequently the production of IL-22. In addition, in zones in which the uptake and delivery of antigens in the colonic lumen is feasible, the delivery of bacterial or dietary antigens to dendritic cells allows the production of antigen-specific IgA responses.[11,12]

The gut mucosal immune system

Due to the lumen on the GI tract is considered the "outside" of the body and its potentially heavily populated with pathogenic bacteria, the intestinal mucosa is densely populated with immune cells from the innate and adaptive immune system. Intestinal immune cells can be found at the epithelium, at the lamina propria, and organized in gut-associated lymphoid tissue (GALT).[10,14] These lymphoid aggregates are sites for cellular expansion and differentiation within the gut mucosa and connect the intestine to the lymphatic system via mesenteric lymph nodes and their structures depend on their location, where Peyer's patches can be found in the small intestine, whereas in the colon isolated lymphoid follicles, and mesenteric lymph nodes are abundant.[10] The cellular damage observed during the pathogenesis of mucosal injury commonly results in complement/ T cell-mediated cytotoxicity, complement-induced inflammation, activation of Th1 or Th17 lymphocytes within turn secrete proinflammatory cytokines.[10] However, parallel immune responses are involved in the induction of oral tolerance, maintenance of beneficial commensal microbiota, epithelial healing, and recovery. Hence, the clinical outcomes likely reflect the balance between defense mechanisms against pathogens and the host.

Types of immune cells in the colonic mucosa

Aside from the intrinsic role of IECs in the regulation of the mucosal immune system, microfold (M) cells, located over the surface of B-cell follicles at the isolated lymphoid follicles (ILFs) in the colon, are a distinctive type of specialized epithelial cells, which primary function is to sample intestinal microbiota and pathogens from the epithelium to the lymphoid tissues on their basolateral sides.[10,15]

As part of the innate lymphoid system, intestinal macrophages (MΦ) are the most abundant leukocytes in the lamina propria of the large intestine of mammals. In homeostasis, resident MΦ does not produce pro-inflammatory cytokines nor upregulate ROS/NO production in response to TLR ligands but maintains its phagocytic functions. However, under inflammatory conditions, newly infiltrated MΦ are capable of producing pro-inflammatory cytokines such as IL-6.[10] Unlike MΦ, dendritic cells (DCs) can initiate the primary immune response. Depending on the cytokines or ligands present, DCs can activate naïve T-cells and regulate proinflammatory or tolerogenic responses through their antigen-presenting functions, polarizing Th1, Th2, or Tregs. In the sub-mucosa, DCs sample intestinal contents through the epithelial monolayer or M cells by capturing and processing foreign antigens. Thymic stromal lymphopoietin (TSLP), TGF-β, and retinoic acid (RA) derived from IECs promote a tolerogenic profile on both DCs and MΦ.[3] In the presence of RA and TGFβ, intestinal DCs promote the generation of regulatory T cells (Treg) and IgA-secreting B-cells.[10]

Recently discovered, innate lymphoid cells (ILCs) are part of the innate immune cells in the gut mucosal immune system. These cells are defined by the lack of specific antigen

receptors and are now considered essential players in regulating gut epithelial cell barrier integrity, immunity, inflammation, and tissue repair.[10,16] In the context of different development requirements and cytokine expression, ILCs are classified into group 1, group 2, and group 3 ILCs , which share functional similarities with the adaptive CD4+ Th1, Th2, and Th17 cell populations, respectively.[3] While group 1 ILCs (including natural killer cells and innate lymphoid cell subset 1, ILC1) are involved in pro-inflammatory responses, and group 2 ILCs contribute to food allergies and wound repair;[3] group 3 ILCs (ILC3s and lymphoid tissue inducer (LTi) cells) produce Th17 and Th22 cell-associated cytokines, including IL-17A and IL-22, in response to stimulation by IL-23.[3,10,16]

As part of the adaptive immune system, the T-cell population is either recirculated through the body before settling in the gut or primed by intestinal-derived antigen-presenting cells (DCs) in secondary lymphoid tissues, where they exert their tolerogenic or inflammatory effects on the local environment. First, strategically positioned between IECs, specialized intraepithelial lymphocytes (IELs), provide a critical first line of defense, as they are involved in immune surveillance and in modulating intestinal inflammatory responses.[3,17] Upon activation by microbial or dietary antigens by antigen-presenting cells and specific cytokines, $CD4^+$ T cells can differentiate into Tregs and pro-inflammatory type 1 T helper (Th1), type 2 T helper (Th2) and type 17 T helper (Th17) cells.[18] Moreover, an imbalance between the cells of these two subsets results in various disorders ranging from inflammatory and autoimmune diseases to infection and cancer. In this context, Crohn's disease depicts a Th1 cytokine profile, while ulcerative colitis

presents a Th2 profile. Interestingly, Th17 cells are capable of neutralizing pathogens and reconstitute epithelial barrier integrity via IL-17 and IL-22 synthesis, respectively.

Mucosal DCs primed by IECs (RA, NO, IL-10, TGFβ) carrying antigens and live bacteria from the epithelium are responsible for the maturation of naïve B cells into IgA-secreting plasma cells through heavy chain class-switch recombination (CSR).[10,14,19] Naïve B cells present antigens through the major histocompatibility complex II (MHCII) to activated $CD4^+$ T cells, resulting in CSR that allows B cells to proliferate and differentiate into antibody-producing plasma cells or memory B cells. Secretory immunoglobulin A (sIgA) is the most prevalent antibody found in the gastrointestinal tract and is considered a key player in mucosal immunity. sIgA is produced by subepithelial plasma cells and translocated to the mucus at the intestinal lumen. The primary functions of sIgA include protecting pathogenic bacteria in a non-inflammatory manner (via immune exclusion and neutralization of specific bacterial receptor-binding domains), selecting and maintaining the commensal gut microbiota, as well as limiting the spread of intestinal antigens into the circulation.[10,18] More details about differentiation factors and other cytokines/chemokines produced by T cells and the production of antibodies by plasma cells will be discussed in later chapters.

Gut-associated lymphoid organs

The immune system is generally organized in primary, secondary, and tertiary structures. The thymus and bone marrow are part of the primary lymphoid organs and places where

T and B lymphocytes development and selection occur.[20] Lymphocyte activation then occurs in secondary lymphoid tissues such as the spleen and the lymph nodes.[20]

In the colon, the development of secondary lymphoid tissue (cryptopatches, CP and isolated lymphoid follicles, ILFs) occurs postnatally during the first weeks after birth as a response to environmental and commensal stimuli and depends on the activity of LTi cells (lymphoid tissue-inducing) and innate lymphoid cells (ILC) expressing the transcription factor RORγt.[21,22] Contrary to the programmed secondary lymphoid tissue development during embryogenesis, the formation of new lymphoid structures can be recapitulated in adulthood during *de novo* lymphoid neogenesis of tertiary lymphoid tissues (TLTs).[23] TLTs are ectopic structures in the intestinal mucosa and submucosa that develop at sites of inflammation under various pathological processes such as cancer, autoimmunity, infection, or acute and chronic inflammation.[23–25] Hence, the importance of TLT formation relies on their capability to sustain *in situ* adaptive immune responses.[23] While these situationally-dependent structures are not entirely known, their presence has been associated with the promotion of tissue repair, resolution of inflammation, and host defense.[26]

Colorectal cancer as a major health concern

Colorectal cancer (CRC) is the third most common type of cancer in both men and women and the third leading cause of cancer-related death in the U.S. by 2019.[27] CRC accounts for 8.2% of all new cancer cases with a 4.2% lifetime risk in both sexes, a rate of 64.6% 5-year survival rate adjusted by stage at diagnosis has been reported based on data from SEER 18 (2010-2016).[28]

Although the rate of new cases and the mortality rate has decreased over the past few decades due to the availability of numerous screening tests and treatments (chemotherapy, surgery, radiation, and various drugs targeting biological signaling molecules), they are not very effective for patients with advanced stages (distant vs. localized tumors).[28,29]

Epidemiological data suggest that while about 5% of CRC incidence has a genetic component, 95% is still linked to environmental variables.[30] Environmental elements include lifestyle factors such as tobacco and alcohol use, diet, physical activity, exposure to radiation, infections, or toxins.[30] Researchers have suggested that the diet is linked to approximately one-third of cancer mortality in the US.[31] Risk factors include personal/family history of adenomatous colorectal polyps and inflammatory bowel disease, a body mass index greater than 30, and a diet low in fiber, high in red meats and saturated fatty acids.[32–35] CRC is more common in men than women between 65-74 years old and in African Americans.[28]

Mechanisms associated with colorectal cancer development

Pathogenesis and progression.

CRC development is characterized by a long, multi-stage progression of mutations in which normal epithelium acquires and accumulates gene mutations that dysregulate the usual growth and function of IECs until the formation of adenocarcinomas and metastasis occurs (adenoma-to-carcinoma sequence).[36,37] Previous evidence had reported that it takes approximately 17 years for an adenoma (benign tumor) to develop into an advanced carcinoma (malignant tumor), but less than two years for malignant cells to acquire metastatic capabilities.[38] Hence, early identification of premalignant lesions is crucial for diagnosing and developing prevention strategies.

As CRC develops, early histological lesions in the epithelium can be identified as it acquires neoplastic, hyperplastic, or dysplastic features. These histological lesions are defined as aberrant crypt foci (ACF), and their size and number directly correlate with an increased risk of CRC development.[37] Increased mutations lead to disturbance of critical regulatory pathways concerning cell function and overexpression of known oncogenes in the colonic epithelial involved in the activation *APC*/β-catenin pathway, followed by constitutive activation of the *KRAS*/*BRAF* pathway, accompanied with subsequent clonal expansion of genes controlling the expression of *TGF-β, PIk3ca* and *TP53*, among others.[38] Chromosomal and microsomal instability, CpG island methylator phenotype, microsatellite instability, as well as epigenetic modifications lead to loss of cell-cycle regulation, uncontrolled cell growth, and tumor development.[36,39] Non-coding RNAs (microRNAs and long non-coding RNAs) have also been implicated at various CRC

stages.[39] While an adenoma stays in one location above the intestinal epithelium, a carcinoma gains the ability to invade tissues below the colonic epithelium and potentially migrate to other organs (metastasis).

Changes in the microenvironment at the mucosal epithelia driven by dietary factors, gut microbiome, microbial-produced metabolites, oxidative stress, and inflammation have been associated with the promotion of tumorigenesis.[40] There is strong evidence suggesting that microbial dysbiosis can lead to colonic carcinogenesis, where an increased abundance of *Fusobacterium spp*, *Bacteroides fragilis*, and *E. coli* have been postulated as the bacterial strains partially responsible for the initiation of CRC.[36,40] Furthermore, when homeostasis is perturbed by inflammation, the intestine orchestrates the formation of *de novo* intestinal tertiary lymphoid tissue (TLT), which onset has been associated with the generation of an immune-mediated/ anti-tumor response in CRC cases.[26]

Role of inflammation and CRC

Inflammatory bowel diseases (IBDs), including Crohn's Disease and Ulcerative Colitis (UC), are characterized by an increase of both acute and chronic inflammation of the intestinal epithelial lining of the gut and have been associated with an increased risk of CRC.[41] Additionally, the involvement of immune cells, cytokines, and other immune mediators has been described in almost all the steps of colon tumorigenesis. Colitis-associated cancer (CAC) is a subtype of CRC associated with IBD; this type of cancer has a high mortality rate, and more than 20% of these patients develop CAC within 30 years

of the disease onset.[41] CAC follows a classic step-wise progression as described in sporadic CRC cases (chronic inflammation, injury, dysplasia, and colorectal carcinoma) and share common genetic mutations and signaling pathways changes starting with the activation of *APC*/β-catenin, followed by activation of *KRAS*/*BRAF* pathway. Here, the accumulation of genetic mutations initiates the sequential evolution from low-grade dysplasia to high-grade dysplasia and, finally, cancer.[41,42]

Most of the tumors from CAC cases display a strong infiltration by various types of immune cells, which in turn produce pro-tumorigenic inflammatory cytokines and chemokines. Specifically, cells of the innate immune system, including neutrophils, mast cells, dendritic cells, and tumor-associated macrophages, release a series of pro-inflammatory cytokines (IL-6, IL-1, VEGF, IL-23, TNF), chemokines (i.e., CCL2), and immunosuppressant enzymes (arginase).[42] Likewise, cells of the adaptive immune system are recruited to the tumors. T cells (CD3 and CD8) produce cytokines and induce direct toxicity, while a reduction of Treg cells, which produce anti-inflammatory cytokines (IL-10, and TGF-β), has also been described in solid tumors. In sporadic CRC, a balance between immunosurveillance (natural killer cells, $CD8^{+,}$ and $CD4^{+}$ T cells) and tumor-promoting inflammation (innate immune cells) is still maintained through the initiation stage, suppressing premalignant lesions and keeping small tumors inactive.[41] Conversely, in CAC, a pre-established chronic inflammation leads to creating a microenvironment that further promotes the accumulation of additional mutation and epigenetic changes to the DNA inflicted by reactive oxygen species generated by resident immune cells. Equally relevant, constitutive activation of transcription factors involved in inflammatory

pathways such as the nuclear factor-κB (NF-κB) and signal transducer and activator of transcription 3 (STAT3) is observed in CAC cases.[41]

Dietary factors and CRC

Data from a large number of epidemiological studies indicate that foods with a high Dietary Inflammatory Index (DII) (association between dietary factors and inflammatory biomarkers) have been associated with a higher risk of colorectal cancer. Components from these foods include high energy, total fat, cholesterol, vitamin B12, carbohydrates, proteins, iron, and saturated fatty acids.[43,44] Diets low in dietary fiber and high in red meat and saturated fat have been associated with an increased risk of developing CRC.[30]

Obesity-induced by consuming either a Westernized (40% calories from fat) or a high-fat (60% calories from fat) diet has been considered one of the leading environmental risk factors for CRC development as supported by epidemiological, clinical trials, and controlled *in vivo* studies.[45–49] Some mechanisms that have been associated between obesity and an increase CRC risk include: low-grade/ chronic inflammation (increased DNA damage), increase in adipose tissue-derived hormones (estrogen) and adipokines (leptin), increased oxidative stress, insulin, insulin-like growth factor, as well as other cell growth regulators, including mammalian target of rapamycin (mTOR) and AMP-activated protein kinase.[50,51] Specifically, an increased inflammatory response, loss of tumor suppression capacity, and increased stemness of progenitor cells have been suggested as mechanisms linking a diet high in fat (HFD) and increased tumorigenesis in the colon.[52–55] Dietary heme derived from red meat consumption increases the formation of

carcinogenic *N*-nitroso compounds associated with the *KRAS* mutated tumors. Similarly, acrylamide might be associated with somatic DNA mutations.[56] Heavy alcohol consumption (>50 g/day) has been similarly associated with an increased risk of CRC, in which acetaldehyde (ethanol metabolite) can affect the synthesis and repair of DNA, resulting in aberrant glutathione function as well as increased proliferation of the colonic mucosa.[44]

While extensive epidemiological studies, meta-analysis, and clinical trials have failed to demonstrate a positive relationship between fiber consumption and the reduction of colorectal carcinomas, fiber consumption from whole grains has benefit against CRC development. [44] In addition, resistant starch, which induces SCFA production, remains an attractive area of research due to its putative benefits against CRC through the production of butyrate, which in turn has been shown capable of modulating immune response via the suppression of histone deacetylation.[44] Contrary to food components associated with an increased risk of developing CRC, higher intakes of vegetables, fruits, whole grains, nuts and legumes, polyunsaturated fat and omega-3 fatty acids, Vitamin D, Vitamin C, Vitamin E, folic acid, and phytochemicals (polyphenols, terpenoids, organosulfur compounds, and phytosterols), have been widely associated with anti-inflammatory properties and the reduction of CRC risk.[44,57]

Gut microbiome and CRC

Perturbations of the balance of microbial communities are commonly associated with inflammatory bowel disease, and the initiation and progression of sporadic CRC.[4] Host

genetics (immune response and mucosal barriers) and environmental factors (diet and antibiotic use) can lead to shifts in the microbiota composition in which altered immune responses from the host against commensal or pathogenic bacteria may result in inflammation and tumor initiation; this process has been termed "dysbiosis."[58,59] A characteristic reduction of bacterial diversity, evidenced by a decreased abundance of *Firmicutes* and an increased abundance of *Enterobacteriaceae, Proteobacteria,* and *Bacteriodetes,* had been described in patients with IBDs and CRC.[4,60] Although some bacterial species have been identified as suspected to play a role in colon carcinogenesis (*Streptococcus bovis, Helicobacter pylori, Bacteroides fragilis, Enterococcus faecalis, Clostridium septicum, Fusobacterium spp. and Escherichia coli.)*,[61] it is still unclear with confidence which bacterial species are essential for the induction of inflammation or CRC.

Disruption on the host mucosal barrier due to increased mucosal and epithelial permeability increases the risk for pathogenic bacteria to translocate from the lumen to the lamina propria, resulting in over-exposure of bacterial antigens with gut immune cells. Reduction in mucus layer thickness due to the loss of goblet cells or an increase in mucus-degrading bacteria has been reported in IBD and CRC cases (ref?).[62] Similarly, loss of surface receptors or expression of tight junction proteins from IECs due to intestinal damage further increases intestinal permeability.[4] In response, a surge of inflammatory T cells and their pro-inflammatory cytokines (IL-23, IL-17) are considered the major drivers of gut inflammation and can initiate colorectal malignancies by promoting cell growth and survival.[61,63] Alongside, a reduction of Treg cell functions and their secretion of IL-35 and IL-10 (anti-inflammatory cytokines) are positively associated with colonic inflammation.

Toxins produced by pathogenic bacteria such as colibactin (genotoxin) produced by *E. coli* strains, cytotoxin-associated gene A (CagA) from *Helicobacter* species, and Bacteroide fragilis toxin (BFT) from *Bacteroides fragilis* are strongly associated with the development of colon tumors via the induction of epithelial cell proliferation and DNA damage.[4,61] Comparably, an increase in the relative abundance of *Fusobacterium nucleatum* might promote carcinogenesis via the modulation of E-cadherin/β-catenin signaling, pro-inflammation, and the epigenetic silencing of MMR Protein that leads to microsatellite instability in the colon.[4,44]

A current view on bacterial-derived tumorigenesis considered that CRC initiation is initiated by the localized colonization of specific pathogens ("drivers," ETFB or Enterobacteriaceae) and that subsequent changes in the tumor micro-environment allow the colonization of opportunistic ("passenger," *Fusobacteria)* microbes, hence facilitating the progression of the malignancy.[61] Equally important, variations of gut microbiota have been reported across stages of colorectal carcinogenesis.[64] The interactions among bacterial communities (bacterial driver-passenger model) and their subsequent interactions with the host capable of initiating colon malignancies seem highly dependable of their specific spatial organization in the form of higher-order structures termed biofilms.[65] The presence of poly-bacterial biofilms (rich in *Fusobacteria* or *B. fragilis*) has been associated with increased intestinal permeability and bacterial-induced loss of barrier function, as evidenced in biofilm-positive human colon tumors and adenomas, especially in right-sided colon tumors where bacterial attachment is usual. Moreover, biofilms allow bacteria to grow in close proximity to IECs, triggering direct pro-inflammatory damage

and activation of Th17-mediated immune responses favoring CRC initiation and further promotion of epithelium proliferation.[65]

Since the incidence in IBDs and CRC has increased in developing countries where low incidence has been previously reported, environmental factors, such as the diet, are suspected of playing an important role in the development of these diseases. Specifically, consuming a Westernized diet (high in saturated fats and low in fiber) has been associated with reduced microbial diversity in the gut and increasing CRC risk.[4] For example, evidence from a cross-over diet study investigating the role of fiber consumption and CRC risk between African-American and South-African participants indicated that higher fiber intake increased microbial-derived fermentation of carbohydrates and butyrate while suppressing the production of secondary bile acids; resulting in lower mucosal biomarkers (cell proliferation index and immune cell infiltration) of CRC risk.[66] Taken together, the potential pro-carcinogenic effect of the gut microbiota relies on their genotoxicity, their pro-inflammatory effects, microbial-derived metabolism (activation of carcinogens, ROS), and the production of reactive oxygen species.

The aryl hydrocarbon receptor

AhR signaling and function in the gut

The aryl hydrocarbon receptor (AhR) is a ligand-activated nuclear receptor that regulates diverse biological processes, including detoxification of xenobiotics, mucosal inflammation, tissue regeneration, and other gastrointestinal functions.[29,67–69]

The AhR belongs to the Per-Arnt-Sim (PAS) superfamily and shares similarities with other nuclear receptors.[70] On an inactive state, the AhR is sequestered in the cytoplasm by a protein complex containing HSP90, hepatitis B virus protein X-associated protein 2 (XAP2), and p23.[71] Upon ligand activation (direct activation), AhR translocates to the nucleus breaking away from its inactivating protein complex and binds to the AhR nuclear translocator (ARNT), together they interact with the dioxin response elements (DREs) on the promoter region of genes targeted by AhR including cytochrome P450 enzymes (Cyp1A1, Cyp1A2, Cyp1B1), consequently activating their transcription.[67,69]

The AhR has been considered an orphan receptor with no high-affinity endogenous ligands; however, recent studies have identified dietary, microbial, and host-derived compounds that can bind AhR and elicit various beneficial physiological effects.[72–74] In the large intestine, these effects include the regulation of the expression of inflammatory signaling molecules (i.e., IL-6, Il-22 Prostaglandin-Endoperoxide Synthase 2), angiogenesis (i.e., VEGF), gut immunity (innate and adaptive immunity via repression of acute phase response genes, T and B cell differentiation) in the lamina propria of the intestine, tissue regeneration, regulation of the immune system, and proteasomal degradation.[29,67–70,72,73,75] Particularly, an increase in E3 ubiquitin ligase activity involved in the degradation of pro-proliferative factors such as β-catenin has been reported through the activation of AhR by exogenous ligands.[72,76,77] Importantly, the activity of AhR remains elusive due to the selectivity of the receptor to bind to different types of compounds, especially if considered that some structural differences on the ligand-binding domain on the receptor between murine and human isoforms exist. Mouse AhR (AhR^{b1}) exhibits a

10-fold increased affinity for TCDD relative to human AhR (AhR^d), while the human receptor has an increased affinity for indole-derived compounds.[67,75,78] Furthermore, mouse and human AhR differ in their ability to modulate genes expression, and although the expression of AhR-dependent targets are preserved, specific species-specific target do exist, hence the relevance of employing "humanized" AhR murine models to test the putative AhR ligand potential of novel or common compounds.[75]

AhR ligands

Evidence suggests the binding of ligands induces the predominant biological activities of the AhR. Hence, numerous synthetic, environmental, endogenous, and naturally occurring AhR ligands have been characterized in recent years. Although canonical activation of the AhR by 2,3,7,8-Tetrachlorodibenzo-p-dioxin (TCDD) has been shown to promote cell proliferation and tumorigenesis in preclinical models of CRC, the human AhR also binds to structurally and functionally diverse ligands associated with health-promoting properties in the gut-derived endogenously from the diet or the microbiome.[78] A summary of known AhR ligands and their origin is provided in **Table 1.**

Compounds derived from a variety of fruits and cruciferous vegetables (broccoli, brussels sprouts, cabbage, and cauliflower) are considered AhR ligands since they can induce a canonical AhR-dependent activation of CYP proteins. The formation of indolo[3, 2*b*]carbazole (ICZ), and 3,3'-diindolylmethane (DIM), both of which exhibit AHR binding potential and had been widely investigated in both preclinical and clinical within the gastrointestinal tract influencing physiological processes such as immune surveillance

and host-microbiota interactions.[72] Mechanical breakdown of glucobrassicin (plant glucosinolates found in cruciferous vegetables) facilitates the activity of myrosinase, producing several products (with AhR agonist activity), including indole-3-carbinol (I3C) and indole- 3-acetonitrile (I3ACN); once in the stomach, I3C undergoes acid condensation to produce 3,3'-Diindolylmethane (DIM) and other minor metabolic products including indole-3-carboxylic acid and indole-3-carboxaldehyde.[78–80] Likewise, flavones, isoflavones, flavanones, and carotenoids have been shown to elicit AhR activity and are considered AhR ligands.[78] Moreover, compared to the high affinity of AhR to TCDD, most of the dietary AhR ligands are considered weak agonist or event antagonists,[78] and due to their complexity, makes determining their relative contribution to overall physiology particularly challenging.

Tryptophan, an essential amino acid, has been identified as a significant reservoir for the synthesis of AhR ligands via spontaneous and enzyme-catalyzed conversions by the host or the gut microbiota. First, UV-dependent tryptophan exposure results in the synthesis of 6-formylindolo[3,2b] carbazole (FICZ), a high-affinity AhR ligand.[75,78] Second, tryptophan can also undergo the kynurenine pathway, in which tryptophan is initially catalyzed by isoforms of the functionally homologous tryptophan-2,3-dioxygenase (TDO1/2, liver) and indolamine-2,3-dioxygenase (IDO1/2, periphery) enzymes producing kynurenine, kynurenic-, xanthurenic- and cinnabarinic acids, each of which displays AhR ligand-mediated activity.[75,78] Activation of the kynurenine pathway is associated with increased immune tolerance and may contribute to gastrointestinal homeostasis.[78]

Table 1. Known AhR ligands classified by their origin.

Dietary	Flavonoids:
	• Quercetin
	• Galangin
	Indoles:
	• Glucobrassicin (precursor + gastric acid)
	  o Indole-3-carbinol (I3C)
	  o 3,3′-diindolylmethane (DIM)
	  o Indolo[3,2b]carbazole (ICZ)
	• Tryptophan (precursor)

Microbial	• Indole • Indole-3-acetic acid (IAA) • Indole-3-acetate (I3A) • Indole-3-aldehyde (IAld) • Indole-3-acetaldehyde • Tryptamine • Indigo • Indirubin • 7-ketocholesterol • 1,4 dihydroxy-2-naphtoic acid (DHNA) • Malassezin
Endogenous	Tryptophan metabolites: • Kynurenic acid (KA) • Kynurenine (Kyn) • Cinnabarinic acid (CA) • 6-formylindolo[3,2b] carbazole (FICZ) • Indoxyl sulfate
Xenobiotic/ Exogenous	Halogenated aromatic hydrocarbons: • 2,3,7,8-tetrachlorodibenzo-p-dioxin (TCDD) • Dibenzofurans • Biphenyls • Polyaromatic hydrocarbons (i.e., polychlorinated biphenyls) • 3-methylcholanthrene (3-MC) • Benzo[a]pyrene • Benzanthracenes Pharmaceuticals: • Tranilast • Leflutamide • Omeprazole

Sources:[67,72,75,78]

The gut microbiome can also metabolize tryptophan, generating a series of tryptophan metabolites through tryptophanase and other downstream enzymes (bacterial monooxygenases, acetamide hydrolases, decarboxylases), and amino acids transporters.[75,78] These metabolites include indole, indole-3-acetic acid (I3AA), indole-3-aldehyde (I3Ald).[75,78] These compounds can undergo further downstream metabolic transformation to generate additional AhR ligands, such as indoxyl sulfate, indirubin, and indigo from indole (CYP2E1-mediated conversion of indoxyl).[75,78] Considering the abundance of bacteria in the gut and its metabolic capacity, these ligands are present in sufficient concentrations to stimulate AhR activity.[81] By the same token, data from recent studies seem to suggest that tryptophan-derived microbial AHR ligands can influence host-microbe homeostasis through the AHR-dependent modulation of IL22 expression and immunosuppressive Treg differentiation.[17,78] Activation of AhR by dietary and gut microbial tryptophan-derived metabolites (indole, indole-3-acetic acid, tryptamine, indole-3-aldehyde) have shown protective effects against CRC development through the induction of apoptosis, inhibition of cell growth, and modulation of the gut immune responses both *in vivo* and *in vitro*.[67,82–84] Particularly, treatment with 3,3′-Diindolylmethane (DIM) significantly reduces inflammatory markers and clinical signs of acute DSS-induced colitis in mice.[85] Hence, it has been hypothesized that the presence of tryptophan-derived metabolites affects the gut microbial composition, their metabolites, and modulates the host's immune response.[86,87]

As the first ligands discovered to activate the AhR (direct activation) canonically, xenobiotics, mostly including aromatic hydrocarbons and TCDD (dioxins), have been widely studied due to their high concentration in contaminated foods. Acute exposure to high doses of dioxins in industrial settings can cause skin lesions, and chronic environmental exposure can result in immunotoxicity, neurodevelopmental abnormalities, thyroid, and steroid hormone dysfunctions (reproductive issues), as evidenced by epidemiological and experimental data.[71] Conversely, indirect activation of the AhR and consecutive nuclear translocation has been observed with drugs such as omeprazole affecting the c-src-dependent signaling pathway together with cAMP.[71] Altogether, activation via xenobiotic ligands has been involved in mediating the metabolic machinery required for their detoxification or metabolism, which in turn increases the production of pro-carcinogenic compounds resulting in AhR's alleged tumor-promoting activities.

Effect of AhR activation in IEC in CRC and inflammation

Though the effect of AhR expression and activation in cancer has only begun to be investigated, data suggest that this effect appears to be tissue-specific and disease stage-dependent. In particular, high and constitutive expression of AhR has been reported in gastric and colon cancer both *in vivo* and in clinical samples.[67,88,89] Conversely, experimental evidence proposes that AhR activation may also be protective against colon inflammation and malignancies.[76,90–92] In which, the spontaneous development of colon and cecal tumors was reported in several murine models lacking global AhR expression, such as $APC^{min/+}$, $AhR^{-/-}$, and $APC^{min/+}$ x $AhR^{+/-}$.[83,93] Similarly, an increased susceptibility to

develop colon tumors has been described employing AhR-deficient mice ($AhR^{\Delta 2/\Delta 2}$) in a colitis-associated tumorigenesis model and $Apc^{S580/+}$; $Kras^{G12D/+}$ mice.[90,94] Although it has been recently described that IEC-specific AhR deletion enhances inflammation-induced tumorigenesis,[95] and stem cell and crypt injury-induced cell proliferation,[96] there was little information available identifying how AhR ligand availability and diet composition, in particular the fat content of the diet, could affect the development of premalignant CRC lesions and the formation of tertiary lymphoid tissue in the context of AhR-activity in colonocytes.

To investigate the effect of AhR ligands and intestinal inflammation, administration of TCDD, FICZ, DIM, ICZ, DHNA resulted in the reduction of DSS-induced colitis. It was proposed that AhR reduces DSS toxicity while increasing PGE_2, Treg cells, and the expression of anti-inflammatory cytokines such as IL-22, among other mechanisms.[17,78,85,97,98]

AhR activity and intestinal immunity

Similar to its expression in IECs, AhR is also expressed by different intestinal immune cells, such as IELs, Th17 cells, ILCs, macrophages, DCs, and neutrophils, making AhR signaling fundamental to the regulation of mucosal immunity.[17,69] Activation of the AhR has shown to either suppress or repress inflammatory signaling in a context and cell-specific manner. However, in the gastrointestinal tract, most studies support that AhR activation has an anti-inflammatory effect, as evidenced by studies employing $AhR^{-/-}$ mice,[78,90] but failed to establish a ligand-dependent mechanism. To maintain a normal

host-microbiota axis, the gut establishes a well-coordinated immune surveillance in which cytokines and chemokines mediate the response of innate and adaptive immunity as well as its barrier function.[78] Notably, it has been demonstrated that the AhR is capable of modulating the expression of *IL-1β, IL-6, Ccl20, Ccl1,* among other cytokines. Moreover, it is suggested that the AhR directly regulates the synthesis of prostaglandin E_2 (PGE_2)by prostaglandin G/H synthase 2 (Ptgs2).[78] Moreover, microbial-produced AhR ligands are considered a sensory mechanism that, in turn, can potentially increase immune surveillance.

Intestinal epithelial cells express AhR, and its activation is involved in epithelial cell proliferation, renewal, and turnover.[95] Moreover, IECs are capable of regulating the availability of AhR ligands to intestinal immune cells including APCs, ILCs, Th17/Th22 cells, and intraepithelial lymphocytes.[17] Treatment with AhR agonists leads to increased IL-22 expression by differentiated $CD4^+$T cells (Th17/Th22) and ILC3s, resulting in increased wound healing via intestinal stem cells' survival and enhanced anti-bacterial function.[17,78,99]

Environmental and genetic manipulation of AhR activity has shown to be capable of influencing the community structures of the intestinal microbiota according to experimental evidence in which the genotypic segregation of C57BL6/J $Ahr^{-/+}$ and $Ahr^{-/-}$ littermates previously cohoused for 18 days resulted in significant changes in phyla abundance (enrichment in *Verrucomicrobia* and SFB) in $Ahr^{-/-}$ mice.[84]

In the colon mucosa, specialized intraepithelial lymphocytes (IELs) located between the basolateral surface of IECs interact with the variety of immune cells (B cells,

macrophages, DCs, T cells, and ILCs) present in the lamina propria for the overall maintenance of gut homeostasis.[86] Recently, AhR expression and activation have been established as critical for developing and maintaining IELs and ILCs in the gut after birth.[21,86] Other molecular mechanisms in which AhR signaling provides beneficial effects in intestinal homeostasis regulation have been evidenced by the increased apoptotic rates, reduced IL-22 production, and attenuated IL-7/IL-7R expression in intestinal RORγt+ ILCs (ILC3) lacking AhR expression. Likewise, AhR seems to be capable of inducing the transcription of Notch1 and Notch2 proteins.[86]

The primary purpose of this body of research was to investigate the role of AhR in the modulation of sporadic colorectal cancer development and the formation of tertiary lymphoid tissue (TLT) in vivo. Previous studies using AhR-null models reported an increased incidence of colorectal tumors, suggesting that AhR expression is required to ameliorate CRC development. To identify whether AhR expression in the colonic epithelia is required to modulate CRC development in a highly inflammatory environment induced by a HFD, we used an intestinal-specific knockout murine model where AhR expression has been silenced. We also studied the effect of a high-fat diet to promote inflammation, microbial dysbiosis, and the formation of pre-malignant lesions. Additionally, we studied the effects of AhR activity in the IEC on the formation of de novo TLTs under acute inflammatory conditions in adult mice.

CHAPTER II

LOSS OF AHR IN THE INTESTINAL EPITHELIA INDUCES THE FORMATION OF PREMALIGNANT COLORECTAL CANCER LESIONS INMICE FED A HIGH-FAT DIET *

Introduction

Westernization of the diet (low content of dietary fiber and high content in saturated fat) has been associated with CRC development. Suggested mechanisms linking a diet high in fat (High Fat Diet, HFD) and increased tumorigenesis in the colon include increased inflammatory response and loss of tumor suppression capacity.[52–54] Chronic HFD consumption facilitates not only proliferation and survival of tumor cells but also promotes genetic instability leading to increased colon cancer incidence.[100] Under those circumstances, HFD consumption can increase Lgr5+ intestinal stem cells' number and function through the induction of a peroxisome proliferator-activated receptor delta (PPAR-δ) response, increasing their capacity to initiate tumors.[55]

Experiments in rodent models of sporadic colorectal cancer have demonstrated that a high-fat diet (60% kcal from fat), independent of weight gain, can promote a profound pro-carcinogenic environment by increasing the number of premalignant

* Reprinted with permission from sections of "Effects of high-fat diet and intestinal aryl hydrocarbon receptor deletion on colon carcinogenesis" by Garcia-Villatoro, E.L. [1], DeLuca, J.A.A. [1], Callaway, E.S., Allred, K.F., Davidson, L.A., Hensel, M.E., Menon, R., Ivanov, I., Safe, S.H., Jayaraman, A., Chapkin, R.S., and Allred, C.D., 2020. The American Journal of Physiology Gastrointestinal and Liver Physiology, 318(3), G451-G463, Copyright 2020 by The American Physiological Society. [1]Equally contributing co-first authors. Reprint permission has been granted by the co-first authors.

lesions.[46,47,52,53,101,102] In carcinogen-induced CRC in mice fed a HFD, RNA-sequencing revealed both leptin and Wnt as the top two transcripts elevated in the colon.[100]

Activation of the aryl hydrocarbon receptor (AhR) with canonical ligands such as TCDD has been associated with the induction of tumorigenesis in tumor cell lines and animal models, aiding in the development of stem cell-like characteristics,[67] an anti-apoptotic response and induction of inflammatory genes (such as COX-2 and NF-κB).[103] Conversely, human CRC cell lines treated with diet-derived AhR ligands displayed up-regulation of pro-apoptotic cytokines genes (TNF-α/β), thus increasing cell apoptosis.[104] In recent years, an inverse association between expression of AhR and colon carcinogenesis has been reported using AhR-deficient mice (AhR null), which exhibited an increased rate of spontaneous colon-cecal tumors and increased colitis-associated colon tumor formation.[76,90–93] Considering the broad scope of ligands that can bind the AhR, their origin, the different levels of affinity between species, and the increasing evidence of the chemoprotective role of the AhR against different types of cancer, this receptor is now considered an essential target for cancer therapy. Furthermore, it has been reported *in vivo* that consumption of a HFD can deplete gut microbial-derived AhR metabolites such as indole-3-acetate and tryptamine, associated with the reduction of intestinal inflammation.[105]

Since using a global AhR null model limits the ability to understand the significance of its expression within specific cell types, we utilized the IEC-specific, AhR knockout mouse model ($Ahr^{\Delta IEC}$) to further investigate the role of AhR in IEC-related biology. Although it has been recently described that intestinal epithelial cell-specific AhR

deletion enhances inflammation-induced tumorigenesis,[77] before our studies, no data was available identifying how consumption of saturated fat can affect the onset of sporadic CRC formation in the context of AhR activity in colonocytes. Hence, we hypothesized that the loss of AhR in the intestinal epithelial cells would increase the formation of premalignant colon lesions in the presence of a high-fat diet.

Materials and Methods

Animals and model verification. A constitutive, intestinal epithelial cell (IEC)-specific AhR knockout (*Ahr*$^{\Delta IEC}$) was generated by crossing AhR$^{flox/flox}$ mice with mice expressing the Villin-Cre (VCre) promoter on a C57BL/6 background as previously described by Biljes and Walissner.[106,107] Wildtype littermates (AhR$^{flox/flox}$) were used as controls. Mice express the Ahr^{b} allele, commonly known to have higher affinity for ligands that the allele expressed in humans (Ahr^{d} allele).[108,109] Hence, the mouse model used in our experiments expresses the lower affinity Ahr^{d} allele as in humans. Genotyping analysis was performed by our collaborators at Dr. Robert Chapkin's lab (Evelyn Callaway). DNA was extracted from tails using DNeasy Blood and Tissue Kit (Qiagen; 69506). PCR was performed using the following primers: Cre recombinase (F: 5'-CAA GCC TGG CTC GAC GGC C-3', R: 5'-CGC GAA CAT CTT CAG GTT CT-3'), AhR$^{flox/flox}$ (F: 5'-GGT ACA AGT GCA CAT GCC TGC-3', R: 5'-CAG TGG GAA TAA GGC AAG AGT GA-3'). To assess the successful deletion of AhR in the colonic crypts in the *Ahr*$^{\Delta IEC}$ mice (n=4), protein levels of AhR were measured using isolated colonic crypts via Western blot using rabbit anti-

mouse AhR (Enzo Life Sciences, Cat# BML-SA210, 1:2000 dilution) [110]. Protein levels and expression of *Ahr* are sown in **Figure 1**.

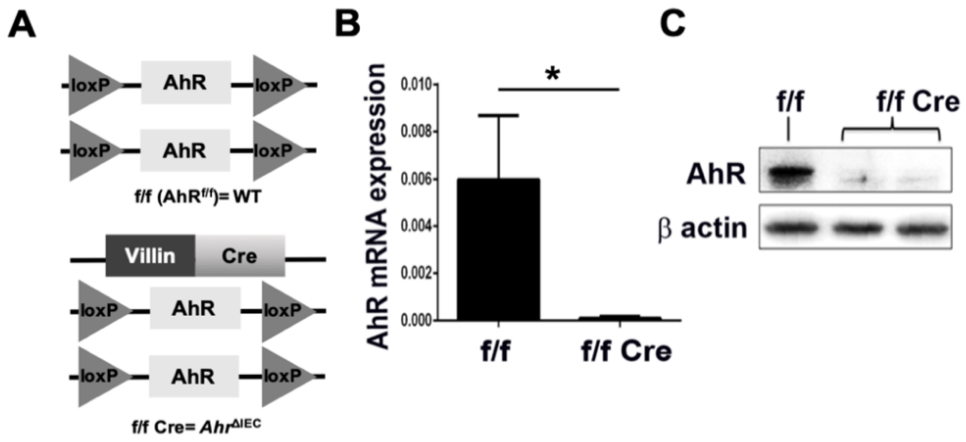

Figure 1 Model verification in the Ahr$^{\Delta IEC}$ mice.

A: Schematic representation of Cre-lox intestinal-specific knockout (*Ahr*$^{\Delta IEC}$) and controls (*AhR*$^{f/f}$) used in the study. **B:** AhR mRNA expression normalized to 18s rRNA. AhR$^{f/f}$ (f/f, WT) vs Ahr$^{f/f}$xVillinCre (f/f Cre, Ahr$^{\Delta IEC}$) from isolated colonic crypts (n= 6) **C:** Representative Western blot analysis of AhR protein expression. β-actin was used as a loading control. *p<0.05 vs. control (WT). Values are means ± SEM. * indicates p ≤ 0.05, ** indicates p ≤ 0.01, *** indicates p ≤ 0.001, and the absence of * indicates p-values >0.05

Sporadic model of colorectal cancer. Wild type-WT (n=4) and IEC-specific AhR knockout (*Ahr*$^{\Delta IEC}$) mice (n=8) were enrolled in the study at four weeks of age and separated by genotype and gender. In the first four weeks of the experiment, mice received a rodent chow diet. Mice were fed an experimental high-fat diet (HFD), providing 60% kcal from fat (Research Diets, D12492) at week four of the experiment, and received food and water *ad libitum*. Mice were housed on a 12 hour/12-hour light-dark cycle at a maximum of five per cage. Body weight was assessed weekly. Sporadic colorectal cancer was chemically induced with one injection of Azoxymethane (AOM; Sigma: A5486) at a

dose of 10 mg/kg of body weight for six consecutive weeks.[111] Animals were terminated 17 weeks after the last AOM injection. All procedures were performed under a protocol approved by the Institutional Animal Care and Use Committee at Texas A&M University. A schematic representation of the study design is included in **Figure 2.**

Figure 2 ACF study pilot timeline

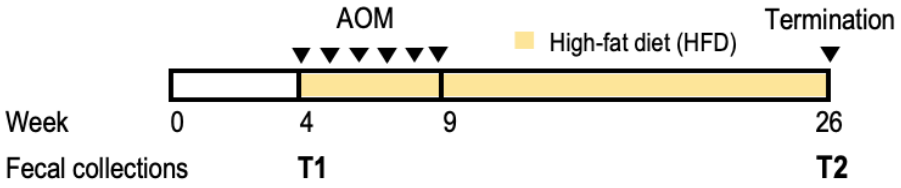

Fecal collection and housing conditions. Cage bedding was changed and mixed weekly for four weeks to homogenize the fecal microbiome among groups before the experimental diets started. Fecal samples from each mouse were collected at week 4 and 26 as indicated in Figure 2. To avoid cross-contamination among samples, mice were individually housed in tiny mouse cages for 30-60 minutes to collect at least four fecal pellets.[112] Samples were snap-frozen and maintained at -80°C until further analysis. Decontamination of surfaces with 70% ethanol and new pair of gloves was required when handling mice on a cage basis for any procedure.

Tissue collection. At week 26 (17 weeks after the last azoxymethane (AOM) injection), mice were sacrificed, and tissues were collected for posterior analyses. Two hours before termination, to assess cell proliferation rates, mice were injected (intraperitoneal) with 5-Ethynyl-2'-deoxyuridine (EdU; A10044, Life Technologies) at a dose of 50 mg/kg body weight. Mice were weighed and anesthetized by an intraperitoneal injection of

ketamine/xylazine (100mg/kg body mass), and blood was collected by cardiac puncture. Subsequently, the entire colon was removed, and the cecum excised. The entire colon was then flushed with sterile, cold PBS to collect fecal pellets, and the length and weight of the colon were measured and recorded. Each colon was then open longitudinally and separated between its anatomical proximal and distal sections. The proximal colon was divided in two, where a 1-cm section was cassetted and fixed in 4% paraformaldehyde (PFA, diluted from 20% PFA aqueous solution, 15713S; Electron Microscopy Sciences) for 4 hours, while mucosal scrapings from the rest of the colon were homogenized in RNA lysis buffer (from the RNAqueous-4-PCR kit, Ambion; AM1914). The colon's entire distal section was flattened between sheets of filter papers and glass plates and fixed in 70% ethanol for 24 hours to assess the development of premalignant lesions.

Histological scoring and Immuno-histo-fluorescence staining. Flattened-fixed colons were stored in 70% ethanol after 24-hour fixation. To morphologically identify and number aberrant crypt foci, tissues were stained with 0.5% methylene blue (Sigma-Aldrich) and analyzed using an inverted Nikon Eclipse fluorescent microscope at a 10X magnification as described previously.[37,113,114] High multiplicity ACF (HM-ACF) were defined as foci involving at least three or more crypts. PFA-fixed/paraffin-embedded proximal colon sections (5 μm) were deparaffinized, rehydrated, and stained with antibodies using standard immunofluorescence (IF). After deparaffinization and rehydration, antigens were retrieved by sub-boiling slides in 10 mM citrate buffer for 20 minutes. Proliferative cells were measured using the Click-iT EdU Alexa Fluor 488 Imaging Kit (Invitrogen, C10637), while apoptotic cells were stained with TACS 2 TdT-

Fluor *in situ* apoptosis detection kit (Trevigen, 4812-30-K) according to the manufacturer's instructions. ProLong Gold AntiFade with DAPI (P36931, Life Technologies) was used to stain the nucleus. Images of colonic crypts were taken with a fluorescence microscope (inverted TE 300 Nikon Eclipse) equipped with × 40/1.30 Nikon Plan Fluor oil immersion objective and a Photometrics Cool Snap EZ digital CCD camera and a SOLA external light source (Nikon, Melville, NY, USA). Images were processed using the NIS Image software, version 3.2 (Nikon). Both proliferation and apoptotic cells were identified and quantified by dividing the total number of cells in the colonic crypt. The localization (bottom, middle, top) of these cells within their corresponding crypt was also assessed. The percentage of proliferative and apoptotic cells was determined by dividing the number of proliferative or apoptotic cells by the total number of cells in the crypt column and multiplying by 100.

RNA sequencing and gene analysis. RNA was isolated from proximal colonic mucosal scrapings using the RNAqueous™ -4PCR Total RNA Isolation Kit (Ambion; AM1914), followed by removal of DNA (Ambion; AM1906), nucleic acid quantification by Nanodrop spectrophotometry and, assessment of RNA integrity on a Bioanalyzer 2100 (Agilent Technologies). Sequencing libraries were prepared by our collaborators in Dr. Robert Chapkin's laboratory, using 250 ng of RNA and the TruSeq RNA Sample Preparation kit (Illumina) following the manufacturer's instructions. ERCC spike-in RNA control mix (Life Technologies) was added to the starting RNA. DNA libraries were sequenced on an Illumina HiSeq 2500 at the Texas AgriLife Genomics and Bioinformatics Services Core Facility (College Station, TX). The sequences' alignment was performed

using Spliced Transcripts Alignment to a Reference (STAR) software with default parameters and referenced against the genome of *Mus musculus* (Ensembl version GRCm38). A list of differentially expressed genes (DEGs) expressed as a ratio of $Ahr^{\Delta IEC}$ /WT was generated using EdgeR based on the matrix of gene counts.[115,116] To further analyze, integrate and interpret the relationship and function of the previously determined DEGs, we utilize the Ingenuity Pathway Analysis (IPA, V. 01-14) (QIAGEN Inc., https://www.qiagenbioinformatics.com/products/ingenuity-pathway-analysis) using an FDR score (q-value) below 0.1 as a cutoff.

Targeted metabolomics. Homogenization and extraction of metabolites from fecal samples at termination (T2) were performed using mass spectrometry and chromatographic separation by our collaborators Dr. Arul Jayaraman and Dr. Rani Menon following previously published methodologies.[117–119] Based on the hypothesis that lack of AhR expression in IECs and the consumption of a HFD could alter the microbial-derived metabolites that will lead to the development of ACFs,[104] the fecal metabolite data were analyzed to identify targeted tryptophan-derived compounds from public metabolite databases.

Colon cancer initiation. Ms. Evelyn Callaway conducted a separate experiment aimed to test whether the carcinogenic potential of AOM was affected by the loss of AhR in IECS through the assessment of DNA damage. Briefly, mice were fed a low-fat diet (LFD) (Research Diets, D12450B) containing 10% kcal from fat for the duration of the study. On day 19 of the study, WT and $Ahr^{\Delta IEC}$ mice received a single intraperitoneal (i.p.) injection of azoxymethane (AOM) (10 mg/kg BW, Sigma: A5486). Twelve hours after AOM

injection, a subgroup was terminated (day 20), while the other subgroup was terminated three days later (day 22). PFA-fixed/paraffin-embedded colon sections (5 μm) were deparaffinized, rehydrated, and stained with antibodies using standard immunofluorescence (IF). Here, DNA double-strand breaks (DSBs) were measured by IF using a rabbit monoclonal phospho-gamma H2AX (γH2AX) Ser139 antibody (9718, Cell Signaling; dilution 1:200), and anti-rabbit Alexa 647 (711-605-152, Jackson ImmunoResearch: dilution 1:400) was used as a secondary antibody. The percentage of DNA-damaged cells per crypt (the number of γH2AX positive cells divided by the total number of cells in each crypt column multiplied by 100) was assessed at both 12 and 72 hours post-AOM.

Statistical analysis. Statistical analysis was performed using GraphPad Prism version 8.1.2 for Mac OS, Graph Pad Software (La Jolla CA, www.graphpad.com). Means were compared using parametric or non-parametric methods according to compliance of normality (Shapiro-Wilk test). Parametric methods included unpaired t-test for comparing two means or one-way ANOVA followed by Fisher Exact test if comparing three or more groups. Non-parametric methods include the Mann-Whitney U (MW) test for comparing two means or the Kruskal-Wallis (KW) for three or more groups. One-tailed p-values are reported in all analyses in accordance with our hypothesis. Differences among groups were considered statistically significant when the p-value was ≤ 0.05. In figures, statistical significance was indicated as follows: * indicates $p \leq 0.05$, ** indicates $p \leq 0.01$, *** indicates $p \leq 0.001$, and the absence of * indicates p-values > 0.05. All values listed are group means, and error bars are presented as SEM.

Results

Carcinogen-induced DNA damage is not associated with AhR activity in intestinal epithelial cells. Since carcinogen activation is partially mediated by IECs,[120] we investigated the effect of the loss of AhR in IECs immediately (12-72 h) following carcinogen exposure (**Figure 3A**). As indicated in figure 3B, no effect of genotype was detected concerning the percentage of DNA-damaged (phospho-γH2AX^{+}) cells in colonic crypts (ANOVA, p=0.2158). Representative images of DNA-damaged cells are shown in **figure 3C**.

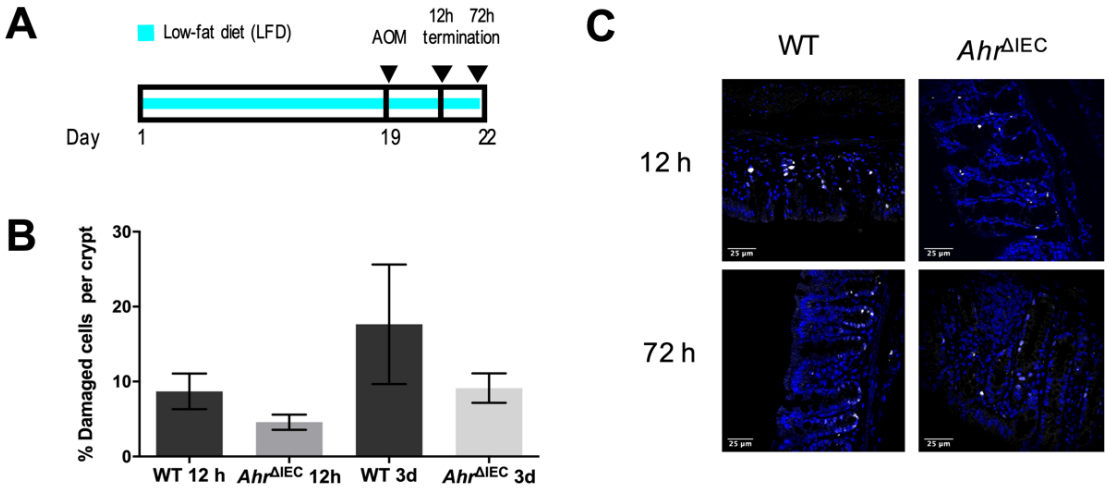

Figure 3. Short-term effects of loss of AhR after colonic-specific carcinogen (AOM) injection

A: Schematic representation of the initiation study design. *B:* Percentage of DNA-damaged cells on intact crypts after 12 and 72 hours post-AOM. 40-60 crypts were scored at the distal end of the colon per animal, n=4 per each of the genotypes and time points. p=0.2158 (One-way ANOVA). *C:* Representative images of immunofluorescence-stained DNA -damaged cells (γH2AX in white) and nuclei (DAPI in blue) on intact crypts of both WT and *Ahr*$^{\Delta IEC}$ models at the 12 and 72 h post AOM injection. Objective 10x (Scale bar=25 μm). Values are expressed as the mean percent of positively stained cells ± SEM. * indicates $p \leq 0.05$, ** indicates $p \leq 0.01$, *** indicates $p \leq 0.001$, and the absence of * indicates p-values >0.05.

Loss of AhR did not have a direct influence on body weight gain. Although all animals consumed a HFD, no significant differences were found between genotypes, as shown in **Figure 4A**. Likewise, body weight was not a predictor of pre-malignant lesion incidence (R^2=0.128) (**Figure 4B**)

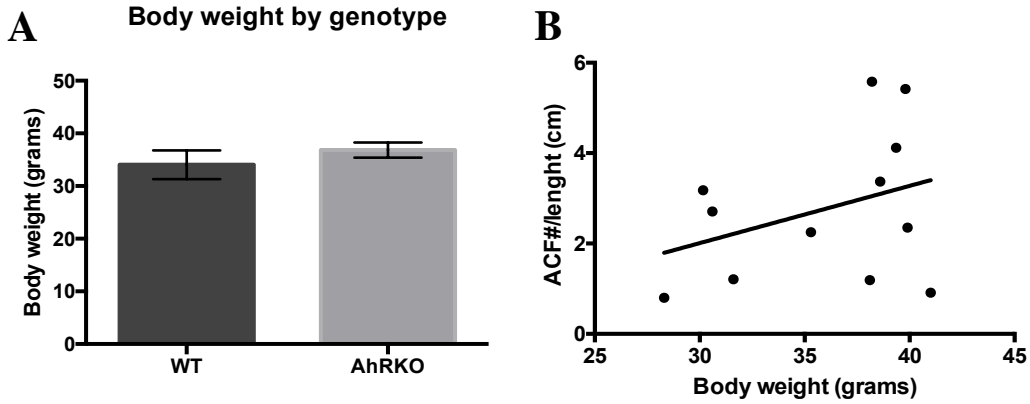

Figure 4. Body weight gain and incidence of ACF

A. Body weight in the WT mice (n=4) is not significantly different ($p > 0.05$) compared with the AhRKO mice (n=8) at the end of the study. ***B.*** ACF number was independent of body weight gain (R^2=0.1281)

Loss of Ahr in IEC enhances the formation of premalignant lesions in the colon. Premalignant CRC lesions (Total number of ACFs and HM-ACFs) were assessed in the distal colon at 17 weeks post final AOM injection. *Ahr*$^{\Delta IEC}$ animals had significantly more ACFs compared to WT ($p < 0.001$ nearly 3-fold, as shown in **Figure 5A**. In addition, the average incidence of High Multiplicity-ACF (HM-ACF) in *Ahr*$^{\Delta IEC}$ mice were approximately 4-fold higher than their WT counterparts ($P \leq 0.05$) (**Figure 5B)**.

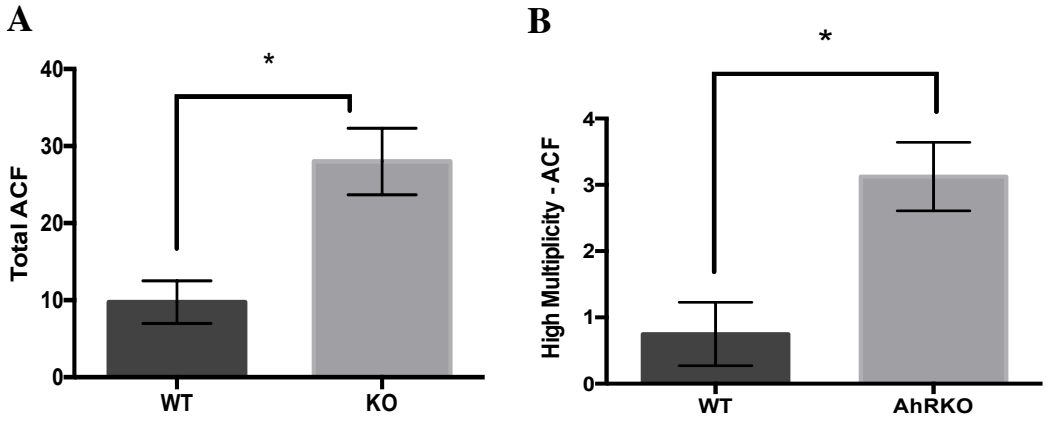

Figure 5. Total number of ACFs and HM-ACFs

A. Total number of ACF identified per animal in distal colons. Columns: WT (n=4, mean 9.750 ACF), *Ahr*$^{\Delta IEC}$ (n=8, mean 28 ACF); bars, SEM. *Statistical significance (P<0.001) when compared with normal controls. ***B.*** High-multiplicity ACFs identified per animal. Columns, WT (n=4, mean=0.750), *Ahr*$^{\Delta IEC}$ (n=8, mean=3.125); bars, SEM. (P=0.0303. HM-ACFs).

Loss of AhR in IEC induces cell proliferation and has no significant effect on apoptotic rates. Significantly higher labeling index (number of proliferative cells per crypt), as well as an expanded proliferative zone, was observed in *Ahr*$^{\Delta IEC}$ compared with WT control mice ($p < 0.0001$ and $P = 0.0152$, respectively) (**Figure 6A and B**). Analysis of the location of proliferative cells in the colonic crypt (top, middle, and bottom) revealed a significant increase in the number of proliferating cells in *Ahr*$^{\Delta IEC}$ mice at the bottom and middle zone ($p \leq 0.05$) but not at the top of the crypt (**Figure 6C**). No significant differences were observed in the number of apoptotic cells between genotypes regardless of their location within the crypt (WT vs. *Ahr*$^{\Delta IEC}$) (**Figure 6D**).

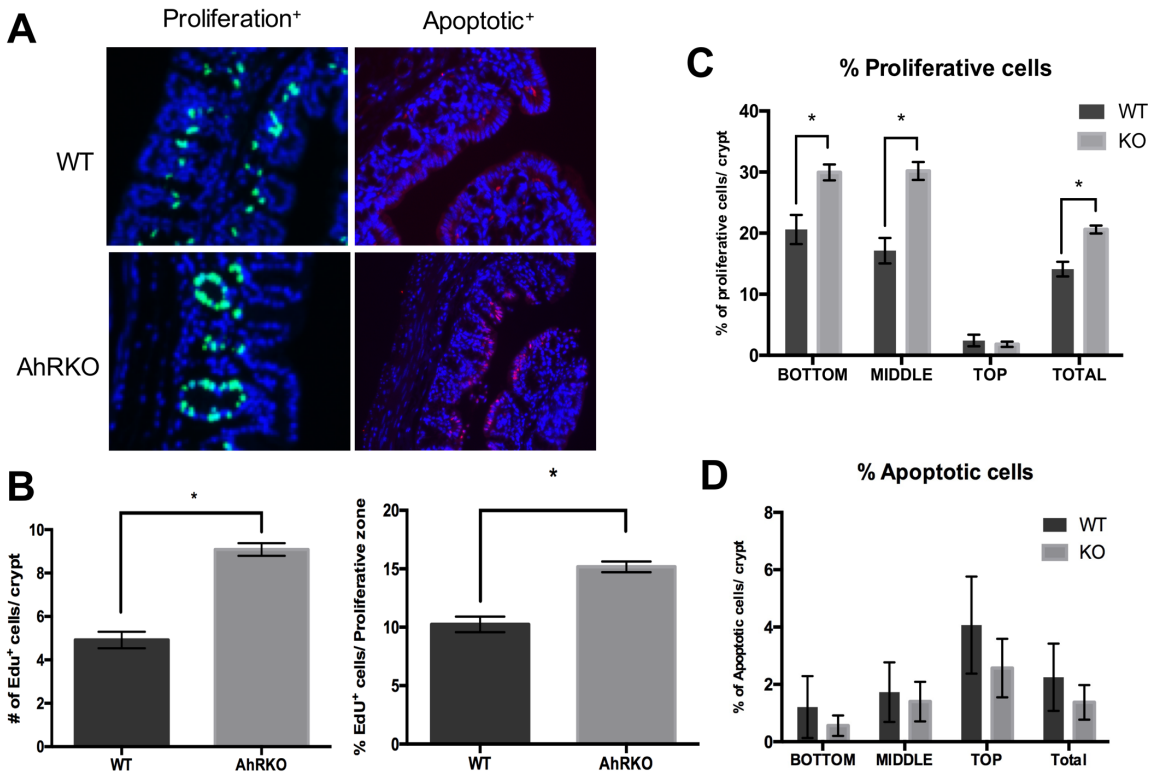

Figure 6. Representative images of IF stained EdU+ and TUNEL+ cells.

A. Representative image of IF stained Edu+ (proliferative, green), TUNEL+ (apoptotic body, red) and nuclei (blue) cells are shown on both WT and AhRKO. Objective 10x. ***B.*** Proliferation expressed as the percentage of Edu+ cells in the crypts by genotype (AhRKO and WT) – Left and expressed by Edu+ cells by proliferative zone ***C.*** Proliferation expressed as the percentage of Edu+ cells and their position within the crypt (bottom, middle, top and total). ***D.*** Apoptosis expressed as the percentage of TUNEL+ cells and their position within the crypt (bottom, middle, top and total). Values are mean percent of positively stained cells ± SEM, WT group, n=4 and AhRKO group, n=8. * Statistical significance ($P<0.05$) when compared within groups

Loss of Ahr in IEC induces the expression of pro-tumorigenic gene signatures. To investigate the effects of the loss of AhR in IEC in relevant molecular pathways and cell functions, IPA® was used to analyze significant differentially expressed genes (DEGs) obtained from our RNA-seq analysis. Data generated from RNA-sequencing of colonic mucosal scrapings resulted in the identification of a total of 185 DEGs, of which 18 genes

were downregulated and 167 upregulated by the loss of AhR in IEC. From these observations, we identified 8 genes with the greatest differential mRNA expression ($p \leq 0.001$, FDR ≤ 0.1) upregulated in the $Ahr^{\Delta IEC}$. Among the genes that were upregulated in the $Ahr^{\Delta IEC}$ compared with WT samples, from highest to lowest $\log_2$-FC, we found *Nos2* (Nitric oxide synthase 2), *C3* (complement 3), *Tnfaip2* (TNF Alpha inducer protein 2), *Akt3* (Akt Serine/Threonine Kinase 3), *Tgfb1* (Transforming Growth Factor Beta 1), *Rac2* (Rac Family Small GTPase 2), *Bcl3* (B-cell CLL/Lymphoma 3), and *Rhof* (Ras homolog family member). According to the IPA's canonical pathway building tool, these genes were shown to be involved in cell proliferation, cell cycle progression, cell migration, inflammation, angiogenesis, and tumor progression (**Figure 7**).

According to IPA's analysis, the top enriched categories of canonical pathways in the $Ahr^{\Delta IEC}$ ($p < 10^{-5}$) are the B-cell Receptor signaling pathway, the PI3K signaling in B lymphocytes, the acute phase response signaling, the leukocyte extravasation signaling, and the Sphingosine-1-phosphate Signaling (**Figure 8A**). Additionally, IPA's analysis of diseases and functions (p-value less than 10^{-11}) was conducted. Diseases related to our system include inflammatory response, cancer, organismal injury and abnormalities, metabolic disease, and hematological disease (**Figure 8B**). In contrast, molecular functions affected by the loss of AhR in IEC included cellular movement, immune cell trafficking, tissue morphology, humoral response, and lymphoid tissue structure and development.

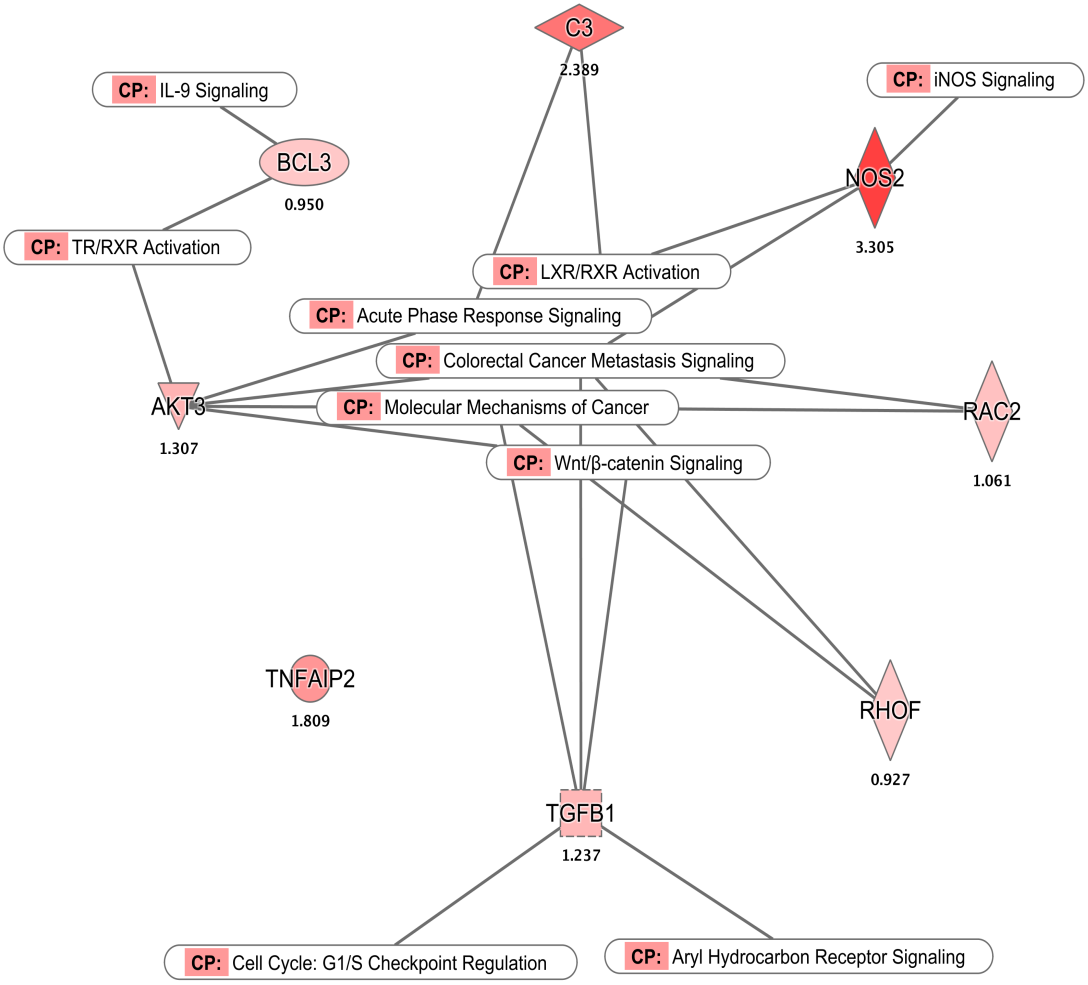

Figure 7. Canonical pathways involved in the ACF development.

Interconnections between significant differentially expressed genes (DEGs) in the dataset and relevant canonical pathways involved in cell proliferation, migration and tumor progression among others are represented. Under each gene legend, Log_2FC values are indicated. Figure was generated in IPA using "My Pathways" building tool based on a set of genes of interest. Canonical pathways shared by our genes of interest are displayed at the middle of the figure, while independent pathways are around the periphery. CP: Canonical Pathway, Red color: more extreme upregulation in $Ahr^{\Delta IEC}$/WT, Pink color: less extreme upregulation in $Ahr^{\Delta IEC}$ /WT.

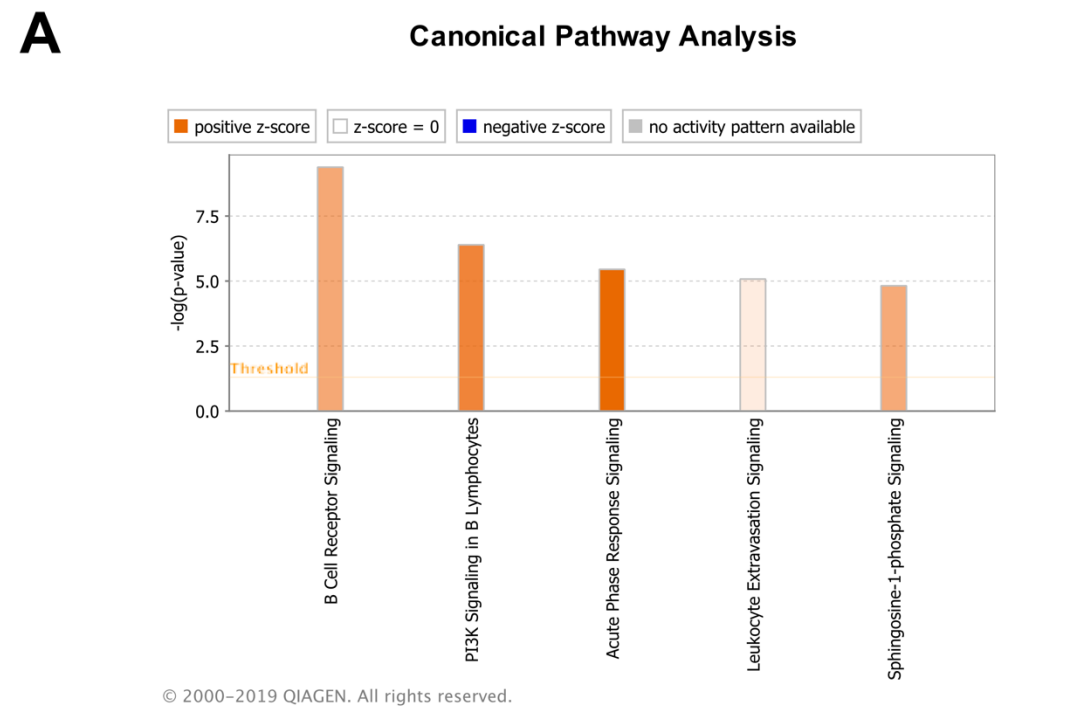

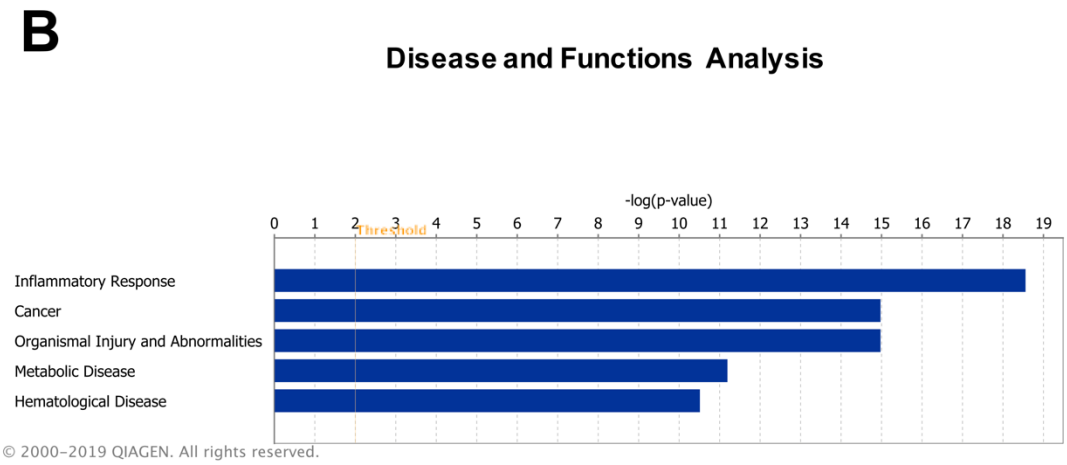

Figure 8. Ingenuity Pathway analysis of significant differentially expressed genes (DEGs) upregulated in the absence of AhR in IEC

A. Top enriched categories of canonical pathways with a p-value less than 10-5 with positive z-scores. The x-axis represents the pathways identified. The y-axis shows the −log of the P value calculated based on Fisher's exact test. Horizontal orange line running through the bars is the threshold for p value for these pathways' enrichment ***B.*** Disease and functions with a p-value less than 10-11 The y-axis shows the −log of the P value calculated based on Fisher's exact test. Vertical orange line running through the bars is the threshold for p value for these diseases and functions.

Loss of AhR in IEC results in an increased abundance of metabolites derived from aromatic amino acids. At 17 weeks post final AOM injection, a total of 10,496 features were detected from all the stool samples and used for quantification of a targeted panel of 21 metabolites. Of these, a significant increase in anthranilic acid, 5-aminovaleric acid, indole 3-carboxaldehyde, and indole-3-lactic acid ($p<0.05$) was observed in fecal samples from *Ahr*$^{\Delta IEC}$ mice compared to the WT mice at termination (**Figure 9**).

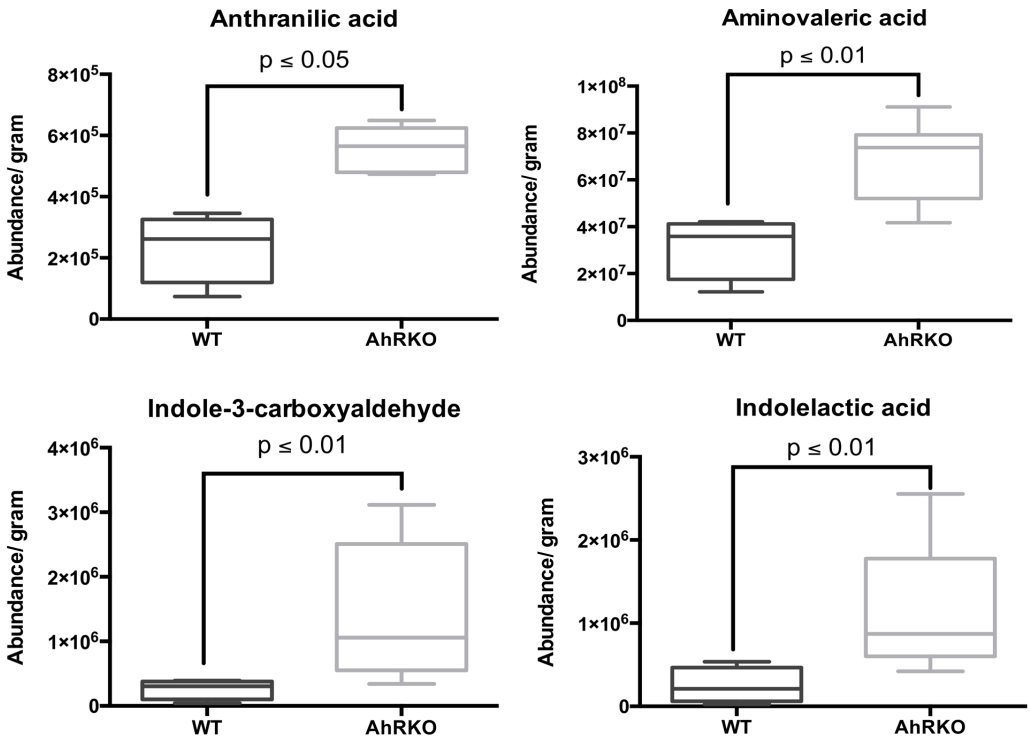

Figure 9. Targeted fecal metabolites affected by the loss of AhR in IECs

At termination, quantification of a panel of 21 metabolites was performed. Significant increase of ***A.*** Anthranilic acid, ***B.*** 5-aminovaleric acid**,** ***C.*** indole 3-carboxaldehyde and ***D***. indole-3-lactic acid ($p<0.05$) was observed in the *Ahr*$^{\Delta IEC}$ compared to the wildtype mice.

Discussion

Although previously published data suggest a tumor suppressor-like activity for the AhR and its ligands, the use of a global AhR null model limits our ability to understand the significance of its expression within specific cell types. In order to address this question, we utilized an IEC-specific AhR knockout mouse (*Ahr*$^{\Delta IEC}$) and demonstrated that the absence of AhR is associated with an increased number of premalignant colon cancer lesions. Given that colon tumor development is a multistage process, it was important to determine the specific stages in which AhR elicits a response. Hence, we demonstrated that loss of AhR plays a critical role in the formation of ACF.

Since the bioactivation of the colon carcinogen AOM is partially mediated by intestinal cytochrome P450s, it was crucial to investigate whether *Ahr*$^{\Delta IEC}$ and WT mice have the same response to DNA damage after carcinogen exposure.[120,121] Because no significant differences in DNA-damaged cells were identified among genotypes, we concluded that a comparable first insult by the carcinogen was achieved, and the differences observed in subsequent stages of carcinogenesis are not likely the result of WT animals receiving a greater exposure to AOM.

Early histological lesions in the epithelium can be identified 9-17 weeks after the last carcinogen dose as the colonic mucosa acquires hyperplastic, dysplastic, and/or neoplastic features. These premalignant lesions have been defined as aberrant crypt foci (ACF), and their size and number have been associated with an increased risk of CRC development.[37] In this study, we established that loss of AhR in IECs could significantly increase the formation and multiplicity of premalignant colon cancer lesions (ACFs) in

the presence of a pro-tumorigenic diet high fat-diet. Furthermore, the loss of AhR in IECs resulted in a significant increase in cellular proliferation rates, specifically at the base and middle section of the colonic crypts, without affecting the apoptosis rates. Since an increased rate of proliferative cells at the bottom of the crypt has been associated with CRC development,[54] our data suggest that loss of AhR activity in IECs can modulate the trajectory of cancer malignancy.

Data collected from the liver, small intestine, and cecum suggest that AhR activation can reduce cell proliferation induced by chemical carcinogens through downregulating the expression of *Myc*, increasing β-catenin degradation, and G0-G1 cell cycle arrest.[29,93,122] Previous studies have shown that exposure to a HFD before and/or during AOM-induced CRC initiation is sufficient to significantly increase colon masses, including polyps and tumors in WT animals regardless of body weight loss or maintenance following a dietary switch.[47,123]

To start identifying the potential molecular mechanisms by which the loss of AhR expression in IECs modulates the risk of CRC development, we identified differentially expressed genes known to play a role in regulating cell proliferation, inflammation, and angiogenesis, increasing the risk of CRC development. To our knowledge, this is the first reported attempt of a comprehensive transcriptome analysis using RNA-sequencing in an intestinal-specific AhR knockout model of AOM-induced CRC. At the premalignant lesion formation stage, deletion of AhR upregulated *Bcl3,* a known oncogene capable of inducing proliferation and cell progression mediated by the STAT3 signaling pathway,[124] and *Akt3,* which promotes processes such as cell survival, cell growth, Wnt/β-catenin

signaling, and proliferation in lymphocytes, breast cancer, and embryonic stem cells.[125] Together, *Bcl3* and *Akt3* are required for TR/RXR (Thyroid Receptor/Retinoid X Receptor) activation and thyroid hormone function (growth, development, and metabolism). Besides, *C3* was upregulated in the absence of AhR, suggesting an enhancement of acute phase response signaling and LXR/RXR (Liver X Receptor/Retinoid X Receptor) signaling.

Similarly, overexpression of *Tnfaip2* has been inversely associated with suppression of proliferation and metastasis in squamous cell carcinoma through activation of Wnt/ β-catenin signaling.[126] Overall, increased expression of *Rhof*, *Tgfb1, Rac2,* and *Nos2* have been implicated in the Wnt/ β-catenin pathway and colorectal cancer metastasis signaling.[127] Considering the role of *Tgfb1* in the regulation of cell cycle, its overexpression suggests a shift from tumor suppressor activity towards the promotion of tumorigenesis.[128] Interestingly, loss of AhR induced the upregulation of *Nos2 (iNOS)* expression, which has been associated with tumor growth and poor survival.[129] Likewise, since genes responsible for reducing oxidative stress and the transcription of pro-inflammatory cytokines such as *Nfr2* were not significantly altered,[130,131] suggest cytokine-inducible molecules such as *Nos2* are not as effectively negatively regulated. In conjunction with increased activation of the Sphingosine-1-Phosphate signaling (cell membrane), members of the Rho (*Rhof)* and Rac (*Rac2)* family are able to induce signaling pathways that lead to cell survival and cell migration.[132] Likewise, AhR activity from IECs can potentially crosstalk with normal B-cell functions, the formation of lymphoid structures, immune cell trafficking, and acute response signaling, as suggested by our IPA

analysis. However, additional research is required to elucidate the role of AhR activity concerning the crosstalk between IECs and the epithelial niche. Taken together, the upregulation of genes involved in the promotion of proliferation, cell growth and tumorigenesis in *Ahr*$^{\Delta IEC}$ mice suggest that AhR activity is crucial for regulating normal intestinal epithelial cell growth.

Conflicting with our previous hypothesis, lack of AhR expression in IECs resulted in a significant increase of beneficial fecal tryptophan-derived amino acids at termination compared with WT mice such as anthranilic acid, indole-3-carboxaldehyde, indole-3-lactic acid, and 5-aminovaleric acid. Specifically, anthranilic acid and 5-aminovaleric acid have been found to be elevated in inflammatory diseases of the gut, such as colitis and Crohn's disease.[133,134] While high levels of indole-3 carboxaldehyde and indole-3-lactic acid, known AhR agonists, have been reported in the absence of AhR.[135,136] Studies using a constitutive Cyp1A1 and a triple Cyp1 knockout murine model have shown that Cyp1 enzymes are crucial to modulate AhR activation by reducing the concentration of AhR ligands and consequently their availability to the IECs.[121,137] In our study, loss of AhR in IECs may, in turn, disrupt the feedback mechanism required to degrade and detoxify these ligands through Cyp1 enzymes resulting in their increased abundance in feces. However, further study is needed to determine if the increase in the levels of these metabolites is the direct result of the altered genotype or if the loss of AhR in IECs leads to a change in microbial populations resulting in altered concentrations of these and other biologically relevant compounds. Albeit chronic HFD consumption is sufficient to modify the gut microbiome and their metabolites, in our study, the phenotypical differences appear to be

driven by the loss of AhR in IECs. However, the physiological effects associated with high concentrations of these metabolites do not recapitulate the increase in ACFs and the expression of pro-tumorigenic genes in mice lacking AhR activity in our experiment.

Taken together, our results provide interesting insights into the vital role of AhR expression in IECs to reduce the formation of premalignant lesions through modulation of cell proliferation and expression of genes associated with cell growth, migration, and survival. Further identification of microbial-derived AhR ligands and the molecular mechanisms underlying AhR's activity will allow us to establish the AhR as a target for therapeutic strategies against colorectal cancer development.

CHAPTER III

EFFECT OF HIGH-FAT DIET AND INTESTINAL ARYL HYDROCARBON RECEPTOR DELETION IN THE FORMATION OF PREMALIGNANT COLORECTAL CANCER LESIONS AND THE GUT MICROBIOME*

Introduction

Based on the data collected in Chapter 2 regarding the significantly increased incidence of premalignant CRC lesions with the lack of AhR expression in IECs in the presence of a HFD, we further investigated whether the development of ACFs was dependent upon both the consumption of saturated fat during the peri-initiation period and loss of AhR activity in IECs. Furthermore, due to the significant effect of both the composition of the diet and the integrity of IECs in the establishment of microbial communities and consequently the role of dysbiosis in colonic inflammation and initiation of CRC,[52–55,58,59] we further investigated the effect of a high-fat diet and loss of AhR in IECs in the formation of premalignant CRC lesions and the gut microbiome.

Recent studies have identified dietary, microbial, and host-derived compounds that can bind AhR and elicit a variety of beneficial physiological effects.[72–74] In the large intestine, these effects include regulation of mucosal inflammation, tissue regeneration,

---

* Reprinted with permission from sections of "Effects of high-fat diet and intestinal aryl hydrocarbon receptor deletion on colon carcinogenesis" by Garcia-Villatoro, E.L. [1], DeLuca, J.A.A. [1], Callaway, E.S., Allred, K.F., Davidson, L.A., Hensel, M.E., Menon, R., Ivanov, I., Safe, S.H., Jayaraman, A., Chapkin, R.S., and Allred, C.D., 2020. The American Journal of Physiology Gastrointestinal and Liver Physiology, 318(3), G451-G463, Copyright 2020 by The American Physiological Society. [1]Equally contributing co-first authors. Reprint permission has been granted by the co-first authors.

regulation of the immune system, proteasomal degradation , and interaction with the microbiome.[29,67–70,72,73] Chronic HFD consumption not only facilitates proliferation and survival of tumor cells,[100] but also is able to alter the gut microbiota composition independently of the host genotype, highlighting the role of the diet in modeling the host's microbial communities.[138] While expression of AhR has been associated with several gastrointestinal cancers (i.e., stomach cancer) in advance stages, [88] increasing experimental evidence suggests that AhR activation may also be protective against colonic inflammation and carcinogenesis in both sporadic and colitis-associated models of CRC.[76,90–92]

The Wnt-β-catenin pathway is often mutated in CRC, and increased expression and nuclear translocation of β-catenin from the cytosol can result in increased colonocyte proliferation through the expression of *c-Myc* and *Cyclin D1*.[139,140] However, AhR activation by exogenous ligands has been associated with increased E3 ubiquitin ligase activity that participates in the degradation of a proliferation-inducing transcription factor such as β-catenin.[76,77] These findings, in combination with studies reporting an increased expression of β-catenin in mice lacking AhR,[22] further support our hypothesis that AhR expression in the intestinal epithelia is vital to modulate CRC development. Thus, in the present study, we investigated the effects of the loss of AhR activity in intestinal epithelial cells (IEC) in the development of premalignant lesions in the context of both high- and low-fat diets as well as the modulation of gut microbial communities towards a pro-carcinogenic and dysbiotic environment.

Materials and Methods

Mouse model, experimental diets, and housing conditions. We employed the intestinal-specific AhR knockout (*Ahr*$^{\Delta IEC}$) as the experimental group and the AhR$^{f/f}$ littermates (WT), as described in Chapter II (Figure 1). Both genders were included in the analysis. A total of 15 mice were assigned to each of the eight treatment groups. Upon enrollment of the study, mice received a chow diet until sexual maturity was reached at eight-weeks of age. During this time, the cage bedding was mixed weekly to establish a baseline of the microbiome. As indicated in figure 9, starting at week six, half of the mice received a low-fat diet (LFD) containing 10% of fat (Research Diets, D12450B) as the control diet, while the other half received a high-fat diet (HFD), providing 60% kcal from fat as the experimental diet (Research Diets, D12492). Mice received food and water *ad libitum* and were housed on a 12 hour/12-hour light-dark cycle at a maximum of five per cage. Body weight was assessed weekly. After three weeks on the experimental diets, sporadic colorectal cancer was chemically induced with one injection of Azoxymethane (AOM; Sigma: A5486) for six consecutive weeks. Since mice consuming a HFD had significantly higher body weight compared to their LFD-fed counterparts, animals weighing less than 40 grams received AOM injections of 10 mg/kg body weight, while those weighing 40 grams or more received AOM at 7.5 mg/kg body weight. Mortality from AOM was observed between 24 and 72 hours after the injection, especially in male mice fed a HFD.

Fecal collections and housing conditions: Housing conditions, handling, diet, and cage effects were controlled during the experiment as indicated in Chapter II.[141]

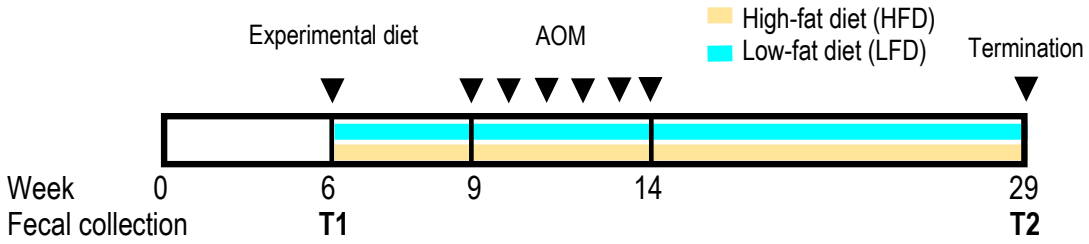

Figure 10. ACF study timeline

Tissue collection. Animals were terminated 15 weeks after the last injection of AOM. As previously described in Chapter 2, two hours before termination, select animals were intraperitoneally injected with a proliferation marker, 5-Ethynyl-2'-deoxyuridine (EdU; A10044, Life Technologies), at a dose of 50 mg/kg body weight. Blood was collected via cardiac puncture. The colons were immediately resected and flushed with sterile PBS. Colon weight and length were recorded at this point. The colon was then opened longitudinally. First, the proximal colon was divided in two, where one 1-cm section was cassetted and fixed in 4% paraformaldehyde (PFA) for 4 hours, while the rest was scrapped to collect the mucosa to be later homogenized in RNA lysis buffer. The colon's distal section was flattened and fixed in 70% ethanol for 24 hours to assess the development of premalignant lesions.

Histological analyses of Aberrant crypt foci. Number and multiplicity of ACFs were assessed as previously indicated in Chapter II.[37,113,114] Data represent the total number of

ACFs divided by the distal colon's length in centimeters (ACF # /distal colon (cm). High multiplicity ACF (HM-ACF) were defined as foci involving three or more crypts. After morphological assessment of ACFs was completed, the remaining distal colons were washed three times in 70% ethanol, cut in half, and arranged in a tissue cassette to be processed and paraffin-embedded for further histological analyses. A total of 3 serial sections of 5 μm of thickness were obtained, in which one was H&E stained for ACF identification at 20X by a veterinary pathologist blinded to treatment groups; images were generated using an Aperio CS2 Scanner (Leica Biosystems). To later analyze nuclear translocation of β-catenin, photomicrographs were taken at 20X to aid in co-localization. Aberrant crypt foci were defined as crypts with more than one of the following features: loss of polarity, nuclear atypia (enlarge nuclei, vesiculate chromatin, crowding), mucin depletion, and crypt multiplicity. The presence of aberrant crypt multiplicity was considered a fundamental change. For this study, only crypts with criteria matching group C, defined by DiGregorio et al., were considered aberrant crypt foci.[142] The location of ACFs was mapped per section using mm measurements from the label corner for future co-localization with β-catenin immunohistochemistry.

β-catenin intensity and subcellular localization in ACF. Serial sections from distal colons previously described were used to measure the nuclear and cytosolic localization of β-catenin in ACF. As previously described by Kim E, et al.,[143] the tissues were stained using a monoclonal β-catenin antibody (610154, BD Transduction, San Jose, CA, USA; dilution 1:500) and an anti-mouse secondary antibody conjugated to Alexa Fluor 647 (A-31571, Life Technologies; dilution 1:200). ProLong Gold AntiFade with DAPI (P36931,

Life Technologies) was sued to stain the nucleus. To assess the subcellular localization of β-catenin in ACF, we first searched for positively identified ACF from the previous histopathological assessment in the previous tissue section and located the same ACF in its parallel immuno-stained section. ACF areas stained with β-catenin and DAPI were captured at 40x magnification. A total of 25 ACFs per tissue were examined. Slides were imaged using an all-in-one fluorescent microscope (Keyence BZ-X700), and the ratio of nuclear-to-cytosolic β-catenin was analyzed using Fiji ImageJ software, version 2.0.0-rc-69/1.52 (imagej.net).[144] For each ACF, a region of interest (ROI) was defined by a positive stain of both β-catenin and DAPI; the latest was used to identify the nuclear region of interest and separate nuclear and cytoplasmic staining within a cell. DAPI staining was used to define the nuclear region of interest and to separate nuclear and cytoplasmic staining within a cell. Briefly, β-catenin intensity in the whole cell (C), and nuclear (N) localization measurements were used to calculate the nuclear-to-cytosolic β-catenin ratio N/(C-N).

Immuno-histo-fluorescence staining. Cell proliferation rates were measured using immunofluorescence staining on intact crypts of proximal colon sections following the same methodology as previously described in Chapter 2. Click-iT EdU (5-ethynyl-2'-deoxyuridine positive) Alexa Fluor 488 Imaging Kit (Invitrogen, C10637) was used as per the manufacturer's instructions to stain proliferative cells, while DAPI (in blue) was used to stain the nucleus. Images of colonic crypts were taken with a fluorescence microscope (inverted TE 300 Nikon Eclipse) equipped with 10x Ph1 DLL Plan Fluor objective with a Photometrics CoolSNAP HQ2 digital camera and a SOLA external light source (Nikon,

Melville, NY, USA). Images were processed using Fiji software.[144] The percentage of proliferative cells was calculated by dividing the number of proliferative cells by the total number of cells in the crypt column and multiplying by 100 (% Proliferative cells/crypt). Crypt length and the proliferative zone (100 times the position of the highest labeled cell divided by the number of cells per crypt column) were also assessed.

Gene expression analysis. RNA was isolated from mucosal scrapings from proximal colon tissues collected during termination to assess the expression levels of *TNF-α, IL-6, IL-22, Muc1*, and *Muc2*. Briefly, total RNA was isolated colonic mucosal scrapings using the Qiagen RNEasy kit (Qiagen, CA). The RNA was further processed to remove DNA by DNase treatment using the Ambion DNA-free kit (Ambion; AM1906). RNA concentration and quality were assessed using a NanoDrop and Bioanalyzer (Agilent), respectively. The generally acceptable RNA quality of A260/A230 ratio was ~2.0. β-actin was used as the housekeeping gene. Gene expression was measured using SYBR Green I-based real-time PCR (04887352001, Roche) on a Roche Light Cycler. Fold-change differences in the expression of different genes were calculated as the expression in $Ahr^{\Delta IEC}$ animals relative to the WT, for both LFD and HFD.

Gut microbiome composition assessment. DNA extracted from fecal samples collected before carcinogen exposure (T1) and before termination (T2) was used to assess the changes in the abundance of microbial communities. The V4 region of 16S rRNA V4 was sequenced on a MiSeq Illumina platform, as previously described.[145] Dr. Arul Jayaraman's laboratory performed DNA extraction and preparations for sequencing. Sequencing was performed on the Analysis, Resources, and Services facility (MARS) at the University of

Connecticut. Raw sequences were aligned, classified, and diversity analysis was conducted.

Statistical analysis. All statistical analyses and figures were generated in GraphPad Prism version 8.1.2 for macOS, Graph Pad Software (La Jolla CA, www.graphpad.com). Means were compared using parametric or non-parametric methods according to compliance of normality (Shapiro-Wilk test). Outliers based on ROUT (Q=1.0%) were excluded. Parametric methods included an unpaired t-test for comparing two means or one-way ANOVA followed by Tukey's multiple comparisons test for comparing three or more means. Two-way ANOVA was used to test interaction effects between variables. Non-parametric methods include the Mann-Whitney U (MW) test for comparing two means or the Kruskal-Wallis (KW) test followed by Dunn's multiple comparisons test for comparing three or more means. One-tailed p-values are reported in all analyses due to the directionality of our hypothesis. All values listed are group means, and error bars are presented as SEM. Differences among groups were considered statistically significant when the p-value was ≤ 0.05. Within figures, * indicates $p \leq 0.05$, ** indicates $p \leq 0.01$, *** indicates $p \leq 0.001$, and the absence of * indicates p-values >0.05.

Results

No significant effect of diet and genotype in body weight gain. At termination, Body weight was assessed once a week throughout the duration of the study (**Figure 11A**). However, neither the genotype (p=0.4463) nor the diet (p=0.2260) significantly affected body weight gain at termination. (**Figure 11B and C**)

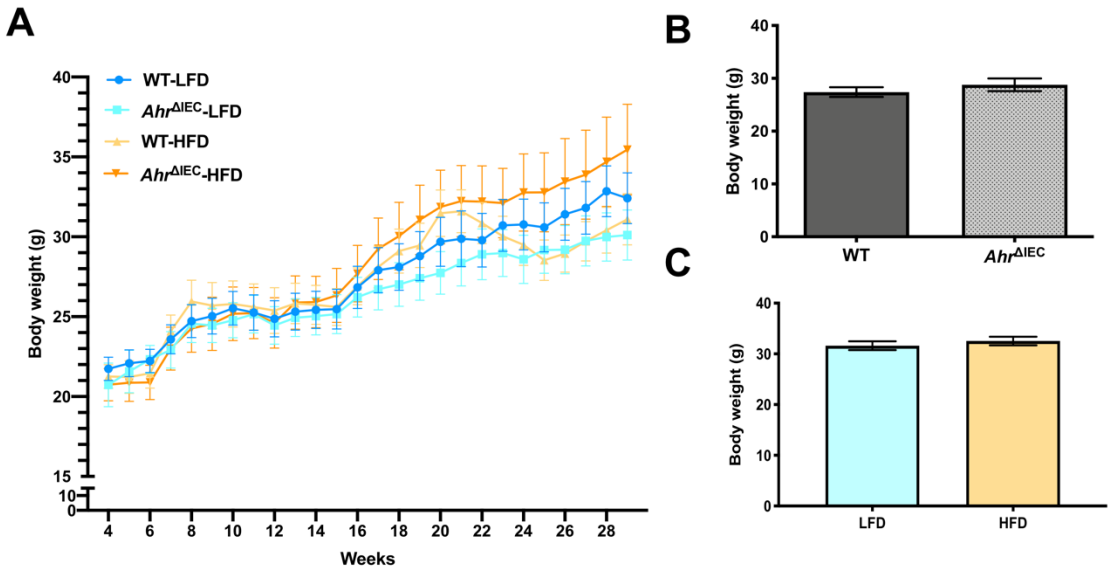

Figure 11. Effect of diet and genotype in body weight

A: Weekly body weight (in grams) is not significantly different between genotype (WT or $Ahr^{\Delta IEC}$) or diet (Low-fat diet, LFD or High-fat diet, HFD). ***B*** and ***C:*** At termination (week 29), no differences in body weight can be observed between genotype and diet.

Loss of AhR in the IECs induces the formation of premalignant lesions in the colon. After fifteen weeks after the last injection of AOM, ACF number (ACF#/cm distal colon) and multiplicity (more than 3 foci/cm distal colon) were assessed (**Figure 12A**) following the same methodology stated in Chapter II. At this stage, $Ahr^{\Delta IEC}$ mice had significantly

more ACFs than their WT (p=0.0088) counterparts, as shown in **Figure 12B**. Specifically, WT control mice had an average of 1.38 ACF, while Ahr$^{\Delta IEC}$ mice 2.29. Although the diet did not significantly affect body weight gain, mice than consumed a HFD had significantly more ACF (p=0.004) that mice fed a LFD (**Figure 12C**). Although separately, diet and genotype seem to have a significant effect on the number of ACFs, collectively, diet and genotype did not have a significant interaction (p=0.4502) (**Figure 12D**). In addition, Ahr$^{\Delta IEC}$ mice displayed a 4-times more high multiplicity ACF (HM-ACF #/ cm distal colon) than their WT counterparts (p=0.0198) (**Figure 12E**).

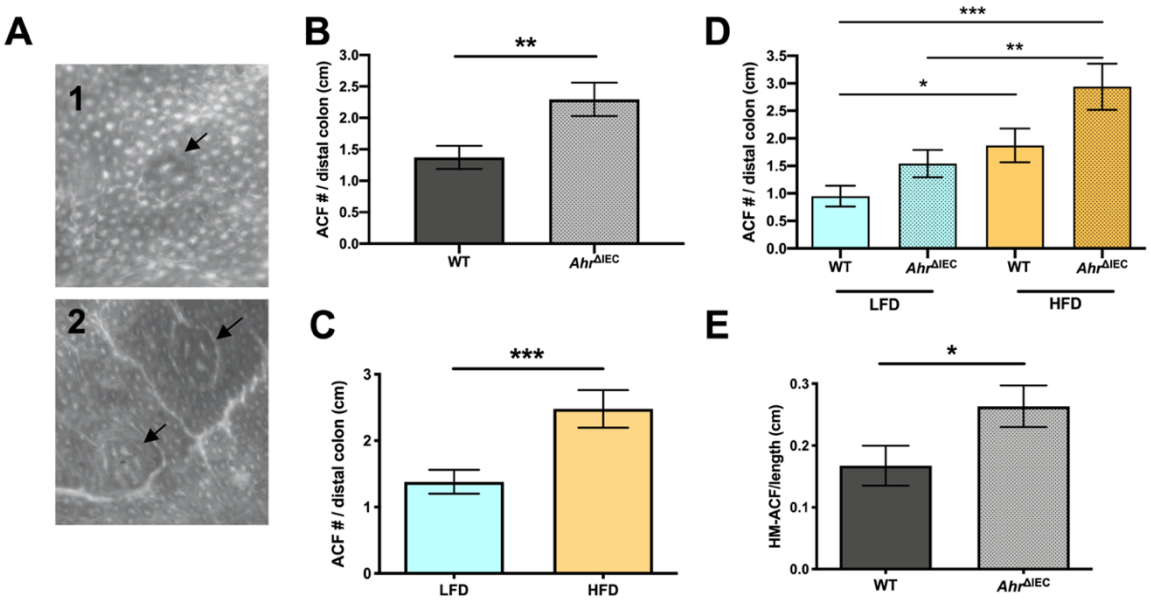

Figure 12. Effect of diet and genotype in ACF formation

A: Topographical view of typical aberrant crypt foci stained with methylene blue (100x) in distal colon tissue with mucosal side up. 1) Aberrant crypt foci with 1 aberrant crypt (arrow) and 2) aberrant crypt foci with 3 or more aberrant crypts (high multiplicity ACF, HM-ACF) (arrow), scale bar=1000 µm. ***B:*** Number of ACFs identified per animal in the distal colon normalized by colon length; p=0.0088 (MW). ***C:*** ACF number normalized by length (cm) compared by diet; p=0.0005 (MW). ***D*:** ACF number normalized by length (cm) compared by genotype and diet; p=0.0004 (KW). No interaction between diet and genotype (p=0.4502), diet effect (P=0.0004), genotype effect (P=0.0102). ***E:*** High Multiplicity-ACF (HM-ACF) normalized by length; p=0.0198 (MW). Values are means ± SEM. * indicates $p \leq 0.05$, ** indicates $p \leq 0.01$, *** indicates $p \leq 0.001$, and the absence of * indicates p-values >0.05.

Loss of Ahr in IEC induces cell proliferation in colonic crypts. Representative images of proliferative cells (EdU^+) in proximal colon tissues classified by genotype and diet are shown in **Figure 13**. At termination, compared to WT mice, $Ahr^{\Delta IEC}$ mice had a significantly higher percentage of proliferative cells per crypt ($p \leq 0.0001$), as displayed in Figure 14A. Comparatively, a significant increase in the percentage of proliferative cells ($p \leq 0.0001$) was observed in mice that consumed a HFD (**Figure 14B**). Subsequent analysis revealed a significant statistical interaction (p=0.0017) between the genotype and the diet (**Figure 14C).** Analysis of the location of proliferative cells within the colonic crypt (bottom, middle, top) revealed a significantly higher percentage ($p \leq 0.01$) of proliferative cells are found at the bottom and middle areas of the crypt of $Ahr^{\Delta IEC}$ mice compared to WT (**Figure 14D).** Additionally, loss of AhR in IECs resulted in a significant increase (p=0.03) of proliferation zone (**Figure 15A**) but without an effect on the colonic crypt length. (Figure 15B)

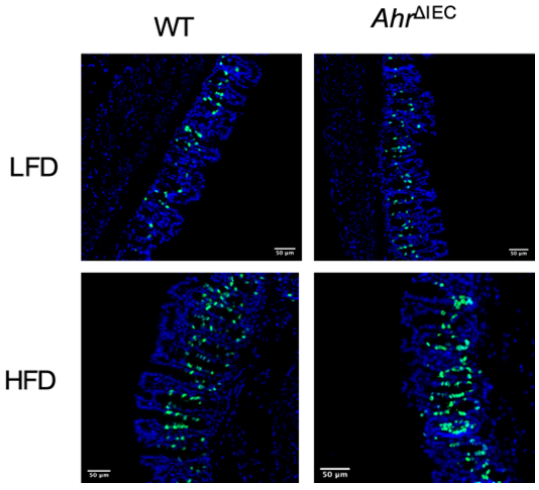

Figure 13. Representative images of immunofluorescence-stained

Proliferative cells are marked in green (EdU^+) and nuclei (DAPI in blue). Data presented by genotype and diet, scale bar=50 µm

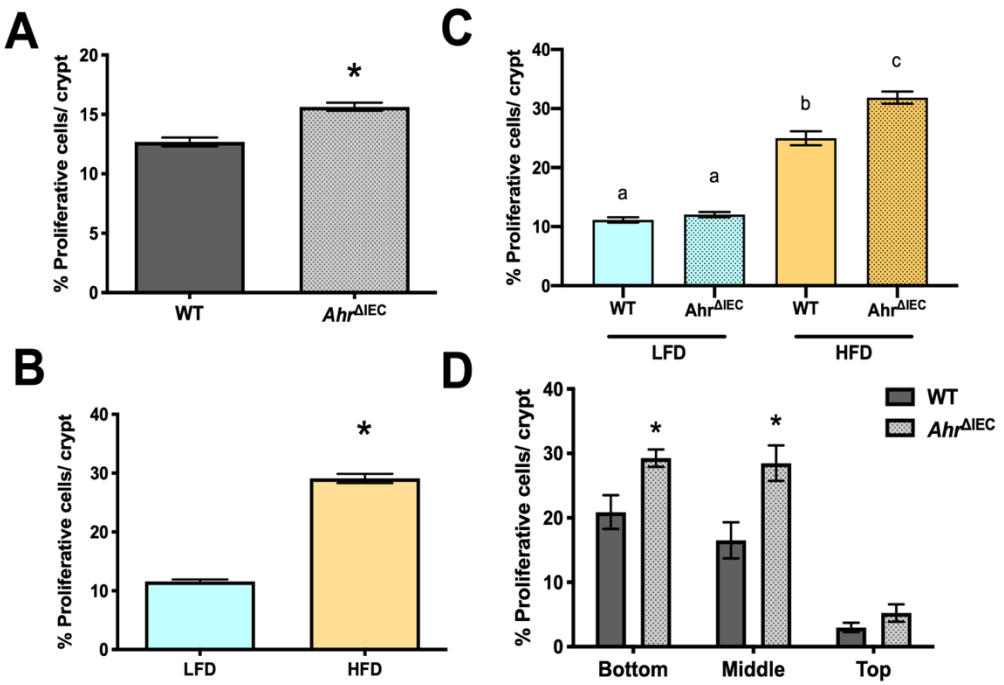

Figure 15. Effect of diet and genotype in cell proliferation in intact crypts at the proximal section of the colon at the ACF formation stage.

A: Percentage of proliferative cells per crypt by genotype; p<0.0001 (MW). ***B:*** Percentage of proliferative cells per crypt by diet; p<0.0001 (MW). ***C:*** Percentage of proliferative cells per crypt by genotype and diet; p<0.0001 (KW). Significant interaction between diet and genotype (p=0.0017). ***D****:* Proliferation expressed as the percentage of EdU^+ cells and their position within the crypt (bottom, middle or top); p<0.0001 (KW). Values are means ± SEM. * indicates $p \leq 0.05$, ** indicates $p \leq 0.01$, *** indicates $p \leq 0.001$, and the absence of * indicates p-values >0.05

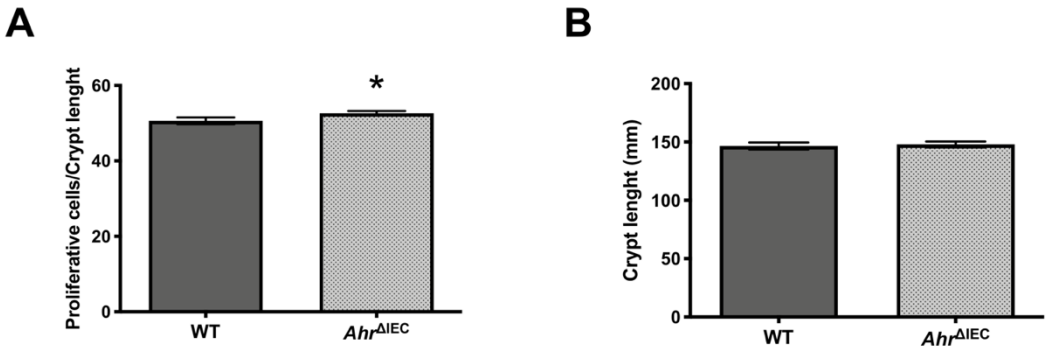

Figure 14. Effect of genotype in cell proliferation in intact crypts at the proximal section of the colon at the ACF formation stage.

A: Proliferative zone EdU^+ cells calculated as 100 times the position of the highest labeled cell divided by their corresponding crypt length in mm, *p=0.03 vs. $Ahr^{\Delta IEC}$. ***B:*** Crypt length in mm by genotype, WT mean 146 mm, and $Ahr^{\Delta IEC}$ mean 148 mm (p=0.2860 (MW). Values are means ± SEM. * indicates $p \leq 0.05$, ** indicates $p \leq 0.01$, *** indicates $p \leq 0.001$, and the absence of * indicates p-values >0.05.

Loss of Ahr in IEC significantly increases β-catenin intensity in the nuclei of colonocytes within ACFs. Representative images of β-catenin staining (in red), overlaid with DAPI (blue) to identify the cell nucleus and regions of interest (ROI, circled in yellow) on individual ACF are shown in **Figure 16A**. Nuclear localization of β-catenin was calculated as the ratio of β-catenin stain localized on the nucleus versus stain in the total cell. Nuclear localization of β-catenin significantly increased within ACFs of tissues lacking AhR compared to those with active AhR (p=0.0020) (**Figure 16B**). Overall, β-catenin is mainly localized in the cytosol of WT mice compared to $Ahr^{\Delta IEC}$ (data not shown).

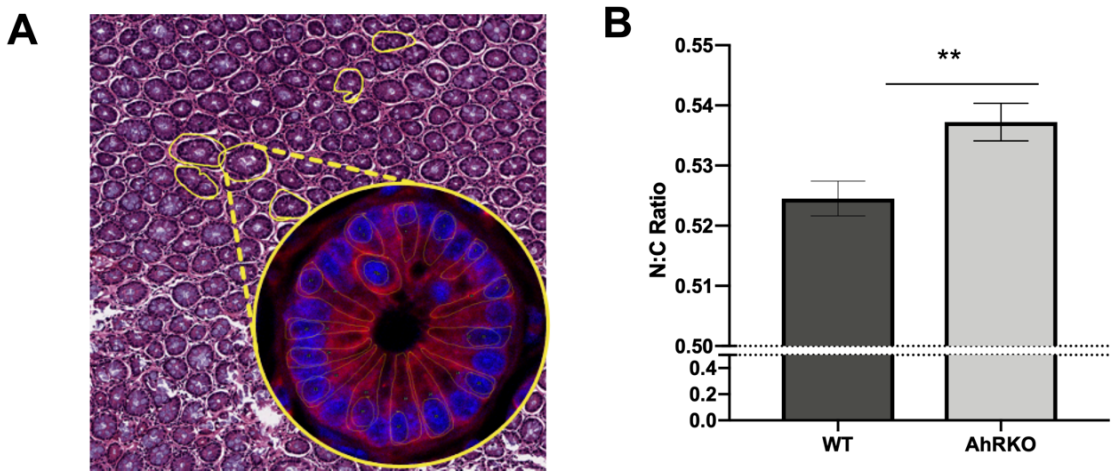

Figure 16. Assessment of β-catenin nuclear localization within ACFs

A*:* Representative image of ACF (circled in yellow) identified in distal colon tissues (H&E stained) at 20X magnification. (Right lower corner circle) Magnified image (40X) of β-catenin (red) translocated into the nucleus (blue). Both cytoplasm and nucleus are circled in yellow**. *B:*** Effect of genotype on β-catenin nuclear localization within ACF; p=0.0020 (MW). β-catenin intensity in the whole cell (C), and nuclear (N) localization measurements were used to calculate the nuclear-to-cytosolic β-catenin ratio N/(C-N); n=25 ACF/tissue. Values are means ± SEM. * indicates $p \leq 0.05$, ** indicates $p \leq 0.01$, *** indicates $p \leq 0.001$, and the absence of * indicates p-values >0.05.

Loss of AhR in IECs reduced the number of tertiary lymphoid tissue. Under the assumption that secondary lymphoid tissue (SLO) development is completed in an adult mouse,[21,25,26] we next sought to determine whether loss of AhR in IECs may influence *de novo* formation of tertiary lymphoid tissue (TLT). Thus, after 15 weeks post-AOM treatment, additional assessment of the number of lymphoid tissues in the colon was performed from H&E-stained whole cross-sectional distal tissue mounts images (Aperio Scan scope), more details regarding the histological features of TLT will be presented in Chapter IV. **Figure 17A** shows that the total number of lymphoid tissues, including colon patches (CP), isolated lymphoid follicles (ILF), and TLT, was significantly reduced in the absence of AhR in IECs (p=0.0390). Furthermore, the exclusion of CP and ILF from the assessment resulted in a significant reduction of TLT number in the AhRKO group compared to WT (p=0.0410), as shown in **Figure 17B**. No differences between diets were observed.

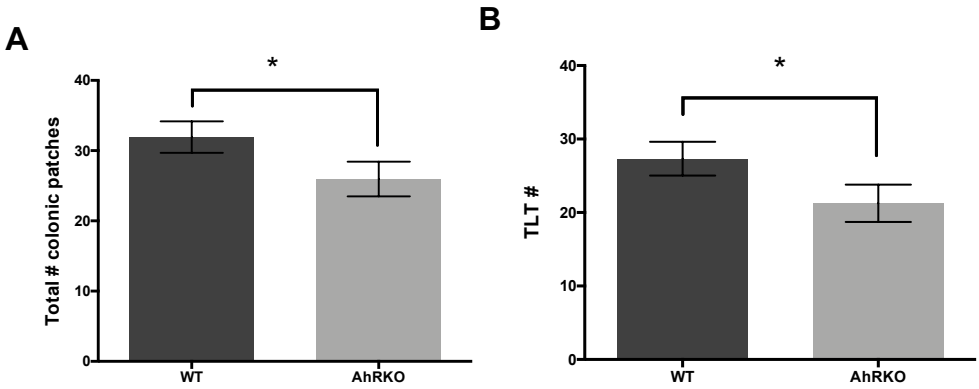

Figure 17. Secondary and Tertiary Lymphoid Tissues in the colon in the Ahr$^{\Delta IEC}$ mice

A. Number of total colonic patches in the distal colon (including ILF, CP and TLTs); WT (n=30, mean=32), AhRKO (n=27, mean 25); bars, SEM. *Statistical significance (p=0.0390) when compared with WT controls. ***B.*** Number of TLTs in the distal colon; WT (n=30, mean 27), KO (n=27, mean 21); bars, SEM. P=0.0410

Loss of AhR in intestinal epithelial cells had a significant effect on bacterial community structure, as indicated by the metagenomics analysis. 16S rRNA was sequenced and aligned as operational taxonomic units (OUT's). Linear discriminant analysis effect size (LefSe) of the OTUs revealed that the loss of AhR in intestinal epithelial cells resulted in significant changes (genotype effect, WT v. Ahr$^{\Delta IEC}$). Relative abundance was analyzed at the phylum level before carcinogen exposure (T1) and before termination (T2) and separated by genotype, sex, and diet (**Figure 9**). Before AOM exposure, male mice fed a HFD, *Firmicutes* increased from 35% in WT to 61% in Ahr$^{\Delta IEC}$ (26% increase), while *Bacteroidetes* decreased from 50% in WT to 19% in Ahr$^{\Delta IEC}$ (30% decrease); no significant differences in phyla were detected in females fed a HFD. Conversely, male mice fed a LFD had no significant differences in phyla, while in female mice (LFD), *Verrucomicrobia* decreased from 28% in WT to 0% in Ahr$^{\Delta IEC}$ (disappears), *Bacteroidetes* increased from 47% in WT to 57% in Ahr$^{\Delta IEC}$ (10% increase), and *Firmicutes* increased from 21% in WT to 31% in Ahr$^{\Delta IEC}$ (10% increase).

At termination (T2), in male mice that received a HFD, *Bacteroidetes* decreased from 54% in WT to 41% in Ahr$^{\Delta IEC}$ (13% decrease), and *Firmicutes* increased from 40% in WT to 52% in Ahr$^{\Delta IEC}$ (12% increase). *Verrucomicrobia* decreased from 4% in WT to 0% in Ahr$^{\Delta IEC}$ (disappeared) in females fed a HFD. In male mice fed a LFD, no significant differences were found. However, *Verrucomicrobia* decreased from 9% in WT to less than 1% in Ahr$^{\Delta IEC}$ (depleted). Overall, the only phylum where significant changes in relative abundance were observed in the absence of AhR in intestinal epithelial cells was

Verrucomicrobia, and this effect was observed in both HFD and LFD samples. A summary of these findings is included in **Table 2**.

Table 2 Genotype effects (WT to *Ahr*$^{\Delta IEC}$) on the microbiome composition before carcinogen exposure (T1) and before termination (T2).

Diet	**Pre-AOM (T1)**		**Termination (T2)**	
	Male	Female	Male	Female
High-fat diet	▪ Firmicutes ↑26% ▪ Bacteroidetes ↓30%	▪ NSD	▪ Firmicutes ↑12% ▪ Bacteroidetes ↓13%	▪ Verrucomicrobia ↓ from 4 to 0%
Low-fat diet	▪ NSD	▪ Verrucomicrobia ↓ to 0% ▪ Firmicutes ↑ 10% ▪ Bacteroidetes ↑10%	▪ NSD	▪ Verrucomicrobia ↓ from 9 to 0%

Loss of AhR upregulates the expression of pro-inflammatory genes at termination. Changes in the expression of genes involved in the production of pro- and anti-inflammatory cytokines and mucin were analyzed using qRT-PCR. Data are expressed as the fold change of their wildtype counterparts by genotype, sex, and diet (**Figure 18**).

The expression of *Tnf-α* significantly increased by 50 to 60% in both knockout males and females (respectively) fed a HFD, whereas no significant changes were detected in mice fed a LFD (**Figure 18A**). Likewise, expression of *Il-6* was significantly increased by 50% in female knockout mice fed LFD, and no changes were detected in other groups (**Figure 18B**). Interestingly, expression of *Il-22* was significantly downregulated (50%) in

knockout females fed a LFD (**Figure 18C**) while its expression was unchanged in the rest of the treatment groups. Lastly, expression of *Muc1* significantly increased by 60% in male knockout mice fed a HFD (**Figure 18D**), whereas *Muc2* expression was significantly downregulated (50%) in female mice fed a LFD and lacking AhR expression in IECs compared to their wildtype and low-fat fed counterparts (**Figure 18E**).

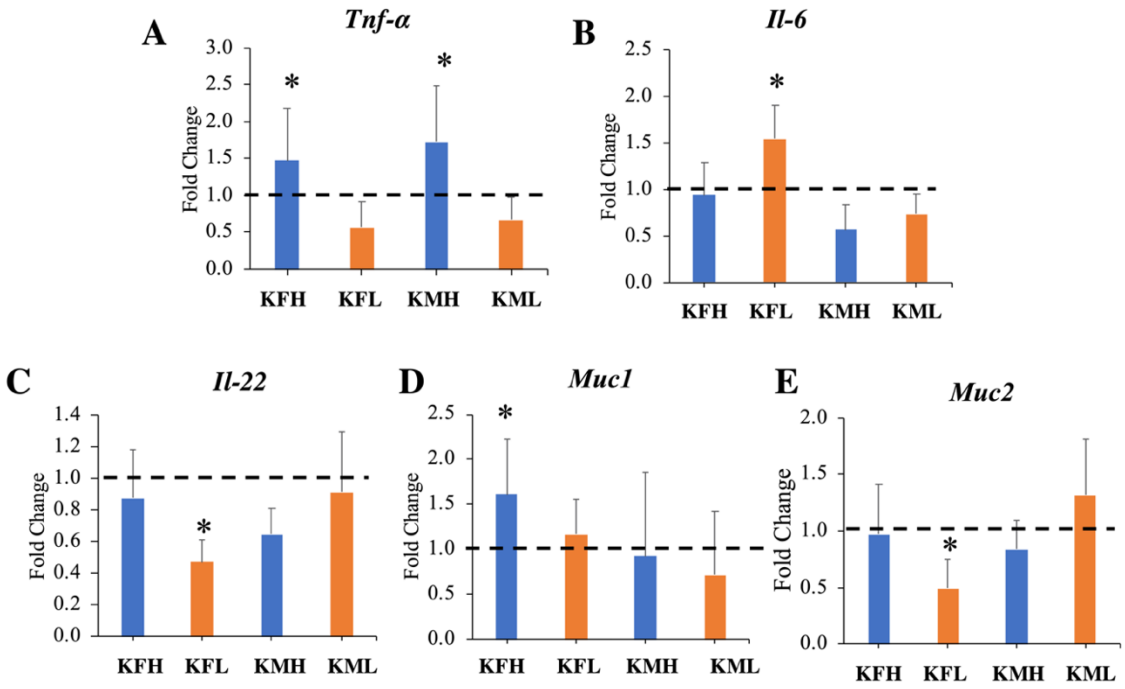

Figure 18. Gene expression data from colonic mucosal scrapings

A: *Tnf-α,* ***B:*** *Il-6,* ***C****: Il-22,* ***D:*** *Muc1 and* ***E:*** *Muc2.* Data are expressed as a fold change of the corresponding control group by genotype, diet and sex (WT is normalized as 1.0, indicated by a dashed line). Genotype (K=AhRKO, W=WT), diet (L=LFD, H=HFD) and sex (M=Male, F=Female). Values are means ± SEM. * indicates $p \leq 0.05$ when compared with their WT counterparts. Menon R. 2018 *Unpublished*

Discussion

AhR plays a significant role not only in regulating detoxification pathways but also in a myriad of cellular processes, such as cell cycle, immune surveillance, epithelial barrier function, cell proliferation, and tumorigenesis.[67,90,146] Moreover, activation of AhR by a varied group of endogenous and dietary ligands has been described to exert beneficial effects in the colon.[67] In recent years, an inverse association between expression of AhR and colon carcinogenesis has been reported using AhR-deficient mice (AhR null), which exhibited an increased rate of spontaneous colon-cecal tumors and increased colitis-associated colon tumor formation.[76,90–94,96] Since using a global AhR null model limits the ability to understand the significance of its expression within specific cell types, we utilized the IEC-specific, AhR knockout mouse model ($Ahr^{\Delta IEC}$) to further investigate the role of AhR in IEC-related biology. Although it has been recently described that intestinal epithelial cell-specific AhR deletion enhances inflammation-induced tumorigenesis,[77] no information is yet available identifying how consumption of saturated fat can affect the different stages of sporadic CRC formation in the context of AhR activity in colonocytes. Furthermore, provided that recent studies suggest that the interaction between the microbiota and the host is bi-directional,[147] and changes in the host can alter the microbiota, which in turn modulates host phenotypes; we also investigated how both the loss of AhR in IECs and the consumption of a HFD, in turn, affects the diversity of the gut microbiome.

By only employing AOM, instead of the widely used model of colitis-associated colon cancer (AOM/DSS) or the genetic background of CRC-prone mouse strains, we were able to isolate the differential contribution of the pro-inflammatory effect of the HFD and the loss of AhR, in the alterations on both the microbial communities and the expression of genes involved in the expression of pro-inflammatory genes and the initiation and promotion of CRC.

In this study, we demonstrate that loss of AhR in IECs, as well as the consumption of a HFD, can significantly increase the formation and multiplicity of premalignant colon cancer lesions. Furthermore, the loss of AhR in IECs resulted in a significant increase in cellular proliferation rates, specifically at the base and middle section of the colonic crypts. Since an increased rate of proliferative cells at the bottom of the crypt has been associated with the development of CRC,[54]our data suggest that loss of AhR activity in IECs can modulate the trajectory of cancer malignancy. Data collected from liver, small intestine, and cecum suggest that AhR can reduce cell proliferation in response to chemical carcinogens via reduced expression of *Myc*, increased β-catenin degradation, and G0-G1 cell cycle arrest.[29,93,122] Additionally, consumption of a diet rich in saturated fat significantly influenced proliferation rates in the colon. However, it is noteworthy that since a significant interaction between genotype and diet was found, both the fat content of the diet and the loss of AhR in IEC have a direct effect on proliferation rate, suggesting a possible increased risk of malignant transformation. As a driver of uncontrolled proliferation of colonocytes in the development of CRC, increased expression and

translocation of β–catenin from the cytosol to the nucleus is commonly used as a biomarker of increased cell proliferation and early colon tumor formation.[148,149] Paired with the significant increase in cell proliferation, loss of AhR in IECs significantly increased nuclear β-catenin levels in ACFs at the pretumor stage. These observations are crucial due to high levels of nuclear β-catenin levels are associated with higher mortality, in particular, CRC and other types of cancer, and numerous efforts have been made to identify inhibitors of β-catenin.[150–154]

Since an increase of colonic polyps, ACFs, and tumors after chemically-induced CRC have been reported in HFD-induced obesity studies,[46,101] an increased inflammatory response has been implicated as a driving mechanism of this phenotype.[45,53] However, it is interesting to note that consuming a diet high in saturated fats did not affect body weight throughout our study. While resistance to body weight gain despite high-fat feeding has been previously reported,[155] it has recently been shown that increased intestinal inflammation and loss of tumor suppression capacity can promote colon carcinogenesis in the presence of a high-fat diet without an increase in weight gain.[52–54,156,157] These results are consistent with our findings that HFD did significantly increase the number of ACFs and proliferation rates but did not affect the intensity nor localization of β-catenin.

A well-defined balance between immunosurveillance ($CD8^+$ T cells, NK cells, and $CD4^+$ T cells) and tumor-promoting inflammation (innate immune cells, B cells, and various subtypes of T cells) is required to maintain gut homeostasis and mediate the early detection and elimination of transformed cells and aberrant crypt foci and also keep small tumors at dormant state.[41] As previously indicated, most of the immune cells in the gut are

distributed through the lamina propria and lower layers of the large intestine and GALT. Adaptive immune responses in the gut are hosted in secondary and tertiary lymphoid tissues and play an essential role in responding to perturbations to the gut mucosa. Here, expression AhR by RORγt^{+}- ILCs and its activation with dietary ligands have been deemed necessary for the formation of secondary lymphoid tissues postnatally.[21] Contrary to the programmed secondary lymphoid tissue development during embryogenesis, tertiary lymphoid structures can be recapitulated in adulthood.[23] Consistent with these observations, our experiment distinctly shows that the constitutive loss of AhR in IECs resulted in significantly fewer TLTs without affecting the number of SLT after carcinogenic exposure. However, more research is needed to distinguish what factors influence the formation of TLTs and how they correlate with the development of premalignant lesions.

The interactions between the microbiota and the host have been identified as bi-directional, in which changes in the microbiota affect the host, and changes in the host can affect the microbial communities and the metabolites they produce. In our study, we analyzed the effect of the loss of AhR in IECs (host), consumption of a HFD, and the exposure to AOM in the microbial communities at the phylum levels and their effect on colonic inflammation. Marked differences between diet, genotype, the timing of carcinogen exposure, and sex were observed. Carcinogen exposure reduced alpha diversity of the intestinal microbiota from the *Ahr*$^{\Delta IEC}$ mouse as evidenced by the increased of relative abundance of *Firmicutes* and *Bacteroidetes* compared to WT (HFD, males) and a significant reduction (to almost 0%) in the relative abundance of the phylum

Verrucomicrobia (LFD, females). A similar pattern was observed at termination (post-AOM) with a more pronounced effect of the loss of AhR in IEC in the reduction of *Verrucomicrobia* in female mice fed a low/high-fat diet compared to their WT counterparts. *Akkermansia muciniphila* is the only currently cultured species of *Verrucomicrobia* known to colonize rodents and humans.[158] *A. muciniphilia* is a mucus-colonizing bacteria that has been proposed to be beneficial for intestinal barrier integrity and negatively-associated with IBDs and obesity by the modulation of genes involved in the differentiation of T cells and other immune responses.[159,160] The decrease in the relative abundance of this species in $Ahr^{\Delta IEC}$ mice suggests increased basal intestinal inflammation in these mice.

Loss of AhR in IECs significantly increased the expression of pro-inflammatory cytokines (*Tnf-α* and *Il-6)* relative to their WT counterparts. Since the expression of these genes was assessed from mucosal scraping samples, which not only include IECs but a variety of cells from the immune system and the lumen, it offers an integral view of the molecular signals from the IECs to its microenvironment in which both inflammation and increased *Muc 1* expression were observed. Moreover, overexpression of a *Muc1* variant has been linked to inflammation-driven tumorigenesis via activation of NF-κβ,[161] activates Lgr5 expression,[162] and represents a marker of poor prognosis of CRC.

Intestinal mucus contains primarily Mucin 2 (*Muc2*) proteins, which are large gel-forming proteins secreted by goblet cells located in the intestinal mucus. Since the reduction in the expression of *Muc2* is observed with the lack of AhR expression in IECs, it is not surprising that a significant reduction in mucus-degrading bacteria, such as

A. muciniphilia, was observed in our experiment as well.[163] Likewise, expression of *Il-22* was downregulated with the loss of AhR in IECs, especially in female mice fed a low-fat diet. Consistent with previously published data, activation of AhR with diet and microbial-derived ligands, have shown to attenuate the severity of DSS-induced colitis through the increased expression of IL-22.[87,99] In a similar manner, chronic HFD consumption not only increased the severity of experimental colitis in mice but significantly decreased expression of *Muc2*, however, both conditions were reversed with the administration of IL-22.[164] Additionally, HFD diet has been reported to not only promote a pro-carcinogenic gene signature but also to induce functional changes in the intestinal microbiota that could further exacerbate colon carcinogenesis via a reduction in AhR ligand availability.[138,165]

The findings of this study provide new insights into the ability of AhR in IECs to prevent the formation of AOM-induced ACFs through modulation of cell proliferation. Loss of AhR expression of AhR in IECs and high-fat content in the diet resulted in reduced formation of tertiary lymphoid tissues and changes in the microbial composition that correlate with inflammation in the gut mucosal epithelium. These data support recommendations that a diet high in saturated fat should be avoided to reduce CRC risk.[55,101] Hence, future studies will investigate the contribution of other relevant cell types in the IEC niche in the context of AhR activity, production of microbial-derived AhR ligands, and high-fat diet consumption.

CHAPTER IV

ARYL HYDROCARBON RECEPTOR ACTIVITY IN THE INTESTINAL EPITHELIAL CELLS AND THE FORMATION AND COMPOSITION OF COLONIC TERTIARY LYMPHOID TISSUES AFTER ACUTE INFLAMMATION

Introduction

In the large intestine, the development of secondary lymphoid tissues (cryptopatches and isolated lymphoid follicles) is AhR-dependent.[21] The process is initiated during the first weeks after birth as a response to environmental and commensal stimuli.[21] The secondary lymphoid tissues subsequently induce the activity of lymphoid tissue-inducing (LTi) cells and innate lymphoid cells (ILC) expressing the transcription factor RORγt^{+}.[21,22] Murine models employing the global loss of AhR expression and specific deletion of AhR in RORγt^{+}- ILCs revealed the requirement of AhR activity for the expansion and formation of secondary lymphoid structures.[21] It has been demonstrated that the development of lymphoid follicles can be altered by modifying the availability of natural AhR ligands at crucial stages. Specifically, mice fed a ligand-depleted diet displayed a phenotype similar to AhR-deficient mice with reduced formation of CP and ILFs at four weeks after birth; conversely, animals fed the same diet supplemented with indole-3-carbinol (I3C) recovered with respect to all parameters.[21] Contrary to the programmed development of secondary lymphoid tissues during embryogenesis, organogenesis of tertiary lymphoid tissues (TLTs) can be recapitulated in adulthood during a *de novo* lymphoid neogenesis (or lymphangiogenesis).[23]

Tertiary lymphoid tissues, also known as tertiary lymphoid structures (TLS) and ectopic lymphoid tissues (ELT) or organs (TLO), are organized congregations of immune tissue that form at sites of inflammation or infection at various areas of the body including the large intestine.[166] They appear to serve as local centers of immune responses against pathogens and tumors,[23–26] while they can also promote self-directed autoimmune diseases or organ transplant rejections.[22] Hence, the importance of TLT formation relies on their capability to sustain *in situ* adaptive immune responses.[23] Extending from the mucosa to the submucosa of the large intestine, TLTs display a high degree of compartmentalization that includes mainly T cells, followed by B cells, dendritic cells (DCs), and a network of $CD21^+$ follicular dendritic cells (FDC). Distinct from secondary lymphoid organs (SLOs), TLT does not possess a capsule and as such is not considered a true organ.[26]

The formation and establishment of TLTs can be divided into four sequential steps: the occurrence of an inflammatory event, the initiation signaling, the recruitment of stromal cell factors that secrete chemokines, and the organization and activation of TLT.[22] First, initiation is described as a pro-inflammatory state directed by immune cells drawn to the site of inflammation. Production of pro-inflammatory cytokines (IL-1β, IL-6, and TNF-α) and lymphotoxin by recruited cells can stimulate resident stromal cells to provide a framework for the developing TLTs and attract T and B cells.[25,166] Stromal cells then secrete chemoattractant molecules, such as chemokine 13 (CXCL13) and chemokine 19 (CXCL19), that further attract T and B cells signifying the recruitment phase.[22] The new formation is considered a TLT once FDCs and blood vessels have been organized locally. While the formation of TLTs has been classified into a series of different events, little is

known about the initial immune response leading to the signaling cascade necessary for their accumulation.

Preclinical and clinical evidence has provided crucial insight into the formation and function of TLTs in the colon. Preclinical models using DSS alone and DSS in combination with AOM to induce colonic inflammation and tumor development have reported a parallel increase in the size and number of TLT,[23] and a favorable prognosis has also been associated with the presence of well-organized and highly-vascularized TLT in CRC patients. [24,26,167–169] However, an increase of TLT formation has been observed in pathologies featuring a chronic inflammation component such as IBDs, or autoimmune diseases,[22,25] and have been associated with both the loss of immune tolerance and a prominent dysbiosis of commensal microflora.[22,24,170]Yet, the contribution of these lymphoid organs to the perpetuation or exacerbation of the inflammatory pathologies was, in the cases where it was tested, less evident. Although contradictory, these data have led the field to hypothesize that the expansion of the lymphoid tissue (*de novo* TLT formation) can both sustain the inflammatory response and its resolution, as well as participate in anti-tumor immune responses.[23] However, more research is needed to distinguish what factors influence the formation of TLTs.

Since dietary and microbial-derived ligands are capable of activating the AhR in different immune cell types, they are considered important regulators of gut mucosal immunity.[17,69] To further investigate the role of AhR activation and TLT formation within the context of acute inflammation, we used preliminary data collected from a previously conducted experiment aiming to analyze the effect of AhR agonists on DSS-induced

colitis. As shown in **Figure 19A**, acute inflammation (DMSO vs. DSS) significantly increased the number of TLT compared to the control group, as reported by other studies using inflammation-associated models.[23] Among the ligands tested in this experiment, I3Ald significantly promoted the formation of TLTs compared with vehicle controls. (**Figure 19B**).

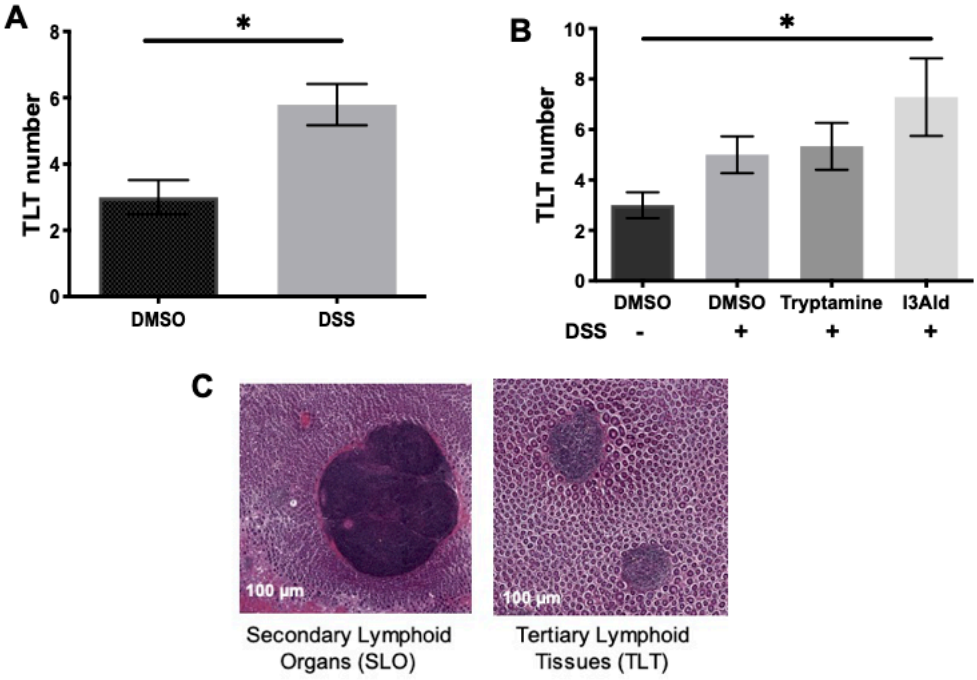

Figure 19. TLT formation in an acute inflammation model

Adult female C57BL/6 mice were gavaged with three doses (10 mg/kg) of known AhR ligands for five days (Tryptamine and I3Ald)[81] and exposed to 2.5% DSS for 5 days to induce a state of acute colitis. Mice were allowed to recover for 5 days after DSS treatment before termination. Whole colon mounts were sectioned, fixed and H&E stained to analyze TLT development. ***A.*** Total number of TLTs in whole colon mounts in control and 2.5% DSS-treated groups (p=0.0445), DMSO (n=8), DSS (n=34). ***B.*** TLT numbers by AhR-ligands treatment compared with control (P=0.0789); No DSS/DMSO (control group/no ligand, n=8), DSS/DMSO (DSS/no ligand), n=9; DSS/Tryptamine, n=9; DSS/ I3Ald, n=9 (p=0.009) ***C.*** Representative images of SLO and TLT in the colon (Scale=100 μm) *Denotes statistical significance. *Yoo J, DeLuca JAA, Unpublished.*

Another well-characterized AhR ligand with significant physiological effects in the intestine, known for attenuating colonic inflammation and tumorigenesis *in vivo*, is 3,3'-Diindolylmethane (DIM).[85,98] As a subproduct of the breakdown of I3C from the glucosinolates glucobrassicin contained in plants of the *Brassicaceae* family (e.g., broccoli and Brussel sprouts), DIM has been characterized as the most abundant bioactive compound resulting from cruciferous vegetable consumption and accounts for ~60% of I3C end products.[171]

Adjacent IECs form tight junctions (TJs) that are essential for the paracellular movement of various substances, including ions, solutes, and water across the intestinal epithelium, while also acting as a barrier against the gut microbiota and xenobiotics.[172] TJs result from the assembly of various proteins consisting of integral transmembrane proteins (including occludin and claudins) that form a network between adjacent cell membranes and peripheral membrane or plaque proteins (such as zonula occludens-1). When the gut epithelial barrier function becomes compromised, antigens from the lumen translocate to the mucosa and submucosa, where the local innate immune system starts an inflammatory cascade to combat a potential infection or respond to the damaged tissue and potentially form TLT.[173] In recent years, experimental evidence suggests that activation of AhR by a series of tryptophan-derived ligands is capable of improving intestinal barrier function.[173] Therefore, we investigated whether AhR activation in IECs was required for the maintenance of intestinal barrier function and the subsequent coordination with subepithelial mucosal cells (i.e. immune cells) during acute inflammation.

Since compounds from the diet greatly influence the function of IECs, nuclear receptors such as the AhR have been identified as a regulators of IEC structure and function,[95] modulator of the immune system,[174] and crucial for the development of gut-associated (secondary) lymphoid tissues.[21] Although the development of SLOs has been reported to be normal in $Ahr^{\Delta IEC}$,[21] it is still unknown whether the expression or activity of AhR in IECs is fundamental for the development of TLTs. As reported in Chapter 3, loss of AhR in the IECs significantly increased the number of ACFs coupled with a significant reduction of TLT number (**Figure 17B)** after exposure to AOM compared to their WT counterparts, suggesting that AhR activity in IECs can modulate the *de novo* formation of TLTs after a pro-carcinogenic stimulus. Additionally, gene expression patterns from mucosal colonic scrapings of the same experiment, exhibited a decrease in *Il-22,* and *Muc2 expression* in $Ahr^{\Delta IEC}$ as shown in **Figure 18C and E,** respectively**.** These proteins are critical regulators of IECs barrier function, such as secretion of mucus, recruitment of immune and stromal cells, and normal pro-/anti-inflammatory signaling;[3,175] this further suggests that loss of AhR activity is able to disrupt IEC homeostasis as well as their response to inflammation.

To understand the process in which loss of AhR in IECs might affect the formation of TLTs, we further analyzed the RNA sequencing data generated in Chapter 2. Several differentially expressed genes involved in the production of chemokines and cytokines that promote the formation of TLTs such as *Cxcl12, Ccl19, Ccl21, Il-22* were significantly downregulated in $Ahr^{\Delta IEC}$.[167,176] At the same time, *Ccr5, Ccr7, Tnfα, Il17a, Lta, Ltb,* and other adaptive immune cell-recruiting molecule*s* were upregulated with the loss of AhR

in IECs, suggesting that major inflammatory signaling required to assemble TLTs is still functional, but TLT formation is halted when AhR activity in IECs is lost. Furthermore, it has been suggested that IL-22 is required to regulate the expression of lymphoid chemokines such as CXCL13 by fibroblasts to aid the recruitment of locally activated B cells within TLTs after mucosal and epithelial damage.[176,177] Since IL-22 expression and chemokines involved in TLT formation were significantly downregulated in the absence of AhR in IECs, we hypothesized that the conditional loss of AhR activity in IECs would reduce the formation of and change the immune cell composition of *de novo* TLTs by reducing the production of lymphoid chemokines in a model of acute inflammation.

To ensure SLO formation was the same across all treatment groups in our study, mice were placed on a standard grain-based rodent diet containing natural AhR ligands until sexual maturity was reached before induction of TLT formation with DSS. To mimic pathologies that occur in adult life, such as IBDs, and assess the impact of AhR signaling on the development of TLT, we induced the IEC-specific knockout of AhR and experimental acute colitis at 11 and 14-weeks old mice, respectively. Furthermore, by controlling the availability of AhR ligands in the diet and the use of an inducible IEC-AhRKO (iAhRKO) we were able to control the timing of AhR activation on *de novo* TLT formation. To that end, this is the first study that has explored the contribution of AhR activation in IEC and the formation of TLTs in the presence of a dietary AhR ligand (DIM) after acute inflammation.

Materials and methods

Mouse model, experimental diets, and housing conditions. In this study, we employed an inducible, intestinal epithelial cell-specific AhR knockout mouse model (CDX2P^{CreT2} x AhR$^{f/f}$)[178] (iAhRKO) with AhR$^{f/f}$ littermates (WT) as controls[108] (**Figure 20**).

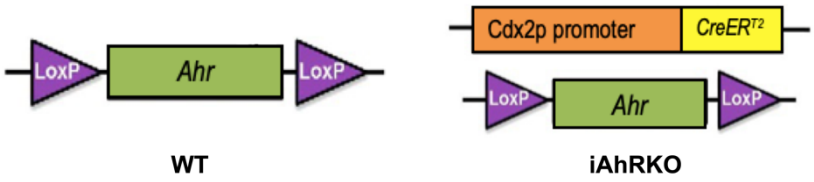

Figure 20. Mouse model used in chapter IV CDX2P^{CreT2} x AhR$^{f/f}$

As indicated in **Figure 21**, mice were enrolled after weaning (4 weeks of age, n=104) and fed a standard rodent diet (Teklad, 8604) for four weeks until sexual maturity (8 weeks) was reached. Both male and female mice were included. Mice were then divided into two experimental diets. The control diet was a semi-purified powder rodent diet containing 10% fat (Research Diets Inc., AIN-76A). The experimental diet consisted of the same control diet supplemented with 3, 3'-Diindolylmethane (DIM) at 20 mg/kg BW (D9568, Sigma-Aldrich). Specifically, DIM (63.75 mg DIM/kg Diet, %w/w) was mixed into the control diet by the investigator.[179] Mice received food and water *ad libitum*; food was replaced every 48 hours, and stored at -20 °C throughout the study. Mice were housed on a 12 hour/12-hour light-dark cycle at a maximum of five per cage. Body weight was assessed weekly. At the beginning of the fourth week, experimental diets were provided

and continued for three weeks before the induction of AhR knockout. At week 7, a subset of animals was terminated to establish a baseline number of TLTs while the rest received a daily intraperitoneal tamoxifen injection for four days. Before exposure to DSS, a waiting period of 15 days was given after tamoxifen injections to ensure effective AhR knockout by a complete crypt turnover.[180,181]

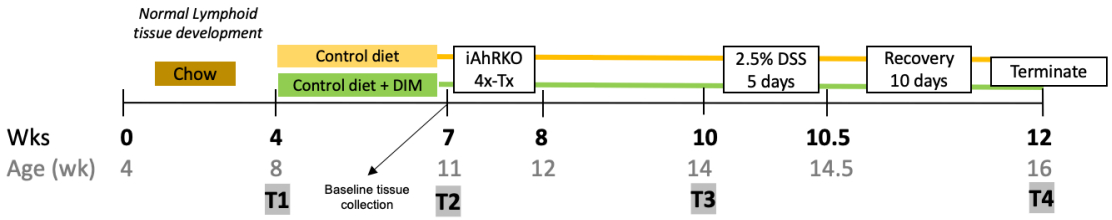

Figure 21. Study design

Induction of colitis. At week 10, dextran sodium sulfate (DSS, MW=36-50 kDa, 9011-18-1, MP Biomedicals) at 2.5% was dissolved in drinking water and provided *ad libitum* for 5 days to induce acute colitis.[182,183] DSS was replaced every 48 hours. Animal controls received normal drinking water. Body weight, fecal consistency, and macroscopic fecal blood scores were evaluated daily until the end of the study to assess the disease activity index (DAI), and the scoring system was adapted from previously published sources.[184,185] A scale was established as follows, body weight loss percentage was evaluated as 0 if weigh gain of 0-1% loss occurred, 1 if 1-5% loss, 3 if 10-15% loss, and 4 if 15% or more loss compared to baseline measurements at Day 0 (Baseline). Rectal bleeding (macroscopic fecal blood) was scored as 0 if a normal stool was present, 1 if the pellet was soft but formed, 2 if the pellet was very soft, 3 if diarrhea (no pellet) was observed, and 4

if dysenteric diarrhea (blood in diarrhea) was present. Lastly, rectal bleeding was scored as 0 if no bleeding was present, 2 if blood was visible in the stool (red/dark pellet), and 4 if there was gross macroscopic bleeding from the anus. All procedures were performed under a protocol approved by the Institutional Animal Care and Use Committee at Texas A&M University.

Fecal and tissue collection. Fecal samples were collected at four different time points, as indicated in Figure 3 (T1-T4). As previously stated in Chapter II, animals were single-housed for up to 2 hours, and feces collected were flash-frozen and stored at –80°C until analysis. At week 12 of the study, 8 hours before termination, food was withdrawn overnight, and a single oral dose of FITC-dextran was given four hours before termination (more details below). Mice were anesthetized by intraperitoneal injection of ketamine/xylazine (100 mg/kg body mass), and blood was collected by cardiac puncture. Plasma was collected and aliquoted after clotting for 45 min. Colon and cecum were resected from the abdominal cavity. Cecal contents were collected and frozen on liquid nitrogen. The entire colon was flushed with cold PBS, contents collected, and length and weight assessed. The colon was opened longitudinally with the mucosal side up along the mesenteric fat line. The distal colon was sectioned in two equal parts and carefully placed on a cassette (with sponge) without stretching the tissue and fixed in 10% neutral buffered formalin (HT501128; Sigma-Aldrich) for 3 hours. Tissues were rinsed in cold PBS three times and stored in 70% ethanol (room temperature) until processing and embedding. To study the differential expression of genes produced by IECs and the rest of the intesitnal wall, the proximal colon was divided into two equal parts. First, the mucosa was scrapped

from the first section, homogenized, and stored in RNA-lysis buffer at -80 ºC; while the second section was processed to extract RNA from isolated colonic crypts as previously described by Davidson L. *et al*.[110] Spleen and liver were removed from the abdominal cavity, weighed, and fixed in 10% neutral buffered formalin for 24 hours.

Intestinal permeability assessment. Intestinal permeability was measured with the fluorescent marker fluorescein isothiocyanate-dextran (FITC-Dextran) (4 kDa, Sigma, #FD4) dissolved in sterile PBS to a final concentration of 80 mg/dl. An oral gavage of 600 mg/kg BW of 80 mg/dl of FITC-dextran solution was gavaged to each mouse four hours before termination. In the dark, blood samples were left to clot for 45 minutes and centrifuged at 12,000 x g for 4 minutes. Serum FITC-dextran levels were determined in a Fluorometer with an excitation of 485 nm and an emission of 528 nm (20 nm bandwidth). Serially diluted FITC-dextran was used as standard (0, 125, 250, 500, 1000, 2000, 4000, 8000 ng/ml).

Histological assessment of Tertiary Lymphoid Tissues. Formalin-fixed distal colon mounts were processed, embedded, sectioned (4 μm), and H&E stained. Crypts were serially sectioned transversally, mucosal side up, to allow the visualization of lymphoid tissues. Slides were digitalized using an Aperio ScanScope at 20X magnification. Identification, quantification, and assessment of the area of tertiary lymphoid tissues (TLT) was performed on QuPath v. 0.1.2.[186] Raw data were collected and processed on Microsoft Excel® for Mac (v. 16.37). First, the entire surface area (measurable area, MA) of the distal colon per mouse was measured (μm^2) using the auto-detection (wand) tool on QuPath. TLTs in the colon mucosa were visualized in horizontal sections as dense and

defined aggregates (clusters) of lymphoid tissues lacking a capsule of connective tissue by morphometric analysis of the distal colon mounts.[23] After identification of TLTs, individual area measurements were recorded. For each histologic section, the total number of TLTs and the area (size) of individual TLTs were recorded. Mean values obtained in all identified regions were calculated and used for subsequent statistical analysis.

Immuno-histo-fluorescence staining of T and B cells. Separately, from DSS-treated animals, two formalin-fixed, paraffin-embedded, 4-μm serial sections of distal colon sections were deparaffinized, rehydrated, and after antigen retrieval in Citrate Buffer (10 mM, pH 6), sections were blocked for one hour at room temperature with 5% goat serum (ab7481, Abcam), and 5% donkey serum (S30-100mL, Millipore) for T-cell and B-cell staining, respectively. Sections were incubated overnight at 4 °C with Armenian hamster (IgG) anti-CD3ε monoclonal antibody (1:50 dilution; Cat. No. 14-0031-82, eBioscience) for T-cells, and rat anti-CD45R monoclonal antibody (1:100 dilution; Cat. No. 14-0452-82, eBioscience) for B-cells. After washing, sections were incubated with their respective secondary antibodies for one hour at room temperature. Goat anti-Armenian hamster (IgG) H&L - Alexa Fluor 647 (1:500 dilution, ab173004, Abcam) and donkey anti-Rat IgG – Alexa Fluor 647 (1:500 dilution, ab150155, Abcam) were used for T and B-cells staining, respectively. All washes (3x, 5 min each) between stages were performed in PBSt (PBS 1X with 0.02% Tween 20). Primary antibodies were omitted in negative control sections. Following the final washing steps, slides were cover slipped with ProLong Gold Antifade Mountant with DAPI (P36930, Invitrogen) and curated overnight until dry. A more detailed protocol can be found in **Appendix F**. Images of T

and B cell-stained tissues focused on the TLT area were acquired at 20X magnification in the all-in-one fluorescent microscope (Keyence BZ-X700) using the Cy5 channel ("red") to capture the Alexa Fluor 647 dye signal. The analysis of T and B cell density as well as the B to T cell ratio (B:T) was performed in ImageJ/Fiji (V. 2.1.0/1.53c) and is described in **Appendix F**.

Gene expression analysis. Samples from mucosal scrapings (MS) and isolated colonic crypts (ICC) were previously homogenized in RNA-lysis buffer and stored at -80 ºC. Total RNA was isolated using the Quick-RNA MiniPrep (R1054, Zymo Research) according to the manufacturer's instructions, including DNase treatment. RNA from ICC was eluted with 40 µl of RNase-free water and RNA from MS with 25 µl. RNA concentration was assessed using a Spectrophotometer (NanoDrop-2000; Thermo Scientific), and purity was confirmed using 260/280 and 260/230 ratios above 2 and 1.8 respectively. cDNA was then synthetized from 1000 ng of total RNA using the Transcriptor First Strand cDNA Synthesis Kit (04896866001; Roche) according to the manufacturer's instructions. Real-time quantitative PCR was performed using the LightCycler 480 SYBR Green I Master (04707516001; Roche) following manufacturer instructions in a Light Cycler 480. Each PCR was conducted in duplicates with 25 µL reaction volume. The sequences of the primers used are shown in **Table 3**. PCR denaturing was set at 94 °C for 5 min; annealing/extending was set at 59 °C for 1 min, for a total of 40 cycles. The expression of each gene was normalized to 18S expression in the individual samples. The threshold cycle (Ct) for each PCR product was calculated on Microsoft Excel® for Mac (v. 16.37), and Ct values obtained for each gene were normalized by subtracting the Ct values

obtained for 18S (housekeeping gene). The resulting ΔCt values were then used to calculate the relative change in mRNA expression as a ratio ($R = 2^{-(\Delta Ct(treatment)-\Delta Ct(control))}$).[187]

Table 3 Primers used in quantitative real-time PCR

Gene	Sense (Forward)	Antisense (Reverse)
Ahr	GCCCTTCCCGCAAGATGTTAT	GCTGACGCTGAGCCTAAGAAC
Zo-1	GATCCCTGTAAGTCACCCAGA	CTCCCTGCTTGCACTCCTATC
Clnd2	GAAAGGACGGCTCCGTTTTCTA	ACAGTGTCTCTGGCAAGCTG
Ocln	TTTTGTGGGATAAGGAACACA	ATAGTCACATGGGGGTGGAG
Muc2	CTGACCAAGAGCGAACACAA	CATGACTGGAAGCAACTGGA
Il-7	TCTGCTGCCTGTCACATCATCT	AAGTTTGGTTCATTATTCGGG
Lcn2	AAGGCAGCTTTACGATGTACAGC	CTTGCACATTGTAGCTGTGTACC
Il-22	ACATCGTCAACCGCACCTTT	CAGCCTTCTGACATTCTTCTGGAT
Il-6	CTGCAAGAGACTTCCATCCAGTT	AAGTAGGGAAGGCCGTGGTT
Cxcl-13	GGCCACGGTATTCTGGAAGC	GGGCGTAACTTGAATCCGATCTA
18S	TCAAGAACGAAAGTCGGAGGTT	GGACATCTAAGGGCATCACAG

Statistical analysis. All statistical analyses and figures were generated in GraphPad Prism version 8.1.2 for macOS, Graph Pad Software (La Jolla CA, www.graphpad.com). Means were compared using parametric or non-parametric methods according to compliance of normality (Shapiro-Wilk test). Outliers based on ROUT (Q=1.0%) were excluded. Parametric methods included an unpaired t-test for comparing two means or one-way ANOVA followed by Tukey's multiple comparisons test for comparing three or more

means. Two-way ANOVA was used to test interaction effects between variables. Non-parametric methods include the Mann-Whitney U (MW) test for comparing two means or the Kruskal-Wallis (KW) test followed by Dunn's multiple comparisons test for comparing three or more means. All values listed are group means, and error bars are presented as SEM. Differences among groups were considered statistically significant when the p-value was ≤ 0.05. Within figures, * indicates $p \leq 0.05$, ** indicates $p \leq 0.01$, *** indicates $p \leq 0.001$, and the absence of * indicates p-values >0.05.

Results

AhR expression was significantly downregulated in iAhRKO mice. *AhR* expression levels were evaluated from isolated colonic crypts and mucosal scraping using real-time quantitative PCR to validate the successful deletion of *AhR* expression in our iAhRKO model after tamoxifen injections. The expression of *AhR* was significantly reduced by 90% reduced (p=0.0430) in the iAhRKO compared to the WT group in isolated colonic crypts (Figure 22A) and 68% in mucosal scrapings (p=0.0071) (Figure 22B).

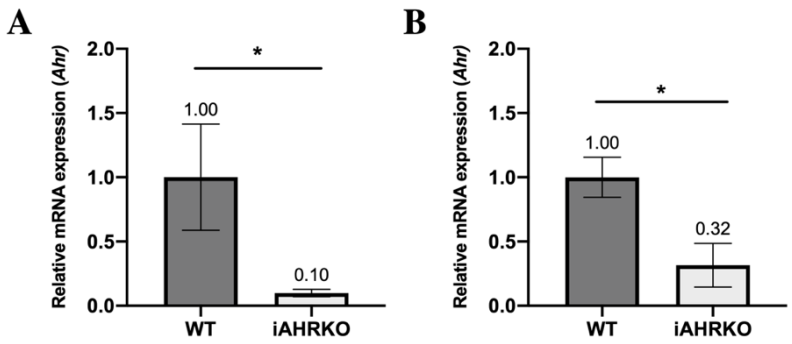

Figure 22. Effect of genotype in the expression of Ahr (Model verification)

A. Relative expression of *Ahr* in isolated colonic crypts (ICC) (p=0.0430) ***B.*** Relative expression of *Ahr* in mucosal scrapings (MS) (p=0.0071). n=3-4. Data presented indicate the mean ± SEM. *p < 0.05

DIM attenuated the severity of DSS-induced acute colitis. Administration of 2.5% dextran sulfate sodium (DSS) for five days induced acute colitis, as evidenced by diarrhea, visible (macroscopic) blood and colon shortening, as well as a decrease in body weight. Mice were terminated ten days after the fifth day of DSS exposure to allow recovery. DAI was measured from baseline (day 0) to termination (day 15). At the end of this experiment,

WT and iAhRKO animals fed a DIM-supplemented diet showed a significant ($p<0.05$) reduction in DAI compared to WT mice fed a semi-purified (control) diet as observed in **Figure 23A**. Moreover, in female mice, a downward trend towards the reduction of DAI was observed in iAhRKO as well as a significant reduction in their WT counterparts ($p<0.05$) compared to WT-males at the end of the study (Figure 23B).

The colons of mice treated with DSS were significantly ($p<0.001$) heavier than their control counterparts and a subsequent analysis revealed a significant interaction ($p=0.0496$) between the genotype, sex, and DSS in colon weight as indicated in **Figure 23C**. Colon shortening was evaluated as a physiological sign of DSS-induced colitis and a significant reduction in colon length was observed in the DSS-treated mice compared to vehicle controls ($p<0.0001$) (**Figure 23D**). Moreover, iAhRKO mice had significantly shorter colons that WT mice at a basal state (**Figure 23D**). No differences were detected between iAhRKO and WT in the presence of DSS (**Figure 23D**).

Treatment with DSS induced a significant increase ($p<0.0001$) in spleen weight compared with non-DSS treated animals (**Figure 23E**), and while a heavier spleen was reported in male mice ($p=0.0060$), neither the diet nor the genotypes had a significant effect on spleen weight. No significant interactions between genotype, sex, diet, or DSS were found in colon length nor spleen weight. Furthermore, a significant increase in mesenteric lymph nodes was observed in DSS-treated mice compared to vehicle-treated controls (**Appendix G**).

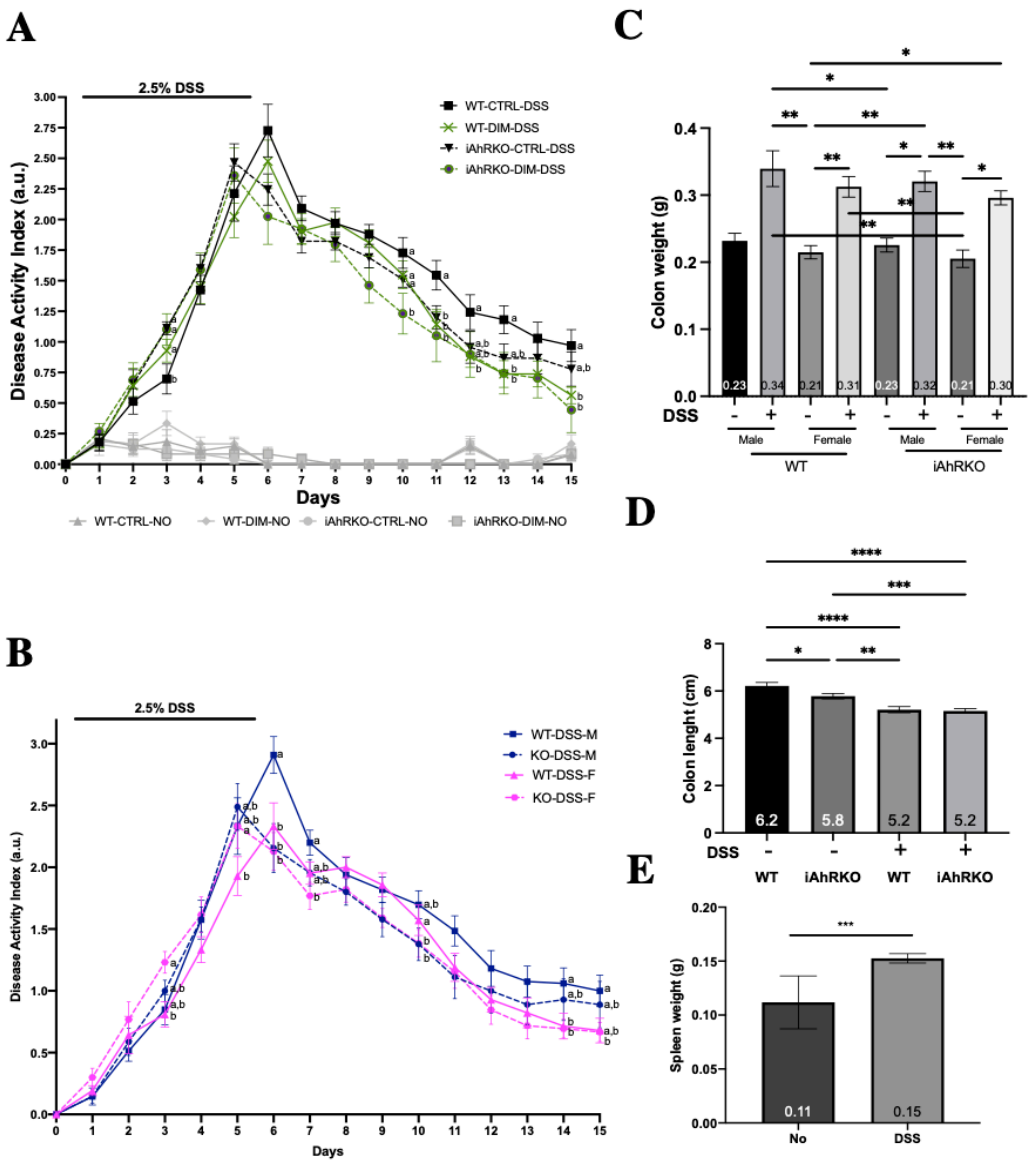

Figure 23. Effect of the loss of AhR in IEC on clinical signs of acute colitis

A. Disease Activity Index (DAI), a composite measure of weight loss, stool consistency and presence of blood in stool. ***B***. DAI (DSS treated animals only), divided by genotype and sex. Different letters denote statistically significant differences with a p value <0.05. (Unless indicated, no significant differences between groups were observed) ***C***. Effect of genotype, sex and DSS on colon weight (interaction, p=0.0496). ***D***. Changes in colon length between genotype and DSS. ***E.*** Effect of DSS on spleen weight. Data presented indicate the mean ± SEM. *p < 0.05, **p < 0.01 and ***p < 0.001.

Effect of loss of AhR in IEC and intestinal permeability. The assessment of gut permeability by oral administration of FITC-dextran showed that the diffusion of this compound through the gastrointestinal epithelium was significantly increased in mice that received DSS compared to vehicle controls ($p<0.0001$) (**Figure 24A**). Although the genotype (**Figure 24B**) or the presence of DIM in the diet (**Figure 24C**) did not have a significant effect on gut permeability, the overall serum concentration of FITC-dextran was significantly higher in female mice than males ($p=0.0060$) (**Figure 24D**). Consequently, a significant interaction ($p=0.0162$) between sex and DSS treatment was detected (**Figure 24E**). When analyzed separately, iAhRKO males that did not receive

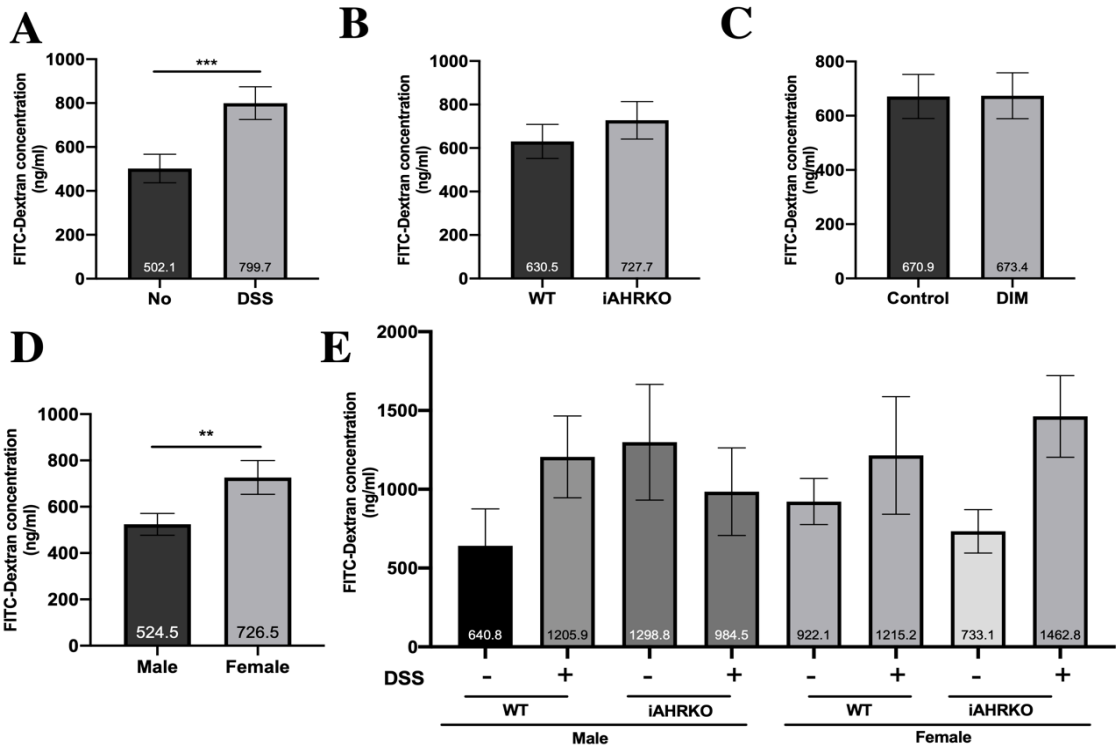

Figure 24. Serum concentration of FITC-dextran at termination

A. Effect of DSS treatment. ***B.*** Effect of the loss of Ahr in IEC ***C.*** Effect diet (DIM supplementation) compared to control diet ***D.*** Effect of sex. ***E.*** Effect of the loss of Ahr in IEC, diet, DSS and sex. Data presented indicate the mean ± SEM. *$p < 0.05$, **$p < 0.01$ and ***$p < 0.001$.

DSS tended to have higher levels of serum FITC-dextran (nsd), that their WT counterparts. However, this effect was not observed in females, in fact, the data trended toward an opposite effect.

The formation of TLT in the colon is a sex and AhR (IEC)-dependent process. While no significant changes in the number of *de novo* tertiary lymphoid tissue (TLT #/area) between genotype (iAhRKO vs. WT, **Figure 25A**) nor diet (DIM-supplemented diet vs. Control, **Figure 25B**) was detected, female mice had significantly more TLTs than males ($p=0.0287$) (**Figure 25C**). Likewise, a significant increase in the number of TLTs present in the colonic mucosa of DSS-treated animals was observed ($p<0.0001$) compared to vehicle controls (**Figure 25D**). Interestingly, a significant interaction between sex, genotype, and DSS-treatment was found ($p=0.0018$); and since DSS-dependent damage significantly promoted the formation of TLTs, the effect of genotype, sex and diet were analyzed in only DSS-treated animals from this point forward. As shown in **Figure 25E**, WT females had significantly more TLTs than their WT male counterparts ($p<0.0001$). However, when treated with DSS, iAhRKO males had significantly more TLTs ($p=0.01999$ than their WT counterparts, while iAhRKO female mice had significantly fewer TLTs than their female WT controls ($p=0.0161$, **Figure 25E**). Although the genotype did not significantly influence the formation of TLTs (**Figure 25F**), female mice had significantly more TLTs than males (**Figure 25G**). In DSS-treated animals, a 3-way ANOVA analysis ($p=0.0183$) revealed a significant interaction between sex and genotype ($p=0.0021$) and between sex and the diet ($p=0.0633$). As illustrated in **Figure 25H**, in females, formation of TLTs was not affected by the presence of DIM on the diet of WT

nor iAhRKO groups when analyzed separately (WC vs WD, KC vs. KD). Representative images of TLT assessment can be seen in **Figure 25I.** However, in males, DIM trended to reduce the formation of TLTs in both WT and iAhRKO mice when compared to their corresponding control diet-fed counterparts (WC vs WD, KC vs. KD). However, when the significant interaction between sex and genotype and diet was considered, the formation of TLT significantly increased in WT females fed a DIM-supplemented diet compared to WT males. Likewise, WT males fed DIM had significantly fewer TLTs that their iAhRKO counterparts fed a control diet, while females lacking AhR (IEC) expression fed a control diet (KC) had significantly fewer TLTs than WT females fed DIM.

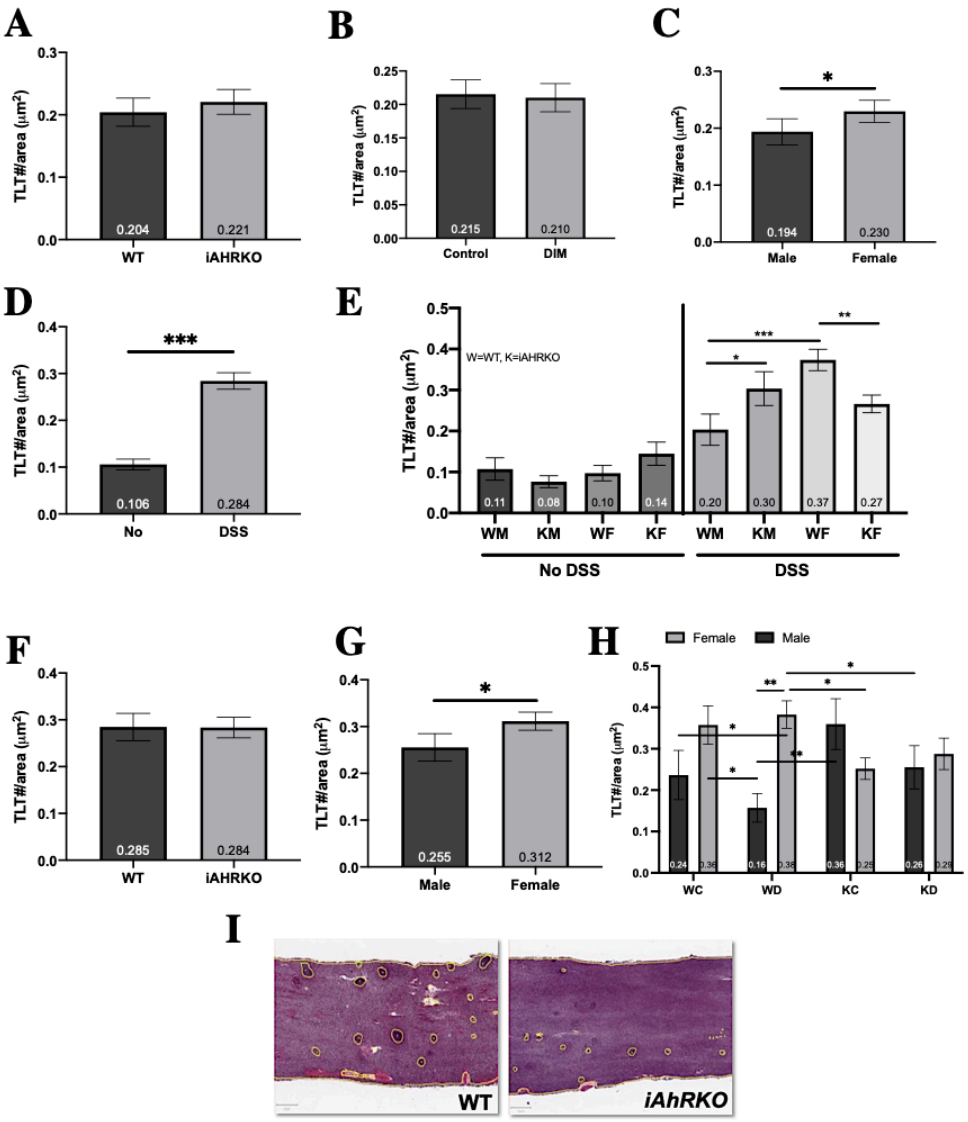

Figure 25. Number of Tertiary Lymphoid tissues (TLT/measurable area (µm^2)

A. Effect of the loss of Ahr in IEC on the number of TLT. ***B***. Effect of diet (DIM supplementation) compared to control diet. ***C***. Effect of sex ***D***. Effect of DSS. Since DSS-dependent damage significantly promoted the formation of TLT, the effect of genotype, sex and diet were analyzed in only DSS-treated groups from here. ***E***. Effect of DSS, genotype and sex. ***F***. Effect of the loss of Ahr in IEC in mice treated with DSS. ***G***. Effect of sex in mice treated with DSS. ***H***. Effect of genotype, diet and sex in mice treated with DSS. ***I.*** Representative TLT images from H&E staining (scale=1 mm). Data presented indicate the mean ± SEM. # $p < 0.075$ *$p < 0.05$, **$p < 0.01$ and ***$p < 0.001$. W=WT, K=iAhRKO, C=control diet, D=DIM-supplemented diet.

Regarding the size of TLTs (average area of TLT, μm^2), no significant changes were observed between genotype (iAhRKO vs. WT, Figure 26A), diet (DIM-supplemented diet vs. Control, **Figure 26B**), and sex (male vs. female, Figure 26C) when analyzed separately. However, since significantly larger TLTs ($p>0.0001$) were reported in mice that received DSS compared to vehicle controls (**Figure 26D**), a significant interaction between the genotype and sex was found ($p=0.0435$) in animals treated with DSS. Loss of AhR in IECs led to significantly smaller TLTs ($p=0.0187$) in males compared to their WT counterparts, while iAhRKO females significantly larger TLTs ($p=0.0236$) compared to iAhRKO males (**Figure 26E**). Moreover, in WT mice, DIM

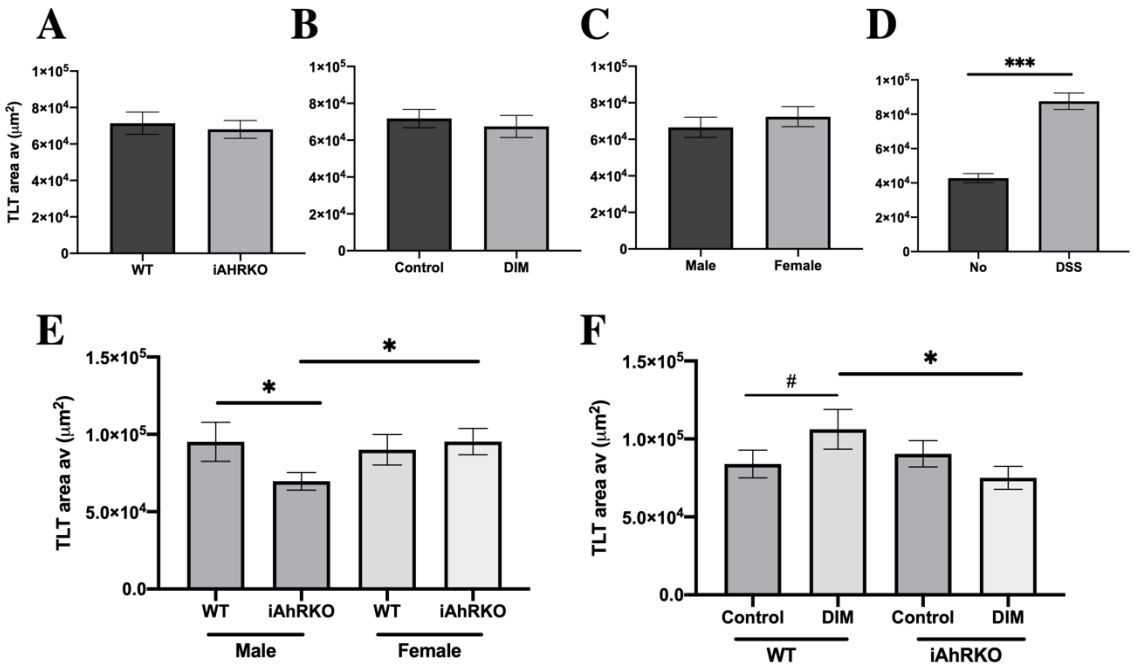

Figure 26. Size of Tertiary Lymphoid tissues (average area of TLT (μm^2)

A. Effect of the loss of Ahr in IEC on the size of TLT. ***B.*** Effect of diet (DIM supplementation) compared to control diet. ***C.*** Effect of sex ***D.*** Effect of DSS. ***E.*** Effect of genotype and sex in mice treated with DSS. ***F.*** Effect of genotype and diet (DIM vs. control) in mice treated with DSS. Data presented indicate the mean ± SEM. # $p < 0.075$ *$p < 0.05$, **$p < 0.01$ and ***$p < 0.001$.

increased the size of TLTs (p=0.0767) compared to the control diet, while in iAhRKO mice, the size of TLTs was not affected by DIM (**Figure 26F**).

AhR activity in IEC affects T-cell aggregation in primary TLT. Since loss of AhR activity in IECs reduced the formation of TLTs in female mice while increasing their formation in males, we analyzed the density of B- and T-cells as well as the ratio of B- to T-cells in *de novo (*primary) tertiary lymphoid tissues. As illustrated in **Appendix H**, following DSS exposure, B-cells were predominantly located inside the newly formed TLTs, while T-cells were found both within TLTs and in their periphery. Except for iAhRKO males and females, where T-cells tend to be located within the TLT (nsd), T-cells were mainly distributed within the TLT and at 1.5 and 2.0 times the area with respect to the TLT regardless of genotype and sex (**Figure 27A**). Due to this observation, we focused our analysis of T-cell density within TLTs. As shown in **Figure 27B**, T-cell density is significantly higher (2.8-fold) in iAhRKO animals than their WT counterparts (p=0.0011). Further analysis revealed a significant interaction between genotype and sex (p=0.0235) and between genotype and diet (p=0.0112). In males, loss of AhR significantly increased T-cell density (p=0.0047) compared to WT-male and female controls, while an increase in T-cell density was observed in iAhRKO-females (nsd) (**Figure 27C**). As illustrated in **Figure 27D,** the DIM-supplemented diet significantly reduced the T-cell density compared to control-fed WT mice (p=0.0397) and iAhRKO animals. DIM had no effect on T-cell density in the absence of AhR in IEC. Later, analysis of B-cell density within TLT, revealed no significant differences between genotype, diet, nor sex (**Figure 27E-F).** Although individual analysis of B- and T-cell density provides a general

perspective of the immune composition of TLT in the context of acute colitis, an assessment of the distribution of B-cells in relation to T-cells (B:T ratio) within TLTs grants a better understanding of the function of this *de novo* structures, since increased B-cell accumulation in TLTs has been associated with immune exclusion, anti-inflammatory responses and antigen clearance.[188] Here, loss of AhR in IEC significantly reduced B:T ratio (-63%, p=0.0054) compared to WT controls (**Figure 27G).** Moreover, after a significant interaction between genotype and sex was identified (p=0.0395), iAhRKO-males presented a significantly reduced B:T ratio than WT-males (-64%, p=0.0166) (**Figure 27H)**. In females, loss of AhR induced a reduction of the B:T ratio by 43% (nsd) compared to WT-female controls (**Figure 27H)**.

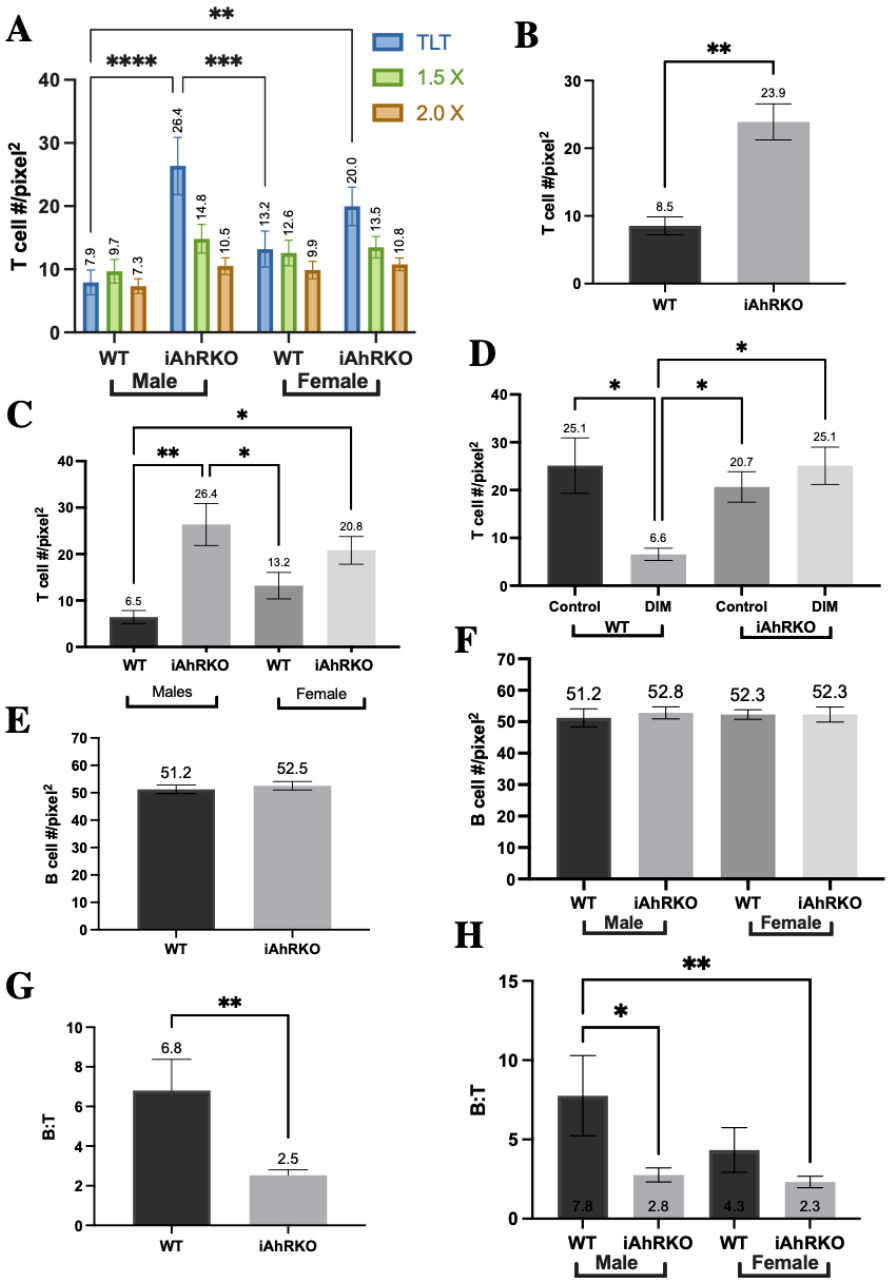

Figure 27. Effect of genotype, sex, and diet in immune cell density within TLT in DSS-treated animals.

A. T cell density distribution at 1.5X and 2.0X the area with respect to TLT by genotype and sex. ***B.*** Effect of genotype in T cell density within TLT (p=0.0011) ***C.*** Effect of genotype and sex in T cell density within TLT (Genotype*Sex, ANOVA (KW) p=0.0235) ***D.*** Effect of genotype and diet in T cell density within TLT (Genotype*Diet, ANOVA (KW) p=0.0112) ***E.*** B cell density within TLT by genotype ***F.*** Effect of genotype and sex in B cell density within TLT. ***G.*** B:T (B cell density/T cell density) within TLT by genotype (p=0.0054) ***H.*** B:T within TLT by genotype and sex (Gen*Sex, ANOVA p=0.0395). Data presented indicate the mean density (Cell #/pixel^2) ± SEM; *p < 0.05, **p < 0.01 and ***p < 0.001.

To begin to assess the differential contribution of IECs from other cell types present in the colonic mucosa, we analyzed RNA from isolated colonic crypts (ICC) before assessing the expression of genes required for the formation of TLTs from colonic mucosal scrapings (MS). For ICC samples, we analyzed the expression levels of *Lcn2, Il-7, Zo-1, Cldn2, Ocln,* and *Muc2* due to their role in the maintenance of intestinal barrier function and the coordination of the host' response to inflammation with subepithelial mucosal cells (immune and stromal cells) present in MS. Moreover, RNA from MS was used to evaluate the expression levels of *Il-22, Il-6, and Cxcl13,* required for the formation of TLTs.

Selected gene expression profiles in isolated colonic crypts (IEC)

Since the expression levels of barrier function-related genes are usually affected by DSS-induced epithelial damage, we analyzed non-DSS and DSS treated animals separately. First, **Figure 28** displays the effect of the genotype and DSS on the relative expression of our genes of interest separated by sex. Next, **in figure 29** we analyze the changes in gene expression relative to the WT/Control-fed/No-DSS group to compare the effect of the genotype, the diet and DSS separated by sex.

DSS upregulated the expression of Lcn2 independently of genotype or sex. Produced by IECs, expression of lipocalin 2 *(Lcn2),* also called neutrophil gelatinase B-associated lipocalin, was assessed as an additional biomarker of inflammation in our study. In both male and female, treatment with DSS increased the expression of *Lcn-2* by more than 17-

fold compared to vehicle controls independently of the genotype (**Figure 28A**) or the diet (**Figure 29A**). In iAhRKO females, DIM significantly reduced the expression of *Lcn2* regardless of the exposure to DSS compared with the control-fed group as indicated in Figure 29A.

Diet and sex affected the expression of Il-7 at the basal state. Expressed by IECs undergoing damage or inflammation, interleukin 7 (*Il-7)* stimulates the differentiation of ILC3s and the secretion of IL- 22 and, consequently, promotes epithelial regeneration.[189] As shown in Figure 28B, iAhRKO males had a significantly (p=0.0022) lower expression of *Il-7* (-60%) at a basal state compared to their WT counterparts; however, no genotypical differences were observed in DSS-treated animals. In females, no significant differences in *Il-7* expression were observed between the genotype or exposure to DSS (**Figure 28B**). As presented in **Figure 29B**, DSS did not significantly affect the expression levels of *Il-7* regardless of diet, genotype, or sex compared to vehicle controls. Moreover, when the effect of the diet was further analyzed (**Figure 29B**) at the basal state, DIM trended to increase the expression of *Il-7* in WT males compared to their control-fed counterparts (interaction between diet, genotype and DSS, p=0.0197). No significant effects were observed in females when comparing experimental diets and treatments in both genotypes.

Expression of Zo-1 was downregulated in the absence of AhR in males. As a TJ protein bound directly to actin fibers in IECs, zonula occludens (*Zo-1*) regulates the paracellular influx of large molecules to the submucosa.[190] In males, *Zo-1* expression was significantly reduced by 60% in the absence of AhR in IECs (p=0.0182) at a basal state compared to WT (**Figure 28C**); when exposed to DSS, both WT and iAhRKO mice displayed a 50%

and 40% reduction of *Zo-1* expression (nsd) compared to vehicle controls, respectively (**Figure 28C).** Contrastingly, no significant differences were observed in the expression of *Zo-1* between WT and iAhRKO mice or with the presence or absence of DSS in female mice (Figure 28C). As presented in **Figure 29C**, in WT males, consumption of a DIM-supplemented diet resulted in a trend towards upregulation of *Zo-1* at the basal state (nsd); however, the effect was lost in the iAhRKO animals regardless of the diet or exposure to DSS. Conversely, expression of *Zo-1* showed a downward trend (nsd) in WT female mice fed the DIM-supplemented diet compared with control-fed WT females (**Figure 29C**). Unexpectedly, expression of *Zo-1* was significantly upregulated (p=0.0393) in iAhRKO female mice that received DSS compared to non-DSS in females (**Figure 29C**).

Clnd2 expression was dependent on sex and AhR activation. Commonly overexpressed in the TJs of leaky epithelia, claudin-2 (*Clnd2)* expression is commonly inversely proportional to the epithelium's damage.[190] In males, although not significant, both DSS and the loss of AhR resulted in a 30-40% reduced expression of *Clnd2* compared to their WT non-DSS treated counterparts (**Figure 28D**). Inversely, in females, loss of AhR led to a clear trend towards the upregulation of *Cldn2* (50-100%, nsd) with or without DSS (**Figure 28D**). As detailed in **Figure 29D**, *Cldn2* expression was not affected by the diet on neither male nor females. Although non-significant, the expression of *Cldn2* increased in DSS-treated iAhRKO female mice fed a control diet compared to their non-DSS treated counterparts.

Expression of Ocln decreased after DSS-induced colitis. Occludin (*Ocln)* is a plasma-membrane protein localized at the TJs of IECs that contributes to their stabilization and

optimal barrier function. In WT males (**Figure 28E**), expression of *Ocln* was not affected by DSS. However, a 60-99% reduction (nsd) of *Ocln* was detected in iAhRKO mice independently of DSS exposure compared to the WT/vehicle controls (**Figure 28E**). Although not significant, **Figure 28E** shows a clear trend in the effect of DSS in the downregulation of *Ocln* expression in both WT and iAhRKO female mice. From figure 29E we can note that in females, DIM consumption increased the expression of *Ocln* (nsd) by more than a 150% in non-DSS animals regardless of the genotype, while this effect was not observed in males.

Muc2 expression was downregulated by the loss of AhR activity in IECs and DSS in males. Mucin 2 (*Muc2)* encodes a member of the mucin protein family (mucin 2) that is secreted towards the lumen and covers and protects the intestinal epithelium. As presented in Figure 28F, the expression of *Muc2* by IECs was downregulated in the presence of DSS in WT male mice by 30% (nsd), 40% by the loss of AhR in IECs (p=0.0481), and 40% by loss of AhR plus treatment with DSS (p=0.0589). In females (**Figure 28F**), a significant increase of *Muc2* expression was found between non-DSS/iAhRKO (+100%, p=0.0152) and DSS/iAhRKO (+220%, p=0.0249) compared to WT vehicle controls. We can observe in **Figure 29F** that WT males fed with DIM had an increase (+90%) in *Muc2* expression at a basal state compared to mice fed a control diet, while exposure to DSS tended towards *Muc2* downregulation regardless of the diet. Furthermore, expression levels of *Muc2* were not affected by the genotype, nor exposure to DSS in females (**Figure 29F**).

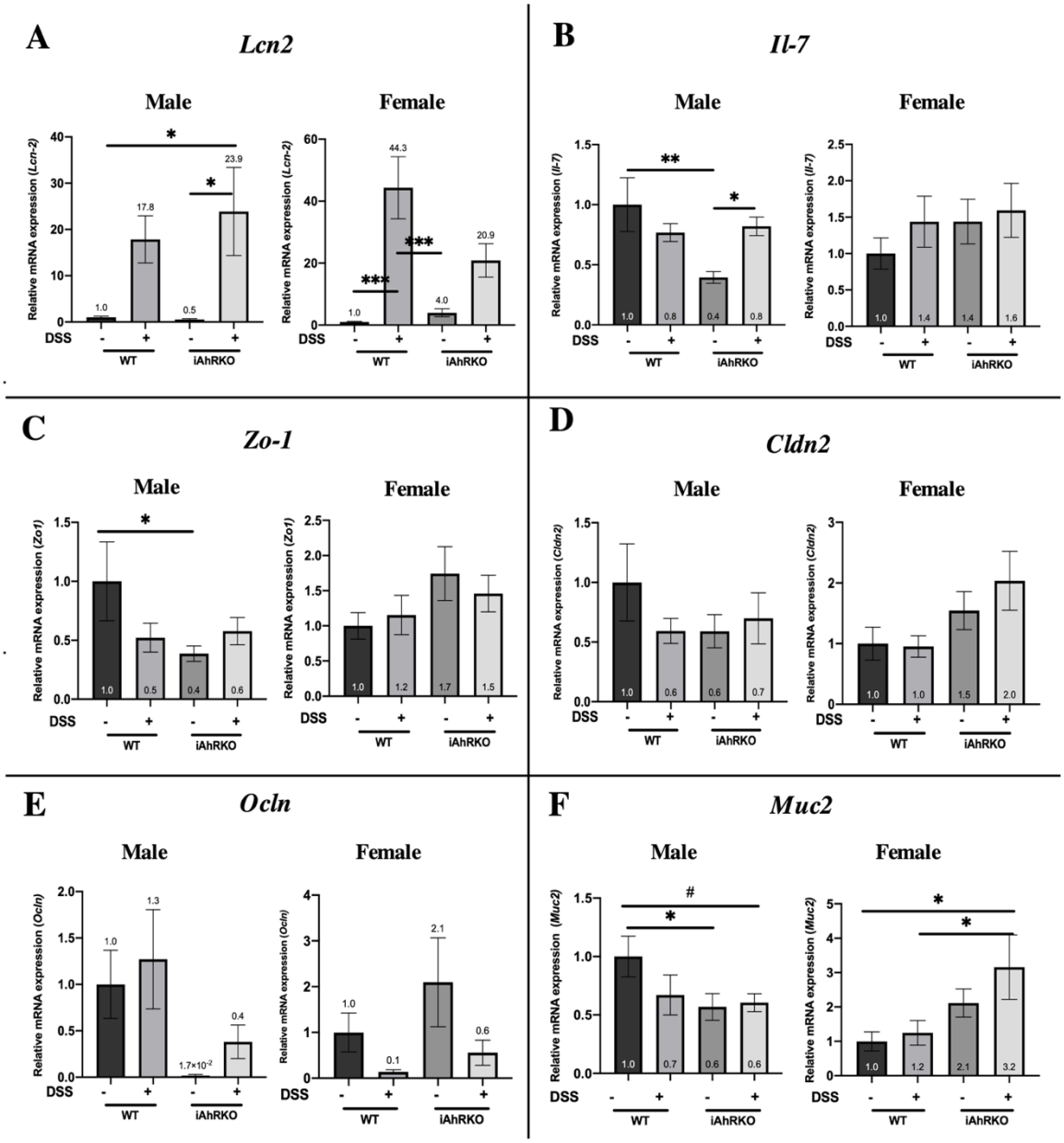

Figure 28. Effect of genotype, DSS and sex in the expression of IEC-derived genes from ICC

A. Relative expression of *Lcn2* (Lipocalin-2). Male (0.0277, one-way ANOVA) and female (p=0.0001, one-way ANOVA). ***B.*** Relative expression of *Il-7* (IL-7). Male (p=0.0071, KW) and female (p=0.6000, one-way ANOVA). ***C.*** Relative expression of *Zo-1* (ZO-1/Tjp1). Male (p=0.1210, KW) and female (p=0.2910, one-way ANOVA). ***D.*** Relative expression of *Cldn2* (Claudin-2). Male (p=0.4943, one-way ANOVA) and female (p=0.0861, one-way ANOVA). ***E.*** Relative expression of *Ocln* (Occludin). Male (p=0.1950, KW) and female (p=0.3108, KW). ***F.*** Relative expression of *Muc2* (Muc2). Male (p=0.1650, one-way ANOVA) and female (p=0.0564, one-way ANOVA). n=7-8, $p < 0.075$ *$p < 0.05$, **$p < 0.01$ and ***$p < 0.001$, p value between 0.5 and 1 is expressed as #.

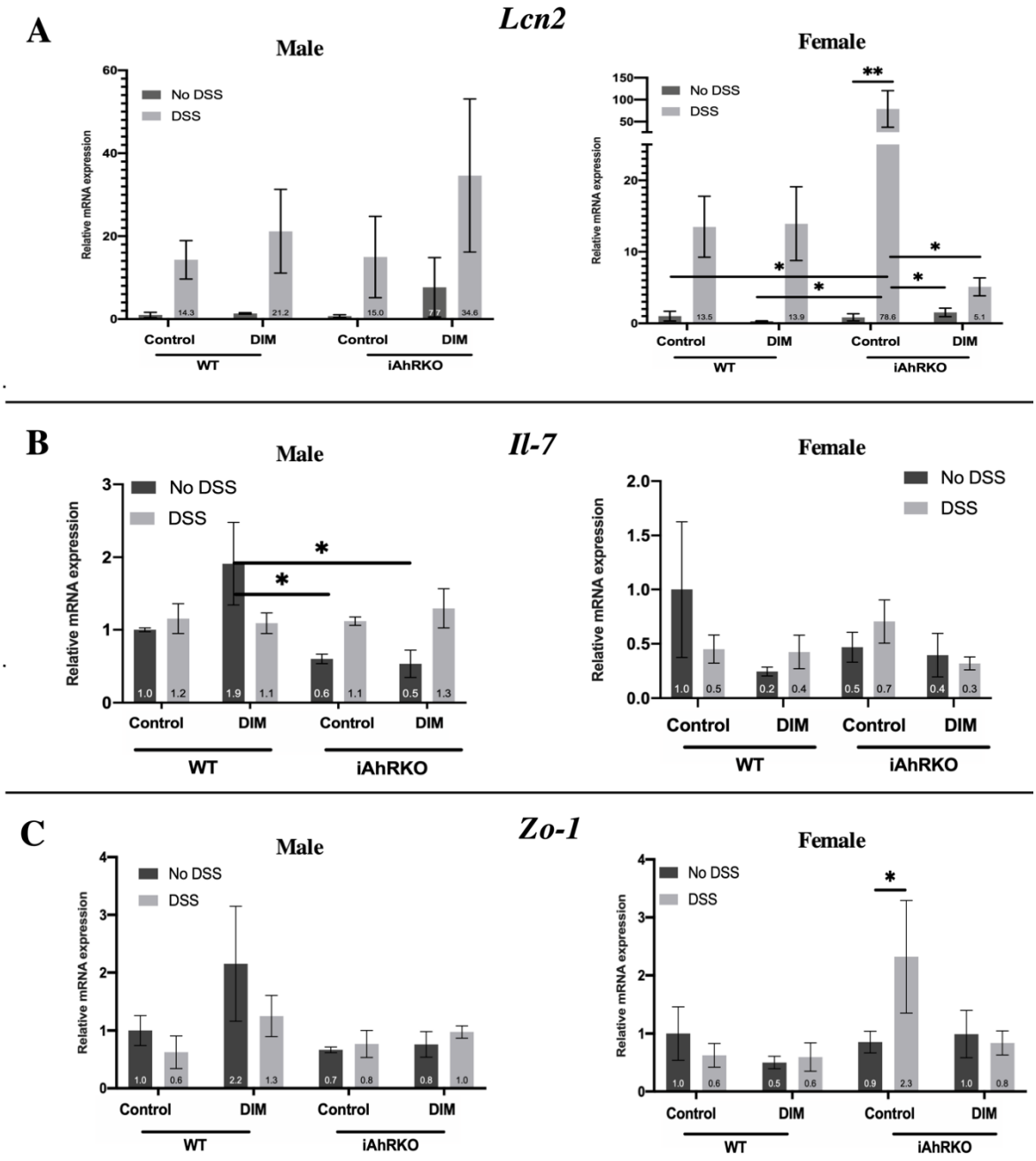

Figure 29. Effect of diet, genotype, DSS, and sex in the expression of IEC-derived genes from isolated colonic crypts (ICC).

A. Relative expression of *Lcn2* (Lipocalin-2), 2-way ANOVA; male (DSS effect, p=0.0215) and female (DSS effect, p=0.0224). ***B.*** Relative expression of *Il-7* (IL-7), 2-way ANOVA; male (Interaction between diet/genotype and DSS, p=0.0197) ***C.*** Relative expression of *Zo-1* (ZO-1/Tjp1) ***D.*** Relative expression of *Cldn2* (Claudin-2) ***E.*** Relative expression of *Ocln* (Occludin) ***F.*** Relative expression of *Muc2* (Muc2). n=3-4, $p < 0.075$ *$p < 0.05$, **$p < 0.01$ and ***$p < 0.001$, p value between 0.5 and 1 is expressed as #.

Figure 29 Continued

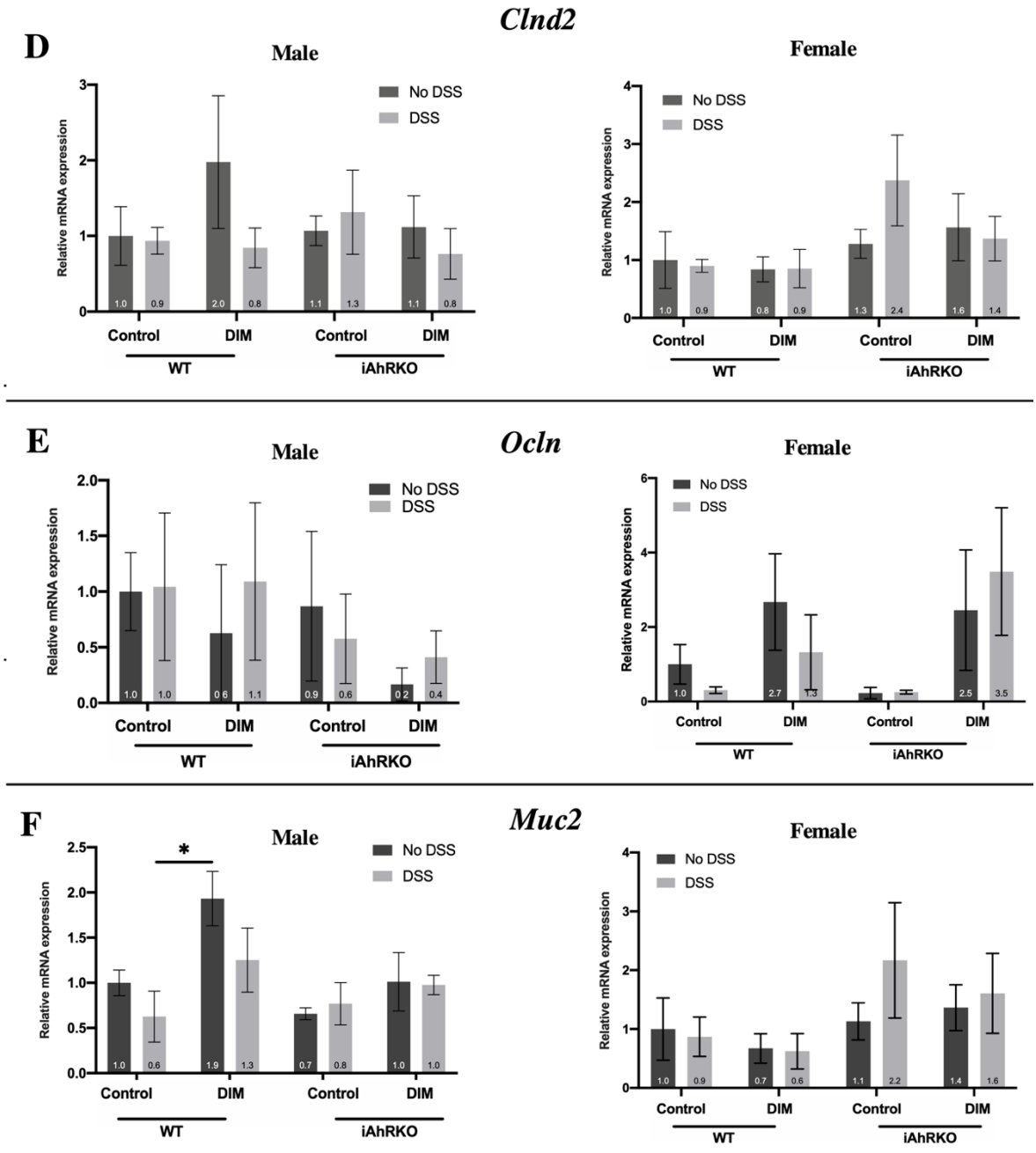

Selected gene expression profile from colonic mucosal scrapings (MS)

To reflect the importance of an inflammatory stimulus for the formation of TLTs, gene expression data from DSS and non-DSS groups were analyzed separately. Here, the relative expression of the selected genes from MS was separated by sex and is presented in **Figure 30**.

Expression of Il-22 was dependent on DSS exposure, sex, and AhR activity. As an important signaling molecule that promotes the integrity of the GI epithelial barrier during inflammation,[11,12] minimal to undetectable levels of interleukin 22 (*Il-22)* were observed in males at basal state; however, in females fed a control diet, a trend towards a 50% reduction of *Il-22* was observed in iAhRKO compared to WT. Likewise, DIM supplementation was not able to increase the expression of *Il-22* in iAhRKO (-99%, p=0.0019) compared to WT mice (**Figure 30A**). In WT/ DSS-treated males (**Figure 30B**), DIM showed an upward trend towards the upregulation of *Il-22* (70%), while a tendency towards increasing *Il-22* expression was also observed in iAhRKO mice (nsd). In contrast, expression of *Il-22* was significantly upregulated in WT females fed the DIM-supplemented diet compared to the control diet (790%, p=0.0005) (**Figure 30B**). Interestingly, in females, *Il-22* expression in both iAhRKO-control and iAhRKO-DIM fed groups was significantly downregulated when compared to the WT-DIM group by 899% (p=0.003) and 860% (p=0.0065), respectively (**Figure 30B**).

Il-6 expression was upregulated in the absence of AhR in IECs at the basal state. Produced by various cell types during acute inflammation, the pro-inflammatory cytokine interleukin-6 (*Il-6*) is an important regulator of innate and adaptive immune function. As

shown in Figure 30C, mice that received DIM in the diet had lower expression levels of *Il-6* regardless of the genotype at a basal state regardless of the genotype and the diet. Specifically, iAhRKO females fed a control diet had significantly higher *Il-6* levels (+520%, p=0.004) compared with their WT counterparts (**Figure 30C**). Similarly, DIM consumption trended to reduce *Il-6* expression by 80% in WT and 90% (p=0.0010) in iAhRKO female mice compared to their control-fed counterparts (**Figure 30C**). In males, DIM significantly decreased *Il-6* expression by 99% (p=0.0338) in WT and by 98% (p=0.0143) in iAhRKO mice compared to their control-fed mice (**Figure 30C**). Although *Il-6* expression was affected by DIM consumption at the basal state, either the diet, or the genotype impacted *Il-6* levels in male and female mice treated with DSS (**Figure 30D**).

Loss of AhR in IECs affected the expression levels of Cxcl13. As a chemokine that selectively attracts B cells (B-cell attracting chemokine 1), expression levels of *Cxcl13* were not significantly affected by the loss of AhR or the presence of DIM in males at a basal state (**Figure 30E**). However, in females, loss of AhR in IECs significantly reduced *Cxcl13* expression by 70% (p=0.0426) in control-fed, and by 97% (p=0.0063) in DIM-fed mice compared with WT-control fed females at the basal state (**Figure 30E**). Compared to control-fed WT males that received DSS (**Figure 30F**), loss of AhR in IECs significantly increased *Cxcl13* expression by more than 10-fold when DIM was present in the diet (p=0.0193) and by 16- and 50-fold (p=0.0002) when compared to iAhRKO control and DIM-fed animals, respectively. In WT females, DIM trended to increase *Cxcl13* expression compared with control-fed mice by 6-fold (p=0.0090) (**Figure 30F**). Likewise, *Cxcl13* expression was significantly downregulated (-90%, p=0.0090) in iAhRKO/

control-fed mice, and by 40% in iAhRKO/DIM-fed mice compared with their WT-control fed counterparts (**Figure 30F).**

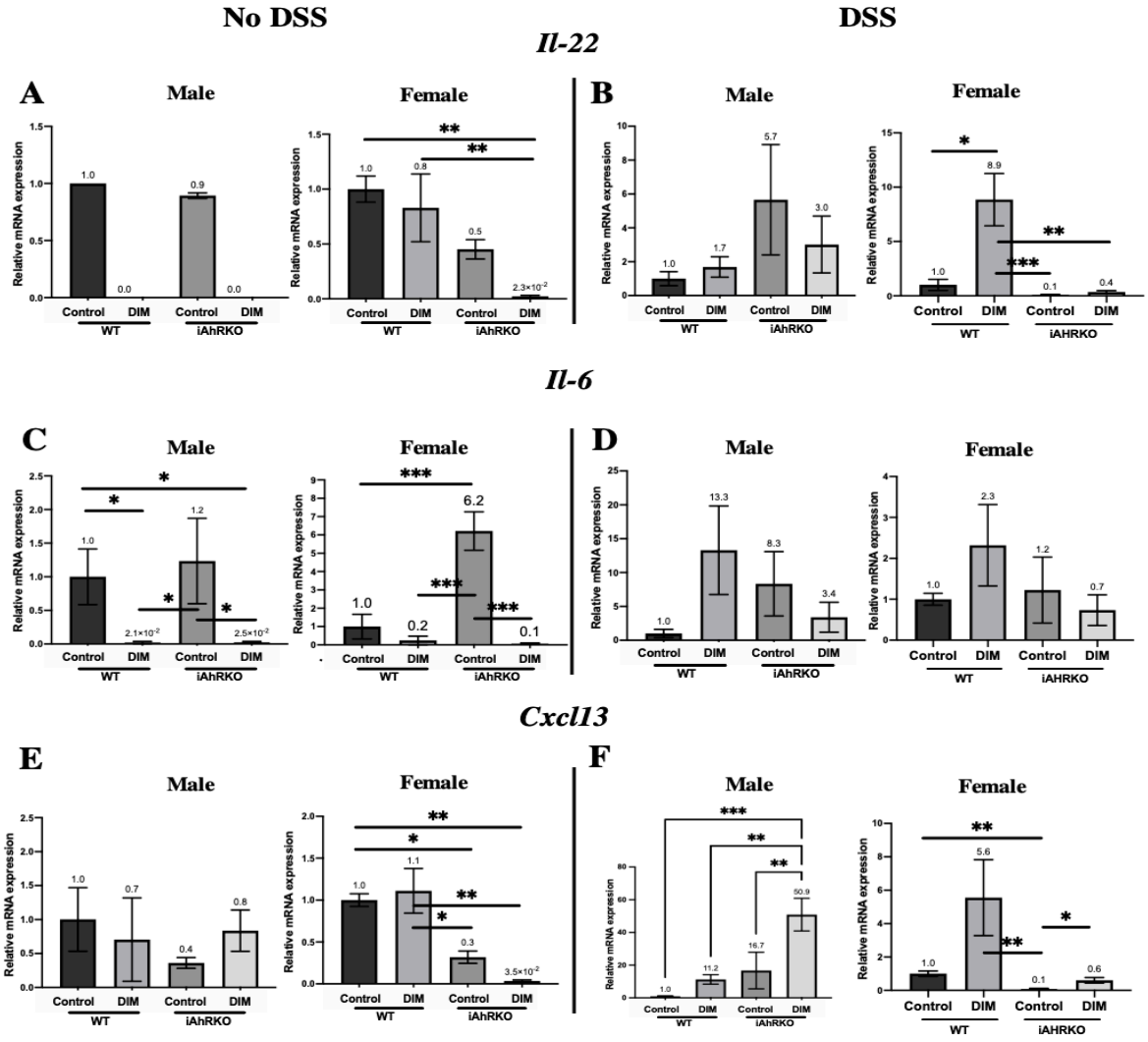

Figure 30 Effect of genotype, diet, DSS and sex in the expression of Il-22, Il-6, and Cxcl13 from MS

A. Relative expression of *Il-22* (IL-22)/No DSS. Male (N/A, 0=undetectable) and female (p=0.0096, one-way ANOVA). ***B.*** Relative expression of *Il-22* (IL-22)/DSS. Male (p=0.3469, one-way ANOVA) and female (p=0.0021, KW). ***C.*** Relative expression of *Il-6* (IL-6)/No DSS. Male (p=0.0021, KW) and female (p=0.0004, one-way ANOVA). ***D.*** Relative expression of *Il-6* (IL-6)/DSS. Male (p=0.2915, one-way ANOVA) and female (p=0.1426, KW). ***E.*** Relative expression of *Cxcl13* (Cxcl13)/No DSS. Male (p=0.5244, one-way ANOVA) and female (p=0.0051, one-way ANOVA). ***F.*** Relative expression of *Cxcl13* (Cxcl13)/DSS. Male (p=0.0015, one-way ANOVA) and female (p=0.0106, one-way ANOVA). n=3-4, $p < 0.075$ *$p < 0.05$, **$p < 0.01$ and ***$p < 0.001$

Discussion

As organized structures containing members of the adaptive immune system that develop at sites of inflammation or infection in the colon, TLTs appear to serve as localized centers for immune responses whose presence have been associated with resolution of colonic inflammation and better prognosis in CRC cases.[166] Different to SLOs which formation is dependent on the expression and activation of the AhR after birth, [21,25] organogenesis of TLT has only been witnessed in adulthood and its relationship with AhR activation has not yet been investigated. In the present study, loss of AhR activity in IECs affected the formation of TLTs due to impaired IEC barrier function in a sex-dependent manner.

The present discussion is organized in three main sections. First, the establishment of colonic inflammation and the formation of TLTs as a result of AhR activity in IECs is discussed. Next, the effect of AhR activation in the expression of genes involved in the preservation of IECs' barrier function is explored. Lastly, the effect of the loss of AhR activity in IECs on the expression of the pro-inflammatory cytokine *Il-6,* the barrier-function promoting *Il-22,* and the chemoattractant molecule *Cxcl13,* required for the sequential formation and establishment of TLTs is established.

Colonic inflammation, formation, and composition of TLTs

Disease activity index (DAI) was evaluated daily in all mice to indirectly identify the severity of experimental colitis.[184,185] As anticipated, exposure to DSS significantly increased DAI in all treatment groups regardless of genotype, diet, and sex compared with

vehicle controls at all timepoints. Compared with WT animals that received a ligand-depleted diet (control), DIM supplementation reduced DAI in both WT and knockout mice. As previously reported, administration of DIM (1-20 mg/kg) before DSS or AOM/DSS exposure resulted in the amelioration of clinical and histological characteristics of DSS-induced colitis in a dose-dependent manner.[85,98] Tough in our experiment we were able to recapitulate these observations using a comparable diet dose of DIM (20 mg/kg BW), the improvements did not appear to be specifically associated with AhR activity in IECs.

Expressed by IECs and used as a biomarker of intestinal inflammation,[191] expression levels of Lipocalin 2 (*Lcn2)* trended to increase in all mice that received DSS compared with vehicle controls, where this effect was more relevant in iAhRKO females fed a control diet compared to their non-DSS controls. Also produced by neutrophils and macrophages in the gastrointestinal tract, Lipocalin 2 promotes the production of pro-inflammatory cytokines.[192,193] Moreover, elevation of *Lcn2* may be associated with the chronic state of low-grade inflammation observed in global AhR knockout mice.[84] Interestingly, in this study, expression of *Lcn2* was significantly reduced in females that lacked AhR expression in IECs and received DIM-supplementation compared with iAhRKO control fed female mice. Taking into consideration that the number and activity of innate lymphoid cells are higher in females than males,[194] it is possible that DIM can activate the AhR in these cells resulting in the attenuation of the overall expression of *Lcn2* compared to female mice fed a control diet. However, the precise role of *Lcn2* in

during acute inflammation in the context of AhR activation in IECs and intestinal regeneration remains to be elucidated as it was beyond the scope of this study.

As previously described,[24,26,167–169] acute exposure to DSS (as an inflammatory stimulus) resulted in a significant increase in the formation and size of colonic TLTs compared to non-DSS treated animals in our study. Moreover, well-defined differences in the number and size of TLT between males and females were observed in our study as evidenced by the significant interaction between sex and AhR activity. At large, loss of AhR activity (IEC) resulted in significantly more yet smaller TLTs in males, while in females, fewer TLTs were observed. Supplementation with DIM increased the size of TLTs in WT animals treated with DSS and had no effect in iAhRKO mice regardless of sex, suggesting a positive association between AhR activation in IECs and the size of TLTs. Ultimately, fewer TLTs were observed in males fed a DIM-supplemented diet regardless of the genotype.

The sex differences observed in TLT numbers may be explained, in part, by the profound differences in immune function associated with sex steroid hormone signaling.[194] Generally, females exhibit higher innate, cell-mediated, and humoral immune responses than males. Specifically, high or consistent levels of estrogen (E_2) can reduce the production of pro-inflammatory cytokines, enhance the expansion of regulatory T cells, and stimulate the production of antibodies by B cells (mainly IgG).[194] As many pro-inflammatory genes have estrogen response elements (EREs) in their promoters, a high concentration of E_2 can inhibit NF- κβ activity and recruit steroid receptor coactivators

that act as transcriptional repressors,[194–197] which may result in higher number of TLTs in WT female mice compared to males.

To further understand the location of TLTs and their cellular composition, immuno-histo-fluorescence staining of B and T-cells in distal colons was performed. Here, we found that B-cells were located within TLTs while T-cells were distributed within TLTs and among colonic crypts on the TLT's periphery in DSS-treated animals. Though this result was not anticipated, it may be associated with the experimental design of our project. To this point, chronic inflammation has been suggested to be a critical factor for members of the adaptive immune system, such as T and B-cells, to become attracted to the inflammation site,[25] while our experiment employed a model of acute colonic inflammation. Looking more closely at the timing of induction and activation of adaptive immune populations in the colon during acute colitis, a significant influx of B-cells occurs at 6-10 days post-DSS (recovery period) while T cells are present in significantly fewer numbers (175 B-cells to 50 T-cells per field of view).[198,199] Maturation of TLTs varies from dense lymphocytic aggregates (early TLTs) to primary and secondary follicle-like TLTs, depending on the presence of other cell-types, such as follicular dendritic cells (FDCs), Tregs, high endothelial venules, and germinal centers. [200,201] TLT maturation stage is also associated with their function, where have a reduction of tumors in the colon and lungs has been associated with fully matured TLTs.[201] Based on these characteristics, the TLTs identified in the present study could belong to the early or primary stages of maturation; however, a more in-depth analysis would be required to differentiate between them. Nevertheless, the structures observed in our experiment showed all the hallmarks of

ILF/TLTs in terms of the presence of B cell follicles and lack of a distinct capsule (as seen in SLOs), but without a distinct T cell area. It is likely that these lymphoid structures indeed represent *de novo*- formed TLTs since they were not observed in vehicle controls.

While density of B-cells within TLTs was uniform between genotype, diet and sex; loss of AhR in IECs significantly increased the density of T-cells within TLTs compared to WT and had a more significant influence in males than females. Similarly, TLTs from iAhRKO animals were characterized by a reduced B:T ratio, with a higher change in males. Together with an increase in DAI in males, it is important to recall that sex-biased immunological responses against inflammatory diseases have been previously reported and appear to be playing a role in the composition of TLTs in the con of our experiment.[194] In females, estrogen (E_2) signaling is characterized by reducing Th1-pro-inflammatory cytokines, stimulating of Th2-anti-inflammatory pathways, enhancing the expansion of Tregs, and stimulating the production of antibodies by B cells; as a result, females developed less severe colitis and recovered faster than males, suggesting a direct contribution of E_2 and the colonic estrogen receptor β (ERβ).[194,202,203] As hypothesized, our experiments demonstrated that supplementation with DIM significantly increased TLT size and reduced T-cell density within TLTs in WT animals with no effect in IEC-AhRKO, suggesting both a correlation with previous findings in the literature where DIM consumption reduced the severity of colitis *in vivo*,[85,98,204] and that AhR activity is required to for DIM to have this physiological effect. Although the mechanism in which AhR activity in IECs affects T- and B-cell recruitment towards TLT is not known, these data support that the maintenance of epithelial barrier function through AhR activity in IECs

serves as a regulator between the luminal signals and the colon mucosa niche microenvironment that can either induce or halt colon inflammation.

AhR-responsive gene expression activity and IEC barrier function

In the present study, several genes involved in the synthesis of numerous TJ proteins were affected by the loss of AhR in IECs, the administration of DSS, and the presence of DIM in the diet in a sex-dependent manner. At the basal state (no-DSS), iAhRKO males showed a substantial downregulation of the expression of both *Zo-1* and *Ocln* compared to their WT counterparts. These observations are consistent with previous findings in the literature in which barrier permeability regulation by occludin requires direct interaction with *Zo-1*.[190] Furthermore, in vehicle control males, AhR activation with DIM trended to increase *Zo-1* expression compared to WT control-fed and iAhRKO males. As reported by Scott S. *et al*.,[173] mice that received DSS while fed a diet supplemented with indole-3-pyruvate or indole-3-aldehyde showed increased levels of occludin and ZO-1 proteins compared to control-fed animals.[173] Similarly, a parallel increased of *Ocln* and *Zo-1* expression was reported from an experiment using *C. Elegans* fed with *E. Coli* that had consumed DIM (100 μM).[205,206]

In female mice, the administration of DSS negatively affected *Ocln* expression regardless of the genotype, suggesting that epithelial damage had caused the loss of TJs and allowed the flux of large particles in a non-selective manner ("unrestricted" pathway), whereas in males the decreased expression of *Ocln* observed in iAhRKO mice at a basal state may be associated with the observed increased in gut permeability compared with

their WT counterparts. Our results share several similarities with previous findings by der Giessen J. *et al*.[207] and Braniste V. *et al*.[208] where activation of the estrogen receptor β (ERβ) with E_2 significantly increased mRNA and protein levels of occludin in the colon, but not ZO-1 *in vivo*.[208] By the same token, *in vitro,* treatment with E_2 and progesterone significantly increased the expression of *Ocln* and *Zo-1*.[207] Together, these data further supports the concept of sex differences on epithelial barrier function and justifies additional investigation.

In the present study, diet supplementation with DIM upregulated *Ocln* in both WT and iAhRKO female mice, but not in males at the basal state, suggesting DIM's effects in the regulation of *Ocln* may be due to an ER-dependent mechanism since basal estrogen levels in females are greater than males. Although DIM is an AhR agonist,[78–80] it has also been shown to activate ERβ to binding to EREs and recruitment of steroid receptor coactivator (SRC)-2.[209,210] In the presence of a ligand, AhR activation is considered to have an "anti-estrogenic" effect since is capable of inducing estrogen metabolism, ER turnover/ proteasomal degradation, and direct inhibition of transcriptional activation through EREs.[211,212] Conversely, without ligands present, ARNT functions as a coactivator of ER-dependent transcription in the presence of E_2, mediating/stabilizing the interaction between ER and EREs.[213–215] This would suggest that the sex differences observed in this study may be attributed to the crosstalk between sex hormones and AhR signaling. For example, in WT males, DIM upregulated the expression of *Zo-1* and *Muc2*, while in females, DIM trended to reduce their expression but increased the expression of *Ocln* which share common transcription pathways between the ERβ and AhR. One possible

explanation for these observations is that, in males, DIM may promote the expression of AhR-dependent genes due to a lower serum concentration of estrogen, while in females, DIM supplementation accompanied with higher estrogen levels would promote the expression of ERβ-dependent genes. In fact, multiple lines of evidence have shown anti-inflammatory effects of estrogen via ERβ signaling in the colon,[216] which could be taking place under the conditions of our study.

Another important regulator of the paracellular flux and ion selectivity in the intact epithelium is the "pore pathway", mainly comprised by claudins. Specifically, the upregulation of *Cldn2* by pro-inflammatory cytokines has been associated with an increase of the pore pathway flux and increasing overall gut permeability.[190] Though no changes in *Clnd2* expression were found in males, in females, *Cldn2* expression increased with the loss of AhR both at the basal and during the post-acute inflammatory state, suggesting that expression of *Clnd2* may be regulated by the expression of the AhR in a sex-dependent manner. However, to the best of our knowledge, the expression of *Clnd2* has not been associated with the activity of the ERβ in the literature.

Since the mucus layer's integrity is often considered a marker of IEC homeostasis, loss of AhR expression in IECs resulted in a significant reduction of *Muc2* in males regardless of DSS. Previous work by Tadesse S. *et al*.[217] established that *Muc2* deficiency in IECs was associated with a higher risk of developing colon tumors and deletion of *Muc2* expression resulted in spontaneous colitis, suggesting the significance of *Muc2* expression to maintain IEC's barrier function, especially after gut barrier damage. This is consistent

with the regulation of mucin-producing genes by the exogenous activation of the AhR/IL-22/Stat3 signaling pathway, commonly observed in the mucosal wound healing process.[218]

In the present study, increased permeability to FITC-dextran was observed not only in DSS-treated mice compared to vehicle controls, but in female mice compared to males. Larger gap junctions between IECs allow more particulates and foreign pathogens into the submucosa, where the local innate and adaptive immune system conducts an inflammatory cascade to combat a potential infection or respond to the damaged tissue.[25] Compared to their WT counterparts, the reduced expression of *Ocln* and *Zo-1* observed in iAhRKO males may be associated with the disruption of TJs resulting in higher DAI and increased gut permeability at a basal state. In females, loss of AhR in IECs led to the downregulation of *Ocln* while increasing *Cldn2* expression compared to WT controls, potentially affecting the leak and the pore pathways at the basal state and when exposed to DSS. This could explain why females had an overall increased gut permeability compared to males when subjected to DSS-induced epithelial damage.

AhR activity in IECs on the TLT formation process

As previously presented in this body of work, the formation of TLTs follows a sequential progression that starts with an inflammatory insult at the large intestine. Since IL-6 has been explicitly documented as a part of the initiation phase of TLT formation in colitis-induced models,[22] we analyzed expression levels of *Il-6* in the context of AhR activation in IECs. However, in our study, no significant differences in *Il-6* expression between groups were found in mice that were exposed to DSS. A possible explanation of this

observation may rely on the fact that *Il-6* expression is greatly affected short after DSS exposure (less than 24 hours), whereas our assessment was completed during a recovery period (10 days after). In contrast, at a basal state, the observed decrease in *Il-6* levels regardless of sex or the genotype might be interpreted as being the result of the IECs' capability to regulate the availability of AhR ligands to the intestinal immune cells underneath the epithelial layer.[17,121,137]

The next step in the formation of TLTs consists in stromal cells increasing the chemokine gradient to induce the homing of B and T-cells to the site of inflammation.[22] In our study, although DIM was present in the diet, the expression of the gene encoding the chemokine CXCL13 was significantly downregulated in females non-expressing AhR in IECs after DSS-induced inflammation. It can thus be suggested that AhR expression and activation in IECs may be required for the recruitment phase of TLT formation. This supports previous findings in the literature where the expression of CXCL13 appears to be regulated by AhR activation in the lung mucosa when smoking.[219] Conversely, the increased expression of *Cxcl13* in iAhRKO males treated with DSS could be associated with the increased number of TLTs observed in this study. Opposite expression patterns of *Cxcl13* between males and females after the loss of AhR in IECS is an interesting observation, since it has been recently reported that some follicular Th cells are capable of producing *Cxcl13;*[200] however, their significance in the context of inflammation and TLT formation is still under investigation.

Recent work has demonstrated a role for IL-22 in the control of both TLT development and function. While expression levels of *Il-22* were low to undetectable at the basal state

in both males and females, expression of *Il-22* appears to be regulated in an AhR (IEC)-dependent manner in females exposed to DSS. Moreover, activation of AhR with DIM significantly increased *Il-22* expression in DSS-treated females while the effect was not retained in their iAhRKO counterparts. According to a disease model in salivary glands (Sjogren's syndrome), the over-expression of CXCL13 facilitated the recruitment of IL-22^{+}ILCs and the subsequent production of IL-22 was critical for developing TLTs, the maintenance of CXCL12/13 levels to facilitate B-cell clustering, and the production of autoantibodies.[22,176] In our study, since the expression of *Il-22* was not significantly affected by activation or lack of AhR expression in males, there is a strong likelihood that the production of IL-22 by ILCs in female mice is a more responsive process in the context of inflammation. To this date, the formation of TLTs as a result of IL-22 signaling has been conducted exclusively on female mice,[176] indicating the need for further studies to establish whether IL-22 production is affected by sex hormone levels in the gut.

Due to a 10-day recovery period was allowed before termination, we can predict that the recovery/ regeneration process of IECs was initiated in mice exposed to DSS-induced epithelial damage. During this stage, IECs can stimulate the production of ILC3-derived IL-22 via interleukin-7 (IL-7).[189] Though we did not observed differences in *Il-7* expression in females, males lacking AhR expression showed a significant downregulation of *Il-7,* while DIM trended to increase its expression in WT animals at a basal state. Moreover, it is possible that expression of *Il-7* was not affected DSS-treated animals as a result of the overall loss of *Il-7*-producing IECs. Though abnormally high levels of IL-7 or its receptor (IL-7R) have been associated with intestinal inflammation,

its expression seems to be affected by AhR activity.[220–222] To the best of our knowledge, limited data related to AhR activity, epithelial recovery, and TLT development are available to this date and requires further investigation.

Our work has led us to conclude that the formation of TLT in the colon is a sex and an AhR (IEC)-dependent process. Paired with increased DAI and lower expression of genes relevant for the preservation of IEC's barrier function, the increased number of TLTs, increased T-cell density, and lower B:T ratio in males lacking AhR expression in IECs may represent an unfavorable prognosis when exposed to DSS-induced epithelial damage. Although WT females have more TLTs than males, loss of AhR activation in IECs reduced their formation without significant changes in disease outcomes in females nor immune cell composition within their TLTs. Equally important, AhR activation in IECs by DIM promoted intestinal barrier integrity through the upregulation of various TJ genes at a basal state, as well as genes involved in the signaling that allows the formation of TLT after an inflammatory event in a sex-dependent manner. Even though our study's design did not allow us to investigate the formation of TLTs in the context of chronic inflammation, our data provides valuable insight into the interaction between the activation of AhR in IECs with dietary ligands and sex-dependent immune responses necessary for the IEC homeostasis and the resolution of inflammation in the colon. A summary of our findings is presented in **Figure 31.**

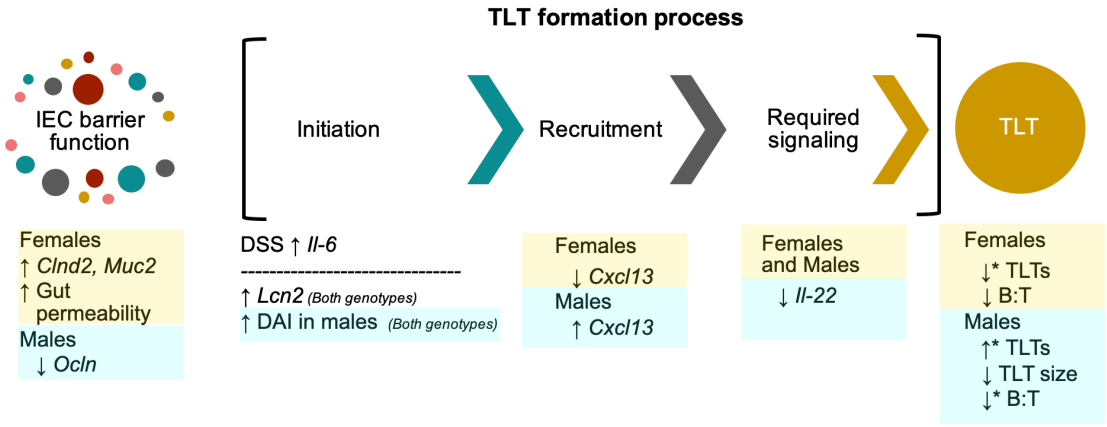

Figure 31. Summary of findings (TLT)

Summary of the effect of loss of AhR activity in IECs (iAhRKO) in mice exposed to DSS-induced colonic inflammation compared to their corresponding WT-vehicle controls (no DSS) as indicated by the direction of the arrows. *p<0.05

Even though uncertainties about the effect of TLTs in different pathologies still exist, several research efforts directed to manipulate the development of these structures have been accomplished.[22] Site-directed delivery of therapeutic compounds that target the function of TLTs may prove a viable path for the treatment of chronic inflammatory diseases or the targeted reduction of solid tumors, with limited effects on the systemic or gut mucosal immunity.[200] According to our data, the formation of TLTs can be potentially modulated by the diet via the activation of the AhR with the purpose of resolving inflammation-associated pathologies in the colon. Since marked sex differences in the expression of a selected group of genes responsible for IECs' barrier function and formation of TLTs were discovered, this study is also the first step towards enhancing our understanding of the impact of sex hormones in the organogenesis of TLTs.

CHAPTER V

SUMMARY AND CONCLUSIONS

AhR activation with dietary and microbial-derived AhR ligands modulates IEC homeostasis and gut mucosal immunity. Previously, it has been demonstrated that global AhR deficiency is associated with increased colonic carcinogenesis, gut microbial dysbiosis, and the disrupted formation of gut-associated lymphoid tissues. In the studies presented in this body of work, we were able to isolate the effect of this receptor exclusively in the intestinal epithelial cells, both conditionally and constitutively using an IEC-specific AhR knockout mouse. The role of diet, microbial communities, and microbial-AhR ligands were assessed in the first two projects that studied the role of AhR in the IEC niche microenvironment. First, we established the host's phenotype in which the loss of AhR in addition to a HFD increased the formation of premalignant lesions; obtaining the first insight into how this genotype can alter cell proliferation, apoptosis, gene expression, and abundance of gut microbial-produced tryptophan-derived AhR metabolites. Next, loss of AhR expression and higher fat content of the diet promoted ACF development, increased the expression of genes associated with colorectal cancer development (cell growth, migration, and survival), disruption of the IEC barrier, and inflammation. Furthermore, lack of AhR expression in IECs altered the composition of microbial communities in a sex-dependent manner. Taken together, our data agrees with the effect of HFD diets in the promotion of a pro-carcinogenic gene signature and induction of functional changes in the intestinal microbiota that could further exacerbate

colon carcinogenesis via a reduction in AhR ligand availability. Interestingly, we found that loss of AhR in IECs resulted in a reduced number of tertiary lymphoid tissues at the premalignant CRC formation stage; observation that we further investigated in our third project.

Since dysfunction of the colonic mucosal epithelial barrier allows intestinal bacteria to gain access to gut immune cells, thereby contributing to intestinal inflammation; it has been demonstrated that AhR activation with xenobiotics, dietary, and microbial-derived ligands can decrease inflammation in the gut via immune-mediated pathways and maintain gut-barrier function. In chapter IV, we investigated whether activation of AhR in IECs with dietary ligands was associated with the maintenance of IEC-barrier function and the subsequent formation of TLTs during acute inflammation. Here, we found that the formation and the immune composition of TLTs in the colon may be considered both an AhR and a sex-dependent process. While the loss of AhR in IECs did not directly affect the disease outcomes after DSS-induced epithelial damage, an increased number of TLTs with a reduced B:T cell ratio were observed in males, while fewer TLTs were found in females. Moreover, paired with higher disease activity index, lower B:T ratio, and lower expression of genes relevant for the preservation of IEC's barrier function, the increased number of TLTs in males lacking AhR expression in IECs may represent an unfavorable scenario. At a basal state, AhR activation in IECs by DIM promoted intestinal barrier integrity through the upregulation of various TJ genes as well as genes involved in the signaling required for the formation of TLTs after an inflammatory event in a sex-dependent manner.

As TLTs represent a niche for adaptive immune responses, they can be considered a putative new target to develop therapies to reduce colonic inflammation and increase the anti-tumor immune response in the large intestine. Equally relevant, identifying the mechanisms in which AhR activation in IECs by dietary or microbial-derived ligands can affect the immune response against acute inflammation and anti-cancer activity will allow us to establish AhR as a target for drug development, immunomodulation, and chemoprevention.

REFERENCES

1. Gordon Betts J., Kelly A. Y, Wise JA, et al. The Small and Large Intestines. In: *Anatomy and Physiology*. Houston, TX: OpenStax; 2013. https://openstax.org/books/anatomy-and-physiology/pages/23-5-the-small-and-large-intestines. Accessed September 21, 2020.

2. Rao JN, Wang J-Y. Intestinal Architecture and Development. 2010. https://www.ncbi.nlm.nih.gov/books/NBK54098/. Accessed September 29, 2020.

3. Peterson LW, Artis D. Intestinal epithelial cells: regulators of barrier function and immune homeostasis. *Nat Rev Immunol*. 2014;14(3):141-153. doi:10.1038/nri3608

4. Kang M, Martin A. Microbiome and colorectal cancer: Unraveling host-microbiota interactions in colitis-associated colorectal cancer development. *Semin Immunol*. 2017;32(February):3-13. doi:10.1016/j.smim.2017.04.003

5. Shreiner AB, Kao JY, Young VB. The gut microbiome in health and in disease. *Curr Opin Gastroenterol*. 2015;31(1):69. doi:10.1097/MOG.0000000000000139

6. Sonnenburg JL, Bäckhed F. Diet–microbiota interactions as moderators of human metabolism. *Nature*. 2016;535(7610):56-64. doi:10.1038/nature18846

7. Rowland I, Gibson G, Heinken A, et al. Gut microbiota functions: metabolism of nutrients and other food components. *Eur J Nutr*. 2018;57(1):1. doi:10.1007/S00394-017-1445-8

8. Liu Y, Hou Y, Wang G, Zheng X, Hao H. Gut Microbial Metabolites of Aromatic Amino Acids as Signals in Host-Microbe Interplay. *Trends Endocrinol Metab*. April 2020. doi:10.1016/j.tem.2020.02.012

9. Bhutia YD, Ogura J, Sivaprakasam S, Ganapathy V. Gut Microbiome and Colon Cancer: Role of Bacterial Metabolites and Their Molecular Targets in the Host. *Curr Colorectal Cancer Rep*. 2017;13(2):111-118. doi:10.1007/s11888-017-0362-9

10. Chassaing B, Kumar M, Baker MT, Singh V, Vijay-Kumar M. Mammalian gut immunity. *Biomed J*. 2014;37(5):246-258. doi:10.4103/2319-4170.130922

11. Okumura R, Takeda K. Roles of intestinal epithelial cells in the maintenance of gut homeostasis. *Exp Mol Med*. 2017;49(5):e338-e338. doi:10.1038/emm.2017.20

12. Sonnenberg GF, Fouser LA, Artis D. Border patrol: regulation of immunity, inflammation and tissue homeostasis at barrier surfaces by IL-22. *Nat Immunol*. 2011;12(5):383-390. doi:10.1038/ni.2025

13. Parks OB, Pociask DA, Hodzic Z, Kolls JK, Good M. Interleukin-22 Signaling in the Regulation of Intestinal Health and Disease. *Front Cell Dev Biol*. 2016;3:85. doi:10.3389/fcell.2015.00085

14. Brandtzaeg P. Immunity in the Gut: Mechanisms and Functions. In: *Viral Gastroenteritis*. Academic Press; 2016:23-46. doi:10.1016/B978-0-12-802241-2.00002-X

15. Dillon A, Lo DD. M Cells: Intelligent Engineering of Mucosal Immune Surveillance. *Front Immunol*. 2019;10:1499. doi:10.3389/fimmu.2019.01499

16. Panda SK, Colonna M. Innate Lymphoid Cells in Mucosal Immunity. *Front Immunol*. 2019;10:861. doi:10.3389/fimmu.2019.00861

17. Lamas B, Natividad JM, Sokol H. Aryl hydrocarbon receptor and intestinal immunity. *Mucosal Immunol*. 2018;11(4):1024-1038. doi:10.1038/s41385-018-0019-2

18. Wang L, Zhu L, Qin S. Gut Microbiota Modulation on Intestinal Mucosal Adaptive Immunity. *J Immunol Res*. 2019:4735040. doi:10.1155/2019/4735040

19. Li Y, Jin L, Chen T. The Effects of Secretory IgA in the Mucosal Immune System. *Biomed Res Int*. 2020;2020:1-6. doi:10.1155/2020/2032057

20. Ohl L, Bernhardt G, Pabst O, Förster R. Chemokines as organizers of primary and secondary lymphoid organs. *Semin Immunol*. 2003.

doi:10.1016/j.smim.2003.08.003

21. Kiss EA, Vonarbourg C, Kopfmann S, et al. Natural aryl hydrocarbon receptor ligands control organogenesis of intestinal lymphoid follicles. *Science (80-)*. 2011;334(6062):1561-1565. doi:10.1126/science.1214914

22. McNamee EN, Rivera-Nieves J. Ectopic tertiary lymphoid tissue in inflammatory bowel disease: Protective or provocateur? *Front Immunol*. 2016;7(308):1-11. doi:10.3389/fimmu.2016.00308

23. Bergomas F, Grizzi F, Doni A, et al. Tertiary intratumor lymphoid tissue in colo-rectal cancer. *Cancers (Basel)*. 2012. doi:10.3390/cancers4010001

24. Colbeck EJ, Ager A, Gallimore A, Jones GW. Tertiary lymphoid structures in cancer: Drivers of antitumor immunity, immunosuppression, or Bystander Sentinels in disease? *Front Immunol*. 2017;8(1830). doi:10.3389/fimmu.2017.01830

25. Buettner M, Lochner M. Development and function of secondary and tertiary lymphoid organs in the small intestine and the colon. *Front Immunol*. 2016;7(342):1-11. doi:10.3389/fimmu.2016.00342

26. Pipi E, Nayar S, Gardner DH, Colafrancesco S, Smith C, Barone F. Tertiary lymphoid structures: Autoimmunity goes local. *Front Immunol*. 2018;9(1952):1-21. doi:10.3389/fimmu.2018.01952

27. Centers for Disease Control and Prevention. Colorectal Cancer Statistics. https://www.cdc.gov/cancer/colorectal/statistics/index.htm. Published 2020. Accessed September 30, 2020.

28. National Cancer Institute. Cancer Stat Facts: Colorectal Cancer. https://seer.cancer.gov/statfacts/html/colorect.html. Published 2020. Accessed September 30, 2020.

29. Xie J. P. G. R. Role of the Aryl Hydrocarbon Receptor in Colon Neoplasia. *Cancers (Basel)*. 2015;7(3):1436-1446. doi:10.3390/cancers7030847

30. Ruiz RB, Hernandez PS. Diet and cancer: Risk factors and epidemiological evidence. *Maturitas*. 2014;77(3):202-208. doi:10.1016/J.MATURITAS.2013.11.010

31. Anand P, Kunnumakkara AB, Kunnumakara AB, et al. Cancer is a preventable disease that requires major lifestyle changes. *Pharm Res*. 2008;25(9):2097-2116. doi:10.1007/s11095-008-9661-9

32. American Cancer Society. Key Statistics for Colorectal Cancer. https://www.cancer.org/cancer/colon-rectal-cancer/about/key-statistics.html. Published 2019. Accessed July 4, 2019.

33. Barone M, Lofano K, De Tullio N, et al. Dietary, Endocrine, and Metabolic Factors in the Development of Colorectal Cancer. *J Gastrointest Cancer*. 2012;43(1):13-19. doi:10.1007/s12029-011-9332-7

34. Centers for Disease Control and Prevention. What Are the Risk Factors for Colorectal Cancer? https://www.cdc.gov/cancer/colorectal/basic_info/risk_factors.htm. Published 2016. Accessed March 4, 2018.

35. Johnson CM, Wei C, Ensor JE, et al. Meta-analyses of colorectal cancer risk factors. *Cancer Causes Control*. 2013;24(6):1207-1222. doi:10.1007/s10552-013-0201-5

36. Marmol I, Sanchez-de-Diego C, Dieste AP, Cerrada E, Yoldi MJR. Colorectal Carcinoma: A General Overview and Future Perspectives in Colorectal Cancer. *Int J Mol Sci*. 2017;18(1):197. doi:http://dx.doi.org/10.3390/ijms18010197

37. Wargovich MJ, Brown VR, Morris J. Aberrant crypt foci: The case for inclusion as a biomarker for colon cancer. *Cancers (Basel)*. 2010;2(3):1705-1716. doi:10.3390/cancers2031705

38. Jones S, Chen W-D, Parmigiani G, et al. Comparative lesion sequencing provides insights into tumor evolution. *Proc Natl Acad Sci U S A*. 2008;105(11):4283-4288. doi:10.1073/pnas.0712345105

39. Tariq K, Ghias K. Colorectal cancer carcinogenesis: a review of mechanisms. *Cancer Biol Med*. 2016;13(1):120-135. doi:10.28092/j.issn.2095-3941.2015.0103

40. O'Keefe SJD. Diet, microorganisms and their metabolites, and colon cancer. *Nat Rev Gastroenterol Hepatol*. 2016;13(12):691-706. doi:10.1038/nrgastro.2016.165

41. Terzić J, Grivennikov S, Karin E, Karin M. Inflammation and Colon Cancer. *Gastroenterology*. 2010;138(6):2101-2114.e5. doi:10.1053/j.gastro.2010.01.058

42. Principi M. Ulcerative colitis: From inflammation to cancer. Do estrogen receptors have a role? *World J Gastroenterol*. 2014;20(33):11496-11504. doi:10.3748/wjg.v20.i33.11496

43. Tabung FK, Brown LS, Fung TT. Dietary Patterns and Colorectal Cancer Risk: A Review of 17 Years of Evidence (2000-2016). *Curr Colorectal Cancer Rep*. 2017;13(6):440-454. doi:10.1007/s11888-017-0390-5

44. Thanikachalam K, Khan G. Colorectal Cancer and Nutrition. *Nutrients*. 2019;11(1). doi:10.3390/nu11010164

45. Day SD, Enos RT, McClellan JL, Steiner JL, Velázquez KT, Murphy EA. Linking inflammation to tumorigenesis in a mouse model of high-fat-diet-enhanced colon cancer. *Cytokine*. 2013;64(1):454-462. doi:10.1016/j.cyto.2013.04.031

46. Sikalidis AK, Fitch MD, Fleming SE. Diet induced obesity increases the risk of colonic tumorigenesis in mice. *Pathol Oncol Res*. 2013;19(4):657-666. doi:10.1007/s12253-013-9626-0

47. Tuominen I, Al-Rabadi L, Stavrakis D, Karagiannides I, Pothoulakis C, Bugni JM. Diet-induced obesity promotes colon tumor development in azoxymethane-treated mice. *PLoS One*. 2013;8(4):e60939. doi:10.1371/journal.pone.0060939

48. Kasdagly M, Radhakrishnan S, Reddivari L, Veeramachaneni DNR, Vanamala J. Colon carcinogenesis: influence of Western diet-induced obesity and targeting stem cells using dietary bioactive compounds. *Nutrition*. 2014;30(11-12):1242-1256. doi:10.1016/j.nut.2014.02.016

49. Day SD, Enos RT, McClellan JL, Steiner JL, Velázquez KT, Murphy EA. Linking inflammation to tumorigenesis in a mouse model of high-fat-diet-enhanced colon cancer. *Cytokine*. 2013;64(1):454-462. doi:10.1016/j.cyto.2013.04.031

50. National Cancer Institute. Obesity and Cancer. Fact sheet. https://www.cancer.gov/about-cancer/causes-prevention/risk/obesity/obesity-fact-sheet. Published 2017. Accessed October 2, 2020.

51. Lauby-Secretan B, Scoccianti C, Loomis D, Grosse Y, Bianchini F, Straif K. Body Fatness and Cancer — Viewpoint of the IARC Working Group. *N Engl J Med*. 2016;375(8):794-798. doi:10.1056/NEJMsr1606602

52. DeClercq V, McMurray DN, Chapkin RS. Obesity promotes colonic stem cell expansion during cancer initiation. *Cancer Lett*. 2015;369(2):336-343. doi:10.1016/j.canlet.2015.10.001

53. Padidar S, Farquharson AJ, Williams LM, Kearney R, Arthur JR, Drew JE. High-fat diet alters gene expression in the liver and colon: links to increased development of aberrant crypt foci. *Dig Dis Sci*. 2012;57(7):1866-1874. doi:10.1007/s10620-012-2092-9

54. Kim E, Davidson LA, Zoh RS, et al. Homeostatic responses of colonic LGR5+ stem cells following acute in vivo exposure to a genotoxic carcinogen. *Carcinogenesis*. 2015;37(2):206-214. doi:10.1093/carcin/bgv250

55. Beyaz S, Mana MD, Roper J, et al. High-fat diet enhances stemness and tumorigenicity of intestinal progenitors. *Nature*. 2016;531(7592):53-58. http://dx.doi.org/10.1038/nature17173.

56. Hughes LAE, Simons CCJM, van den Brandt PA, van Engeland M, Weijenberg MP. Lifestyle, Diet, and Colorectal Cancer Risk According to (Epi)genetic Instability: Current Evidence and Future Directions of Molecular Pathological Epidemiology. *Curr Colorectal Cancer Rep*. 2017;13(6):455-469. doi:10.1007/s11888-017-0395-0

57. González-Vallinas M, González-Castejón M, Rodríguez-Casado A, Ramírez de Molina A. Dietary phytochemicals in cancer prevention and therapy: a

complementary approach with promising perspectives. *Nutr Rev*. 2013;71(9):585-599. doi:10.1111/nure.12051

58. Turner ND, Ritchie LE, Bresalier RS, Chapkin RS. The microbiome and colorectal neoplasia: Environmental modifiers of dysbiosis. *Curr Gastroenterol Rep*. 2013;15(9):0-10. doi:10.1007/s11894-013-0346-0

59. Rothschild D, Weissbrod O, Barkan E, et al. Environment dominates over host genetics in shaping human gut microbiota. *Nature*. February 2018. doi:10.1038/nature25973

60. Gao Z, Guo B, Gao R, Zhu Q, Qin H. Microbiota disbiosis is associated with colorectal cancer. *Front Microbiol*. 2015;6(FEB):1-9. doi:10.3389/fmicb.2015.00020

61. Gagnière J, Raisch J, Veziant J, et al. Gut microbiota imbalance and colorectal cancer. *World J Gastroenterol*. 2016;22(2):501-518. doi:10.3748/wjg.v22.i2.501

62. Grondin JA, Kwon YH, Far PM, Haq S, Khan WI. Mucins in Intestinal Mucosal Defense and Inflammation: Learning From Clinical and Experimental Studies. *Front Immunol*. 2020;11:2054. doi:10.3389/fimmu.2020.02054

63. Lasry A, Zinger A, Ben-Neriah Y. Inflammatory networks underlying colorectal cancer. *Nat Immunol*. 2016;17(3):230-240. doi:10.1038/ni.3384

64. Nakatsu G, Li X, Zhou H, et al. Gut mucosal microbiome across stages of colorectal carcinogenesis. *Nat Commun*. 2015;6:1-9. doi:10.1038/ncomms9727

65. Li S, Konstantinov SR, Smits R, Peppelenbosch MP. Bacterial Biofilms in Colorectal Cancer Initiation and Progression. *Trends Mol Med*. 2017;23(1):18-30. doi:10.1016/j.molmed.2016.11.004

66. O'Keefe SJD, Li J V, Lahti L, et al. Fat, fibre and cancer risk in African Americans and rural Africans. *Nat Commun*. 2015;6:6342. doi:10.1038/ncomms7342

67. Iain AM, Andrew DP, Gary HP. Aryl hydrocarbon receptor ligands in cancer: friend and foe. *Nat Rev Cancer*. 2014;14(12):801-814. doi:10.1038/nrc3846

68. Kerley-hamilton JS, Trask HW, Ridley CJA, Dufour E, Ringelberg CS. Obesity Is Mediated by Differential Aryl Hydrocarbon Receptor Signaling in Mice Fed a Western Diet. 2012;1252(9):1252-1259. doi:10.1093/toxsci/kfs155

69. Ikuta T, Kurosumi M, Yatsuoka T, Nishimura Y. Tissue distribution of aryl hydrocarbon receptor in the intestine: Implication of putative roles in tumor suppression. *Exp Cell Res*. 2016;343(2):126-134. doi:10.1016/j.yexcr.2016.03.012

70. Stevens EA, Mezrich JD, Bradfield CA. The aryl hydrocarbon receptor: a perspective on potential roles in the immune system. *Immunology*. 2009;127(3):299-311. doi:10.1111/j.1365-2567.2009.03054.x

71. Larigot L, Juricek L, Dairou J, Coumoul X. AhR signaling pathways and regulatory functions. *Biochim Open*. 2018;7:1-9. doi:10.1016/J.BIOPEN.2018.05.001

72. Busbee PB, Rouse M, Nagarkatti M, Nagarkatti PS. Use of natural AhR ligands as potential therapeutic modalities against inflammatory disorders. *Nutr Rev*. 2013;71(6):353-369. doi:10.1111/nure.12024

73. Xie G, Raufman J-P. Role of the Aryl Hydrocarbon Receptor in Colon Neoplasia. *Cancers (Basel)*. 2015;7(3):1436-1446. doi:10.3390/cancers7030847

74. Beischlag T V, Luis Morales J, Hollingshead BD, Perdew GH. The aryl hydrocarbon receptor complex and the control of gene expression. *Crit Rev Eukaryot Gene Expr*. 2008;18(3). doi:10.2964/jsik.kuni0223

75. Hubbard TD, Murray IA, Perdew GH. Indole and Tryptophan Metabolism: Endogenous and Dietary Routes to Ah Receptor Activation. *Drug Metab Dispos*. 2015;43:1522-1535. doi:10.1124/dmd.115.064246

76. Kawajiri K, Kobayashi Y, Ohtake F, et al. Aryl hydrocarbon receptor suppresses intestinal carcinogenesis in ApcMin/+ mice with natural ligands. *Proc Natl Acad Sci*. 2009;106(32):13481-13486. doi:10.1073/pnas.0902132106

77. Metidji A, Omenetti S, Crotta S, et al. The Environmental Sensor AHR Protects from Inflammatory Damage by Maintaining Intestinal Stem Cell Homeostasis and Barrier Integrity. *Immunity*. August 2018. doi:10.1016/j.immuni.2018.07.010

78. Murray IA, Perdew GH. Ligand activation of the Ah receptor contributes to gastrointestinal homeostasis. *Curr Opin Toxicol*. 2017;2:15-23. doi:10.1016/j.cotox.2017.01.003

79. Baenas N, Suárez-Martínez C, García-Viguera C, Moreno DA. Bioavailability and new biomarkers of cruciferous sprouts consumption. *Food Res Int*. 2017;100(July):497-503. doi:10.1016/j.foodres.2017.07.049

80. Fujioka N, Ainslie-Waldman CE, Upadhyaya P, et al. Urinary 3,30-diindolylmethane: A biomarker of glucobrassicin exposure and indole-3-carbinol uptake in humans. *Cancer Epidemiol Biomarkers Prev*. 2014;23(2):282-287. doi:10.1158/1055-9965.EPI-13-0645

81. Cheng Y, Jin U-H, Allred CD, Jayaraman A, Chapkin RS, Safe S. Aryl Hydrocarbon Receptor Activity of Tryptophan Metabolites in Young Adult Mouse Colonocytes. *Drug Metab Dispos*. 2015;43(10):1536-1543. doi:10.1124/dmd.115.063677

82. Jin U-H, Lee S-O, Sridharan G, et al. Microbiome-Derived Tryptophan Metabolites and Their Aryl Hydrocarbon Receptor-Dependent Agonist and Antagonist Activities. *Mol Pharmacol*. 2014;85(May):777-788. doi:10.1124/mol.113.091165

83. Kolluri SK, Jin U-H, Safe S. Role of the aryl hydrocarbon receptor in carcinogenesis and potential as an anti-cancer drug target. *Arch Toxicol*. 2017;91(7):2497-2513. doi:10.1007/s00204-017-1981-2

84. Murray IA, Nichols RG, Zhang L, Patterson AD, Perdew GH. Expression of the aryl hydrocarbon receptor contributes to the establishment of intestinal microbial community structure in mice. *Sci Rep*. 2016;6(33969):1-14. doi:10.1038/srep33969

85. Jeon E-J, Davaatseren M, Hwang J-T, et al. Effect of Oral Administration of 3,3′-Diindolylmethane on Dextran Sodium Sulfate-Induced Acute Colitis in Mice. *J*

Agric Food Chem. 2016;64(41):7702-7709. doi:10.1021/acs.jafc.6b02604

86. Stockinger B, Di Meglio P, Gialitakis M, Duarte JH. The aryl hydrocarbon receptor: multitasking in the immune system. *Annu Rev Immunol*. 2014;32:403-432. doi:10.1146/annurev-immunol-032713-120245

87. Murray IA, Perdew GH. Ligand activation of the Ah receptor contributes to gastrointestinal homeostasis. *Curr Opin Toxicol*. 2016;1:15-23. doi:10.1016/j.cotox.2017.01.003

88. Peng TL, Chen J, Mao W, et al. Potential therapeutic significance of increased expression of aryl hydrocarbon receptor in human gastric cancer. *World J Gastroenterol*. 2009;15(14):1719-1729. doi:10.3748/wjg.15.1719

89. Andersson P, McGuire J, Rubio C, et al. A constitutively active dioxin/aryl hydrocarbon receptor induces stomach tumors. *Proc Natl Acad Sci U S A*. 2002;99(15):9990-9995. doi:10.1073/pnas.152706299

90. Díaz-Díaz CJ, Ronnekleiv-Kelly SM, Nukaya M, et al. The Aryl Hydrocarbon Receptor is a Repressor of Inflammation-associated Colorectal Tumorigenesis in Mouse. *Ann Surg*. 2016;264(3):429-436. doi:10.1097/SLA.0000000000001874

91. Wang Q, Yang K, Han B, et al. Aryl hydrocarbon receptor inhibits inflammation in DSS-induced colitis via the MK2/p-MK2/TTP pathway. *Int J Mol Med*. 2017;41(2):868-876. doi:10.3892/ijmm.2017.3262

92. Benson JM, Shepherd DM. Aryl hydrocarbon receptor activation by TCDD reduces inflammation associated with Crohn's disease. *Toxicol Sci*. 2011;120(1):68-78. doi:10.1093/toxsci/kfq360

93. Kawajiri K, Kobayashi Y, Ohtake F, et al. Aryl hydrocarbon receptor suppresses intestinal carcinogenesis in ApcMin/+ mice with natural ligands. *PNAS*. 2009;106(32):13481-13486. doi:10.1073/pnas.0902132106

94. Han H, Davidson LA, Hensel M, et al. Loss of aryl hydrocarbon receptor promotes colon tumorigenesis in ApcS580/þ; KrasG12D/þ mice. *Mol Cancer Res*. 2021;19(5):771-783. doi:10.1158/1541-7786.MCR-20-0789

95. Metidji A, Omenetti S, Crotta S, et al. The Environmental Sensor AHR Protects from Inflammatory Damage by Maintaining Intestinal Stem Cell Homeostasis and Barrier Integrity. *Immunity*. 2018;49(2):353-362.e5. doi:10.1016/j.immuni.2018.07.010

96. Han H, Davidson LA, Fan Y, et al. Loss of aryl hydrocarbon receptor potentiates FoxM1 signaling to enhance self-renewal of colonic stem and progenitor cells. *EMBO J*. 2020;39(19). doi:10.15252/embj.2019104319

97. Alrafas HRD, Busbee B, Nagarkatti P, Nagarkatti M. Effect of 3,3′-Diindolylmethane on Gut Microbiome in Colorectal Cancer. *J Immunol*. 2018;200(1).

98. Kim YH, Kwon HS, Kim DH, et al. 3,3′-Diindolylmethane Attenuates Colonic Inflammation and Tumorigenesis in Mice. *Inflamm Bowel Dis*. 2009;15(8):1164-1173. doi:10.1002/ibd.20917

99. Qiu J, Guo X, Chen Z-ME, et al. Group 3 innate lymphoid cells inhibit T-cell-mediated intestinal inflammation through aryl hydrocarbon receptor signaling and regulation of microflora. *Immunity*. 2013;39(2):386-399. doi:10.1016/j.immuni.2013.08.002

100. Penrose HM, Heller S, Cable C, et al. High-fat diet induced leptin and Wnt expression: RNA-sequencing and pathway analysis of mouse colonic tissue and tumors. *Carcinogenesis*. 2017;38(3):302-311. doi:10.1093/carcin/bgx001

101. Chen J, Huang X-F. High fat diet-induced obesity increases the formation of colon polyps induced by azoxymethane in mice. *Ann Transl Med*. 2015;3(6):79. doi:10.3978/j.issn.2305-5839.2015.03.46

102. Gruber L, Kisling S, Lichti P, et al. High Fat Diet Accelerates Pathogenesis of Murine Crohn's Disease-Like Ileitis Independently of Obesity. *PLoS One*. 2013;8(8). doi:10.1371/journal.pone.0071661

103. Bekki K, Vogel H, Li W, et al. The aryl hydrocarbon receptor (AhR) mediates resistance to apoptosis induced in breast cancer cells. *Pestic Biochem Physiol*. 2015;120:5-13. doi:10.1016/j.pestbp.2014.12.021

104. Ronnekleiv-Kelly SM, Nukaya M, Díaz-Díaz CJ, et al. Aryl hydrocarbon receptor-dependent apoptotic cell death induced by the flavonoid chrysin in human colorectal cancer cells. *Cancer Lett*. 2016;370(1):91-99. doi:10.1016/j.canlet.2015.10.014

105. Krishnan S, Ding Y, Saedi N, et al. Gut Microbiota-Derived Tryptophan Metabolites Modulate Inflammatory Response in Hepatocytes and Macrophages. *Cell Rep*. 2018;23(4):1099-1111. doi:10.1016/j.celrep.2018.03.109

106. Biljes D, Hammerschmidt-kamper C, Merches K, Esser C. The Aryl Hydrocarbon Receptor In T Cells Contributes To Sustaining Oral Tolerance Against Ovalbumin In A Mouse Model. *EXCLI J*. 2017;16:291-301.

107. Walisser JA, Glover E, Pande K, Liss AL, Bradfield CA. Aryl hydrocarbon receptor-dependent liver development and hepatotoxicity are mediated by different cell types. *Pnas*. 2005;102(49):17858-17863. doi:10.1073/pnas.0504757102

108. The Jackson Laboratory. 006203 - STOCK Ahr/J. https://www.jax.org/strain/006203. Accessed October 17, 2017.

109. Walisser JA, Glover E, Pande K, Liss AL, Bradfield CA. Aryl hydrocarbon receptor-dependent liver development and hepatotoxicity are mediated by different cell types. *Proc Natl Acad Sci*. 2005;102(49):17858-17863. doi:10.1073/pnas.0504757102

110. Fan Y-Y, Davidson LA, Chapkin RS. Murine Colonic Organoid Culture System and Downstream Assay Applications. *Methods Mol Biol*. August 2016. doi:10.1007/7651_2016_8

111. Rosenberg DW, Giardina C, Tanaka T. Mouse models for the study of colon carcinogenesis. *Carcinogenesis*. 2009. doi:10.1093/carcin/bgn267

112. Goodrich JKK, Di Rienzi SC, Poole ACC, et al. Conducting a Microbiome Study. *Cell*. 2014;158(2):250-262. doi:10.1016/j.cell.2014.06.037

113. Weige CC, Allred KF, Allred CD. Estradiol Alters Cell Growth in Nonmalignant

Colonocytes and Reduces the Formation of Preneoplastic Lesions in the Colon. *Cancer Res*. 2009;69(23):9118-9124. doi:10.1158/0008-5472.CAN-09-2348

114. Davidson LA, Nguyen D V., Hokanson RM, et al. Chemopreventive n-3 polyunsaturated fatty acids reprogram genetic signatures during colon cancer initiation and progression in the rat. *Cancer Res*. 2004;64(18):6797-6804. doi:10.1158/0008-5472.CAN-04-1068

115. Dobin A, Davis CA, Schlesinger F, et al. STAR: Ultrafast universal RNA-seq aligner. *Bioinformatics*. 2013;29(1):15-21. doi:10.1093/bioinformatics/bts635

116. Robinson MD, McCarthy DJ, Smyth GK. edgeR: a Bioconductor package for differential expression analysis of digital gene expression data. *Bioinformatics*. 2010;26(1):139-140. doi:10.1093/bioinformatics/btp616

117. Sridharan G V., Choi K, Klemashevich C, et al. Prediction and quantification of bioactive microbiota metabolites in the mouse gut. *Nat Commun*. 2014;5. doi:10.1038/ncomms6492

118. Whitfield-Cargile CM, Cohen ND, Chapkin RS, et al. The microbiota-derived metabolite indole decreases mucosal inflammation and injury in a murine model of NSAID enteropathy. *Gut Microbes*. 2016;7(3):246-261. doi:10.1080/19490976.2016.1156827

119. Sridharan G V., Choi K, Klemashevich C, et al. Prediction and quantification of bioactive microbiota metabolites in the mouse gut. *Nat Commun*. 2014. doi:10.1038/ncomms6492

120. Megaraj V, Ding X, Fang C, Kovalchuk N, Zhu Y, Zhang QY. Role of hepatic and intestinal P450 enzymes in the metabolic activation of the colon carcinogen azoxymethane in mice. *Chem Res Toxicol*. 2014;27(4):656-662. doi:10.1021/tx4004769

121. Schiering C, Wincent E, Metidji A, et al. Feedback control of AHR signalling regulates intestinal immunity. *Nature*. 2017;542(7640):242-245. doi:10.1038/nature21080

122. Fan Y, Boivin GP, Knudsen ES, Nebert DW, Xia Y, Puga A. The aryl hydrocarbon receptor functions as a tumor suppressor of liver carcinogenesis. *Cancer Res*. 2010;70(1):212-220. doi:10.1158/0008-5472.CAN-09-3090

123. Velázquez KT, Enos RT, Carson MS, et al. Weight loss following diet-induced obesity does not alter colon tumorigenesis in the AOM mouse model. *Am J Physiol Liver Physiol*. 2016;311(4):G699-G712. doi:10.1152/ajpgi.00207.2016

124. Chang TP, Vancurova I. Bcl3 regulates pro-survival and pro-inflammatory gene expression in cutaneous T-cell lymphoma. *Biochim Biophys Acta - Mol Cell Res*. 2014;1843(11):2620-2630. doi:10.1016/j.bbamcr.2014.07.012

125. Wang L, Huang D, Jiang Z, et al. Akt3 is responsible for the survival and proliferation of embryonic stem cells. *Biol Open*. 2017;6(6):850-861. doi:10.1242/bio.024505

126. Xie Y, Wang B. Downregulation of TNFAIP2 suppresses proliferation and metastasis in esophageal squamous cell carcinoma through activation of the Wnt/β-catenin signaling pathway. *Oncol Rep*. 2017;37(5):2920-2928. doi:10.3892/or.2017.5557

127. Gouw LG, Reading NS, Jenson SD, Lim MS, Elenitoba-Johnson KSJ. Expression of the Rho-family GTPase gene RHOF in lymphocyte subsets and malignant lymphomas. *Br J Haematol*. 2005;129(4):531-533. doi:10.1111/j.1365-2141.2005.05481.x

128. Lebrun J-J. The Dual Role of TGFβ in Human Cancer: From Tumor Suppression to Cancer Metastasis. *ISRN Mol Biol*. 2012;2012:381428. doi:10.5402/2012/381428

129. Vanini F, Kashfi K, Nath N. The dual role of iNOS in cancer. *Redox Biol*. 2015;6:334-343. doi:10.1016/j.redox.2015.08.009

130. Kobayashi EH, Suzuki T, Funayama R, et al. Nrf2 suppresses macrophage inflammatory response by blocking proinflammatory cytokine transcription. *Nat Commun*. 2016;7(1):11624. doi:10.1038/ncomms11624

131. Graham DB, Jasso GJ, Mok A, et al. Nitric Oxide Engages an Anti-inflammatory Feedback Loop Mediated by Peroxiredoxin 5 in Phagocytes. *Cell Rep*. 2018;24(4):838-850. doi:10.1016/J.CELREP.2018.06.081

132. Mendelson K, Evans T, Hla T. Sphingosine 1-phosphate signalling. *Development*. 2014;141(1):5 LP - 9. doi:10.1242/dev.094805

133. Nikolaus S, Schulte B, Al-Massad N, et al. Increased Tryptophan Metabolism Is Associated With Activity of Inflammatory Bowel Diseases. *Gastroenterology*. 2017;153(6):1504-1516.e2. doi:10.1053/j.gastro.2017.08.028

134. Santoru ML, Piras C, Murgia A, et al. Cross sectional evaluation of the gut-microbiome metabolome axis in an Italian cohort of IBD patients. *Sci Rep*. 2017;7(1):9523. doi:10.1038/s41598-017-10034-5

135. Zelante T, Iannitti RG, Cunha C, et al. Tryptophan Catabolites from Microbiota Engage Aryl Hydrocarbon Receptor and Balance Mucosal Reactivity via Interleukin-22. *Immunity*. 2013;39:372-385. doi:10.1016/j.immuni.2013.08.003

136. Cervantes-Barragan L, Chai JN, Tianero MD, et al. Lactobacillus reuteri induces gut intraepithelial CD4+CD8αα+T cells. *Science (80-)*. 2017;357(6353):806-810. doi:10.1126/science.aah5825originally

137. Dragin N, Shi Z, Madan R, et al. Phenotype of the Cyp1a1 / 1a2 / 1b1 (-/ -) Triple-Knockout. *Mol Pharmacol*. 2008;73:1844-1856. doi:10.1124/mol.108.045658.

138. Carmody RN, Gerber GK, Luevano JM, et al. Diet dominates host genotype in shaping the murine gut microbiota. *Cell Host Microbe*. 2015;17(1):72-84. doi:10.1016/j.chom.2014.11.010

139. Sellin JH, Umar S, Xiao J, Morris AP. Increased beta-catenin expression and nuclear translocation accompany cellular hyperproliferation in vivo. *Cancer Res*. 2001;61(7):2899-2906.

140. Clevers H, Nusse R. Wnt/β-Catenin Signaling and Disease. *Cell*. 2012;149(6):1192-1205. doi:10.1016/J.CELL.2012.05.012

141. Laukens D, Brinkman BM, Raes J, De Vos M, Vandenabeele P. Heterogeneity of the gut microbiome in mice: Guidelines for optimizing experimental design. *FEMS Microbiol Rev*. 2015;40(1):117-132. doi:10.1093/femsre/fuv036

142. Di Gregorio C, Losi L, Fante R, et al. Histology of aberrant crypt foci in the human colon. *Histopathology*. 1997;30(4):328-334. doi:10.1046/j.1365-2559.1997.d01-626.x

143. Kim E, Davidson LA, Zoh RS, et al. Rapidly cycling Lgr5+ stem cells are exquisitely sensitive to extrinsic dietary factors that modulate colon cancer risk. *Cell Death Dis*. 2016;7(11):e2460-e2460. doi:10.1038/cddis.2016.269

144. Schindelin J, Arganda-Carreras I, Frise E, et al. Fiji: an open-source platform for biological-image analysis. *Nat Methods*. 2012;9(7):676-682. doi:10.1038/nmeth.2019

145. Kozich JJ, Westcott SL, Baxter NT, Highlander SK, Schloss PD. Development of a Dual-Index Sequencing Strategy and Curation Pipeline for Analyzing Amplicon Sequence Data on the MiSeq Illumina Sequencing Platform. *Appl Environ Microbiol*. 2013;79(17):5112-5120. doi:10.1128/AEM.01043-13

146. Kawajiri K, Fujii-Kuriyama Y. The aryl hydrocarbon receptor: a multifunctional chemical sensor for host defense and homeostatic maintenance. *Exp Anim*. 2017;66(2):75-89. doi:10.1538/expanim.16-0092

147. Korecka A, Dona A, Lahiri S, et al. Bidirectional communication between the Aryl hydrocarbon Receptor (AhR) and the microbiome tunes host metabolism. *npj Biofilms Microbiomes*. 2016;2(1):16014. doi:10.1038/npjbiofilms.2016.14

148. Novellasdemunt L, Antas P, Li VSW. Targeting Wnt signaling in colorectal cancer. A Review in the Theme: Cell Signaling: Proteins, Pathways and Mechanisms. *Am J Physiol Cell Physiol*. 2015;309(8):C511-21. doi:10.1152/ajpcell.00117.2015

149. Zhan T, Rindtorff N, Boutros M. Wnt signaling in cancer. *Oncogene*. 2017;36(11):1461-1473. doi:10.1038/onc.2016.304

150. Xing Pei Hao, Pretlow TG, Rao JS, Pretlow TP. β-catenin expression is altered in human colonic aberrant crypt foci. *Cancer Res*. 2001;64(22):8085–8088. https://cancerres.aacrjournals.org/content/61/22/8085.article-info.

151. Zhang D, Fei F, Li S, et al. The role of β-catenin in the initiation and metastasis of TA2 mice spontaneous breast cancer. *J Cancer*. 2017;8(11):2114-2123. doi:10.7150/jca.19723

152. De P, Carlson JH, Wu H, et al. Wnt-beta-catenin pathway signals metastasis-associated tumor cell phenotypes in triple negative breast cancers. *Oncotarget*. 2016;7(28):43124-43149. doi:10.18632/oncotarget.8988

153. Yang C-M, Ji S, Li Y, Fu L-Y, Jiang T, Meng F-D. β-Catenin promotes cell proliferation, migration, and invasion but induces apoptosis in renal cell carcinoma. *Onco Targets Ther*. 2017;10:711-724. doi:10.2147/OTT.S117933

154. Damsky WE, Curley DP, Santhanakrishnan M, et al. β-Catenin Signaling Controls Metastasis in Braf-Activated Pten-Deficient Melanomas. *Cancer Cell*. 2011;20(6):741-754. doi:10.1016/j.ccr.2011.10.030

155. Yang Y, Smith DL, Keating KD, Allison DB, Nagy TR. Variations in body weight, food intake and body composition after long-term high-fat diet feeding in C57BL/6J mice. *Obesity*. 2014;22(10):2147-2155. doi:10.1002/oby.20811

156. Karunanithi S, Levi L, DeVecchio J, et al. RBP4-STRA6 Pathway Drives Cancer Stem Cell Maintenance and Mediates High-Fat Diet-Induced Colon Carcinogenesis. *Stem cell reports*. 2017;9(2):438-450. doi:10.1016/j.stemcr.2017.06.002

157. Doerner SK, Reis ES, Leung ES, et al. High-fat diet-induced complement activation 1 mediates intestinal inflammation and neoplasia, independent of obesity 2 3. 2016. doi:10.1158/1541-7786.MCR-16-0153

158. Derrien M, Vaughan EE, Plugge CM, de Vos WM. Akkermansia municiphila gen. nov., sp. nov., a human intestinal mucin-degrading bacterium. *Int J Syst Evol Microbiol*. 2004;54(5):1469–1476. doi:10.1099/ijs.0.02873-0

159. Derrien M, Belzer C, de Vos WM. Akkermansia muciniphila and its role in regulating host functions. *Microb Pathog*. 2017;106:171-181. doi:10.1016/j.micpath.2016.02.005

160. Derrien M, Van Baarlen P, Hooiveld G, Norin E, Müller M, de Vos WM. Modulation of Mucosal Immune Response, Tolerance, and Proliferation in Mice Colonized by the Mucin-Degrader Akkermansia muciniphila. *Front Microbiol*. 2011;2:166. doi:10.3389/fmicb.2011.00166

161. Niv Y. MUC1 and colorectal cancer pathophysiology considerations. *World J Gastroenterol*. 2008;14(14):2139-2141. doi:10.3748/wjg.14.2139

162. Li W, Zhang N, Jin C, et al. MUC1-C drives stemness in progression of colitis to colorectal cancer. *JCI Insight*. 2020;5(12). doi:10.1172/JCI.INSIGHT.137112

163. van der Lugt B, van Beek AA, Aalvink S, et al. Akkermansia muciniphila ameliorates the age-related decline in colonic mucus thickness and attenuates immune activation in accelerated aging Ercc1−/Δ7 mice. *Immun Ageing*. 2019;16(1):6. doi:10.1186/s12979-019-0145-z

164. Gulhane M, Murray L, Lourie R, et al. High Fat Diets Induce Colonic Epithelial Cell Stress and Inflammation that is Reversed by IL-22. *Sci Rep*. 2016;6:28990. doi:10.1038/srep28990

165. Zhang C, Zhang M, Pang X, Zhao Y, Wang L, Zhao L. Structural resilience of the gut microbiota in adult mice under high-fat dietary perturbations. *ISME J*. 2012;6(10). doi:10.1038/ismej.2012.27

166. Leslie M. Immunity goes local. *Science (80-)*. 2016;352(6281):21-23. doi:10.1126/science.352.6281.21

167. Sautès-Fridman C, Lawand M, Giraldo NA, et al. Tertiary lymphoid structures in cancers: Prognostic value, regulation, and manipulation for therapeutic intervention. *Front Immunol*. 2016;7(OCT):1-11. doi:10.3389/fimmu.2016.00407

168. Di Caro G, Bergomas F, Grizzi F, et al. Occurrence of tertiary lymphoid tissue is associated with T-cell infiltration and predicts better prognosis in early-stage

colorectal cancers. *Clin Cancer Res*. 2014;20(8):2147-2158. doi:10.1158/1078-0432.CCR-13-2590

169. Olivier BJ, Cailotto C, van der Vliet J, et al. Vagal innervation is required for the formation of tertiary lymphoid tissue in colitis. *Eur J Immunol*. 2016;46(10):2467-2480. doi:10.1002/eji.201646370

170. Lochner M. Tertiary lymphoid tissues in the colon: Friend and foe. *Gut Microbes*. 2011;2(3):193-197. doi:10.4161/gmic.2.3.16732

171. Thomson CA, Ho E, Strom MB. Chemopreventive properties of 3,30-diindolylmethane in breast cancer: Evidence from experimental and human studies. *Nutr Rev*. 2016;74(7):432-443. doi:10.1093/nutrit/nuw010

172. Lee B, Moon KM, Kim CY. Tight junction in the intestinal epithelium: Its association with diseases and regulation by phytochemicals. *J Immunol Res*. 2018;2018(Figure 2). doi:10.1155/2018/2645465

173. Scott SA, Fu J, Chang P V. Microbial tryptophan metabolites regulate gut barrier function via the aryl hydrocarbon receptor. *Proc Natl Acad Sci U S A*. 2020;117(32):19376-19387. doi:10.1073/pnas.2000047117

174. Gutiérrez-Vázquez C, Quintana FJ. Regulation of the Immune Response by the Aryl Hydrocarbon Receptor. *Immunity*. 2018. doi:10.1016/j.immuni.2017.12.012

175. Owens BMJ, Simmons A. Intestinal stromal cells in mucosal immunity and homeostasis. *Mucosal Immunol*. 2013;6(2):224-234. doi:10.1038/mi.2012.125

176. Barone F, Nayar S, Campos J, et al. IL-22 regulates lymphoid chemokine production and assembly of tertiary lymphoid organs. *Proc Natl Acad Sci*. 2015;112(35). doi:10.1073/pnas.1503315112

177. Saez de Guinoa J, Barrio L, Mellado M, Carrasco YR. CXCL13/CXCR5 signaling enhances BCR-triggered B-cell activation by shaping cell dynamics. *Blood*. 2011;118(6):1560-1569. doi:10.1182/blood-2011-01-332106

178. The Jackson Laboratory. CDX2P-CreERT2. Mouse Strain Datasheet - 022390. https://www.jax.org/strain/022390. Published 2018. Accessed March 8, 2019.

179. Diet Dose Calculator- Research Diets, Inc. - Research Diets, Inc. https://www.researchdiets.com/opensource-diets/add-test-compounds/diet-dose-calculator. Accessed July 12, 2020.

180. Dame MK, Jiang Y, Appelman HD, et al. Human colonic crypts in culture: segregation of immunochemical markers in normal versus adenoma-derived. *Lab Investig*. 2014;94(2):222-234. doi:10.1038/labinvest.2013.145

181. CREAMER B, SHORTER RG, BAMFORTH J. The turnover and shedding of epithelial cells. I. The turnover in the gastro-intestinal tract. *Gut*. 1961;2(2):110-118. doi:10.1136/gut.2.2.110

182. Solomon L, Mansor S, Mallon P, et al. The dextran sulphate sodium (DSS) model of colitis: An overview. *Comp Clin Path*. 2010;19(3):235-239. doi:10.1007/s00580-010-0979-4

183. Chassaing B, Aitken JD, Malleshappa M, Vijay-Kumar M. Dextran Sulfate Sodium (DSS)-Induced Colitis in Mice. *Curr Protoc Immunol*. 2014;104(1):Unit. doi:10.1002/0471142735.im1525s104

184. Singh N, Gurav A, Sivaprakasam S, et al. Activation of Gpr109a, Receptor for Niacin and the Commensal Metabolite Butyrate, Suppresses Colonic Inflammation and Carcinogenesis. *Immunity*. 2014;40(1):128-139. doi:10.1016/j.immuni.2013.12.007

185. Murthy SNS, Cooper HS, Shim H, Shah RS, Ibrahim SA, Sedergran DJ. Treatment of dextran sulfate sodium-induced murine colitis by intracolonic cyclosporin. *Dig Dis Sci*. 1993;38(9):1722-1734. doi:10.1007/BF01303184

186. Bankhead P, Loughrey MB, Fernández JA, et al. QuPath: Open source software for digital pathology image analysis. *Sci Rep*. 2017;7(1):1-7. doi:10.1038/s41598-017-17204-5

187. AppliedBiosystems. *Real-Time PCR: Understanding Ct*.; 2016.

https://www.thermofisher.com/content/dam/LifeTech/Documents/PDFs/PG1503-PJ9169-CO019879-Re-brand-Real-Time-PCR-Understanding-Ct-Value-Americas-FHR.pdf. Accessed July 23, 2020.

188. Spencer J, Sollid LM. The human intestinal B-cell response. *Mucosal Immunol*. 2016;9(5):1113-1124. doi:10.1038/mi.2016.59

189. Hageman JH, Heinz MC, Kretzschmar K, van der Vaart J, Clevers H, Snippert HJG. Intestinal Regeneration: Regulation by the Microenvironment. *Dev Cell*. 2020;54(4):435-446. doi:10.1016/j.devcel.2020.07.009

190. Odenwald MA, Turner JR. The intestinal epithelial barrier: a therapeutic target? *Nat Rev Gastroenterol Hepatol*. 2017;14(1):9-21. doi:10.1038/nrgastro.2016.169

191. Chassaing B, Srinivasan G, Delgado MA, Young AN, Gewirtz AT, Vijay-Kumar M. Fecal Lipocalin 2, a Sensitive and Broadly Dynamic Non-Invasive Biomarker for Intestinal Inflammation. *PLoS One*. 2012;7(9):3-10. doi:10.1371/journal.pone.0044328

192. Moschen AR, Adolph TE, Gerner RR, Wieser V, Tilg H. Lipocalin-2: A Master Mediator of Intestinal and Metabolic Inflammation. *Trends Endocrinol Metab*. 2017;28(5):388-397. doi:10.1016/j.tem.2017.01.003

193. Toyonaga T, Matsuura M, Mori K, et al. Lipocalin 2 prevents intestinal inflammation by enhancing phagocytic bacterial clearance in macrophages. *Sci Rep*. 2016;6(1):35014. doi:10.1038/srep35014

194. Klein SL. Immune cells have sex and so should journal articles. *Endocrinology*. 2012;153(6):2544-2550. doi:10.1210/en.2011-2120

195. Taneja V. Sex Hormones Determine Immune Response. *Front Immunol*. 2018;9:1931. doi:10.3389/fimmu.2018.01931

196. Scharff AZ, Rousseau M, Mariano LL, et al. Sex differences in IL-17 contribute to chronicity in male versus female urinary tract infection. *JCI Insight*. 2019;4(13). doi:10.1172/JCI.INSIGHT.122998

197. Galligan CL, Fish EN. Sex Differences in the Immune Response. In: *Sex and Gender Differences in Infection and Treatments for Infectious Diseases*. Cham: Springer International Publishing; 2015:1-29. doi:10.1007/978-3-319-16438-0_1

198. Perše M, Cerar A. Dextran sodium sulphate colitis mouse model: Traps and tricks. *J Biomed Biotechnol*. 2012;2012. doi:10.1155/2012/718617

199. Hall LJ, Faivre E, Quinlan A, Shanahan F, Nally K, Melgar S. Induction and activation of adaptive immune populations during acute and chronic phases of a murine model of experimental colitis. *Dig Dis Sci*. 2011;56(1):79-89. doi:10.1007/s10620-010-1240-3

200. Paijens ST, Vledder A, de Bruyn M, Nijman HW. Tumor-infiltrating lymphocytes in the immunotherapy era. *Cell Mol Immunol*. 2021;18(4):842-859. doi:10.1038/s41423-020-00565-9

201. Posch F, Silina K, Leibl S, et al. Maturation of tertiary lymphoid structures and recurrence of stage II and III colorectal cancer. *Oncoimmunology*. 2018;7(2). doi:10.1080/2162402X.2017.1378844

202. Jacenik D, Krajewska WM. Significance of G Protein-Coupled Estrogen Receptor in the Pathophysiology of Irritable Bowel Syndrome, Inflammatory Bowel Diseases and Colorectal Cancer. *Front Endocrinol (Lausanne)*. 2020;11:390. doi:10.3389/fendo.2020.00390

203. Klein SL, Flanagan KL. Sex differences in immune responses. *Nat Rev Immunol*. 2016;16(10):626-638. doi:10.1038/nri.2016.90

204. Alexeev EE, Lanis JM, Kao DJ, et al. Microbiota-Derived Indole Metabolites Promote Human and Murine Intestinal Homeostasis through Regulation of Interleukin-10 Receptor. *Am J Pathol*. 2018;188(5):1183-1194. doi:10.1016/j.ajpath.2018.01.011

205. Kim JY, Le TAN, Lee SY, et al. 3,3′-Diindolylmethane Improves Intestinal Permeability Dysfunction in Cultured Human Intestinal Cells and the Model Animal *Caenorhabditis elegans*. *J Agric Food Chem*. 2019:acs.jafc.9b03039. doi:10.1021/acs.jafc.9b03039

206. Zhang Y, Li Y. Inflammatory Bowel Disease: Crossroads of Microbes, Epithelium and Immune Systems. *World J Gastroenterol*. 2014;20(1):91-99. doi:10.3748/wjg.v20.i1.91

207. van der Giessen J, van der Woude C, Peppelenbosch M, Fuhler G. A Direct Effect of Sex Hormones on Epithelial Barrier Function in Inflammatory Bowel Disease Models. *Cells*. 2019;8(3):261. doi:10.3390/cells8030261

208. Braniste V, Leveque M, Buisson-Brenac C, Bueno L, Fioramonti J, Houdeau E. Oestradiol decreases colonic permeability through oestrogen receptor beta-mediated up-regulation of occludin and junctional adhesion molecule-A in epithelial cells. *J Physiol*. 2009;587(Pt 13):3317-3328. doi:10.1113/jphysiol.2009.169300

209. Vivar OI, Saunier EF, Leitman DC, Firestone GL, Bjeldanes LF. Selective activation of estrogen receptor-beta target genes by 3,3'-diindolylmethane. *Endocrinology*. 2010;151(4):1662-1667. doi:10.1210/en.2009-1028

210. Leong H, Riby JE, Firestone GL, Bjeldanes LF. Potent ligand-independent estrogen receptor activation by 3,3'-diindolylmethane is mediated by cross talk between the protein kinase A and mitogen-activated protein kinase signaling pathways. *Mol Endocrinol*. 2004;18(2):291-302. doi:10.1210/me.2003-0196

211. Matthews Ja, Gustafsson J-Å. Estrogen receptor and aryl hydrocarbon receptor signaling pathways. *Nucl Recept Signal*. 2006;4(e016). doi:10.1621/nrs.04016

212. Safe S, Wormke M. Inhibitory aryl hydrocarbon receptor-estrogen receptor α cross-talk and mechanisms of action. *Chem Res Toxicol*. 2003;16(7):807-816. doi:10.1021/tx034036r

213. Swedenborg E, Pongratz I. AhR and ARNT modulate ER signaling. *Toxicology*. 2010;268(3):132-138. doi:10.1016/J.TOX.2009.09.007

214. Rüegg J, Swedenborg E, Wahlström D, et al. The Transcription Factor Aryl Hydrocarbon Receptor Nuclear Translocator Functions as an Estrogen Receptor β-Selective Coactivator, and Its Recruitment to Alternative Pathways Mediates Antiestrogenic Effects of Dioxin. *Mol Endocrinol*. 2008;22(2):304-316. doi:10.1210/me.2007-0128

215. Brunnberg S, Pettersson K, Rydin E, Matthews J, Hanberg A, Pongratz I. The basic helix-loop-helix-PAS protein ARNT functions as a potent coactivator of estrogen receptor-dependent transcription. *Proc Natl Acad Sci*. 2003;100(11):6517-6522. doi:10.1073/pnas.1136688100

216. Saleiro D, Murillo G, Benya R V., Bissonnette M, Hart J, Mehta RG. Estrogen receptor-β protects against colitis-associated neoplasia in mice. *Int J Cancer*. 2012;131(11):2553-2561. doi:10.1002/ijc.27578

217. Tadesse S, Corner G, Dhima E, et al. MUC2 mucin deficiency alters inflammatory and metabolic pathways in the mouse intestinal mucosa. *Oncotarget*. 2017;8(42):71456-71470. doi:10.18632/oncotarget.16886

218. Wang J, Wang P, Tian H, et al. Aryl hydrocarbon receptor/IL-22/Stat3 signaling pathway is involved in the modulation of intestinal mucosa antimicrobial molecules by commensal microbiota in mice. *Innate Immun*. 2018;24(5):297-306. doi:10.1177/1753425918785016

219. Wang G-Z, Cheng X, Zhou B, et al. The chemokine CXCL13 in lung cancers associated with environmental polycyclic aromatic hydrocarbons pollution. *Elife*. 2015;4(e09419). doi:10.7554/eLife.09419

220. Barata JT, Durum SK, Seddon B. Flip the coin: IL-7 and IL-7R in health and disease. *Nat Immunol*. 2019;20(12):1584-1593. doi:10.1038/s41590-019-0479-x

221. Ji T, Xu C, Sun L, et al. Aryl Hydrocarbon Receptor Activation Down-Regulates IL-7 and Reduces Inflammation in a Mouse Model of DSS-Induced Colitis. *Dig Dis Sci*. 2015;60(7):1958-1966. doi:10.1007/s10620-015-3632-x

222. Qiu J, Heller JJ, Guo X, et al. The aryl hydrocarbon receptor regulates gut immunity through modulation of innate lymphoid cells. *Immunity*. 2012;36(1):92-104. doi:10.1016/j.immuni.2011.11.011

223. Leivonen SK, Pollari M, Brück O, et al. T-cell inflamed tumor microenvironment predicts favorable prognosis in primary testicular lymphoma. *Haematologica*. 2019;104(2):338-346. doi:10.3324/haematol.2018.200105

224. Visikol. In Vitro Immuno-Oncology Immune Cell Infiltration. https://visikol.com/services/in-vitro/t-cell-infiltration/. Accessed May 25, 2021.

225. Gong C, Anders RA, Zhu Q, et al. Quantitative characterization of CD8+ T cell clustering and spatial heterogeneity in solid tumors. *Front Oncol*. 2019;9(JAN):649. doi:10.3389/fonc.2018.00649

APPENDIX A

DIET COMPOSITION: LOW-FAT DIET

Open formula purified diets for lab animals

OpenSource DIETS®

Report ▸ Repeat ▸ Revise

Product Data - D12450B

Description
Rodent Diet with 10% kcal% fat.

Used in Research
Obesity
Diabetes

Packaging
Product is packed in 12.5 kg box. Each box is identified with the product name, description, lot number and expiration date.

Lead Time
IN-STOCK.
Ready for next day shipment.

Gamma-Irradiation
Yes. Add 10 days to delivery time.

Form
Pellet, Powder, Liquid

Shelf Life
Most diets require storage in a cool dry environment. Stored correctly they should last 6 months.

Control Diets
Used as a control diet for D12451 and D12492

Sucrose Content
35% Sucrose
See D12450J, K, H for other options.

Formula

Product #D12450B		gm%	kcal%
Protein		19.2	20
Carbohydrate		67.3	70
Fat		4.3	10
	Total		100
	kcal/gm	3.85	

Ingredient	gm	kcal
Casein, 30 Mesh	200	800
L-Cystine	3	12
Corn Starch	315	1260
Maltodextrin 10	35	140
Sucrose	350	1400
Cellulose, BW200	50	0
Soybean Oil	25	225
Lard*	20	180
Mineral Mix S10026	10	0
DiCalcium Phosphate	13	0
Calcium Carbonate	5.5	0
Potassium Citrate, 1 H2O	16.5	0
Vitamin Mix V10001	10	40
Choline Bitartrate	2	0
FD&C Yellow Dye #5	0.05	0
Total	**1055.05**	**4057**

Formulated by E. A. Ulman, Ph.D., Research Diets, Inc., 8/26/98 and 3/11/99.

*Typical analysis of cholesterol in lard = 0.72 mg/gram.
Cholesterol (mg)/4057 kcal = 54.4
Cholesterol (mg)/kg = 51.6

RESEARCH DIETS INC.
www.ResearchDiets.com
Where NutriPhenomics Begins

Research Diets, Inc.
20 Jules Lane
New Brunswick, NJ 08901 USA
Tel: 732.247.2390
Fax: 732.247.2340
info@researchdiets.com

APPENDIX B

DIET COMPOSITION: HIGH-FAT DIET

Open formula purified diets for lab animals

Product Data - D12492

OpenSource DIETS®

Report ▸ Repeat ▸ Revise

Description
Rodent Diet with 60% kcal% fat.

Used in Research
Fatty Liver
Inflammation
Obesity
Diabetes

Packaging
Product is packed in 12.5 kg box. Each box is identified with the product name, description, lot number and expiration date.

Lead Time
IN-STOCK.
Ready for next day shipment.

Gamma-Irradiation
Yes. Add 10 days to delivery time.

Form
Pellet, Powder, Liquid

Shelf Life
Most diets require storage in a cool dry environment. Stored correctly they should last 6 months. Because of the high fat content is best if kept frozen.

Control Diets
D12450B, D12450J, D12450K

Formula

Product #D12492		gm%	kcal%
Protein		26.2	20
Carbohydrate		26.3	20
Fat		34.9	60
	Total		100
	kcal/gm	5.24	

Ingredient	gm	kcal
Casein, 30 Mesh	200	800
L-Cystine	3	12
Corn Starch	0	0
Maltodextrin 10	125	500
Sucrose	68.8	275.2
Cellulose, BW200	50	0
Soybean Oil	25	225
Lard*	245	2205
Mineral Mix S10026	10	0
DiCalcium Phosphate	13	0
Calcium Carbonate	5.5	0
Potassium Citrate, 1 H2O	16.5	0
Vitamin Mix V10001	10	40
Choline Bitartrate	2	0
FD&C Blue Dye #1	0.05	0
Total	**773.85**	**4057**

Formulated by E. A. Ulman, Ph.D., Research Diets, Inc., 8/26/98 and 3/11/99.

*Typical analysis of cholesterol in lard = 0.72 mg/gram.
Cholesterol (mg)/4057 kcal = 216.4
Cholesterol (mg)/kg = 279.6

RESEARCH DIETS INC.
www.ResearchDiets.com
Where NutriPhenomics Begins

Research Diets, Inc.
20 Jules Lane
New Brunswick, NJ 08901 USA
Tel: 732.247.2390
Fax: 732.247.2340
info@researchdiets.com

APPENDIX C

DIET COMPOSITION: AIN-76A

Open formula purified diets for lab animals

Product Data - D10001

OpenSource DIETS®

Report ▸ Repeat ▸ Revise

Description
AIN-76A- widely used, balanced, purified rodent diet.

Used in Research
Obesity
Diabetes
Osteoporosis
Hypertension
Atherosclerosis
Metabolic Syndrome

Packaging
Product is packed in 12.5 kg box. Each box is identified with the product name, description, lot number and expiration date.

Lead Time
IN-STOCK.
Ready for next day shipment.

Gamma-Irradiation
Yes. Add 10 days to delivery time.

Form
Pellet, Powder, Liquid

Shelf Life
Most diets require storage in a cool dry environment. Stored correctly they should last 6 months.

Control Diets
Used as a control diet, compound addition, for imaging studies, phytoestrogen-free diet.

Formula

Product # D10001		gm%	kcal%
Protein		20.3	20.8
Carbohydrate		66.0	67.7
Fat		5.0	11.5
	Total		100.0
	kcal/gm	3.90	

Ingredient	gm	kcal
Casein, 30 Mesh	200	800
DL-Methionine	3	12
Corn Starch	150	600
Sucrose	500	2000
Cellulose, BW 200	50	0
Corn Oil	50	450
Mineral Mix S10001	35	0
Vitamin Mix V10001	10	40
Choline Bitartrate	2	0
Total	**1000**	**3902**

References

D10001 (a.k.a. AIN-76A)

1. American Institute of Nutrition. AIN report of the AIN ad hoc committee on standards for nutritional studies.J. Nutr. 107: 1340-1348, 1977.
2. American Institute of Nutrition. AIN second report of the AIN ad hoc committee on standards for nutritional studies. J. Nutr. 110:1726, 1980.
3. Clinton SK , Mulloy AL, Li SP, Manglan HJ, & Visek WJ. Dietary Fat and Protein Intake Differ in Modulation of Prostate Tumor Growth, Prolactin Secretion and Metabolism, and Prostate Gland Prolactin Binding Capacity in Rats. J. Nutr. 127:225-237, 1997.

RESEARCH DIETS INC.
www.ResearchDiets.com
Where NutriPhenomics Begins

Research Diets, Inc.
20 Jules Lane
New Brunswick, NJ 08901 USA
Tel: 732.247.2390
Fax: 732.247.2340
info@researchdiets.com

APPENDIX D

MIXING TEST COMPOUNDS INTO A POWERED STANDARD RODENT DIET

Materials

- 3,3′-Diindolylmethane (D9568, Sigma-Aldrich)
- Powder semi-purified diet AIN-76A (Research Diets Inc., D10001)

Equipment

- Mixing bowls of different sizes (cleaned and dried)
- Commercial stand mixer (10 Qt.) (Clean and dry mixing bowl in advance)
- Commercial stand mixer (60 Qt.) (Clean and dry mixing bowl in advance)
- Spatulas (silicon)
- Platform (industrial) scale
- Precision lab scale

Safety

- Use PPE (gloves, lab coat and googles) for the entirety of the procedure.

Procedure

1. Pre-weight 1,402 mg of DIM using a precision lab scale
2. In a small bowl mix equal parts of DIM and powder diet thoroughly for 5 minutes.
3. Duplicate the combined amounts (3 grams) of powder diet and mix. Duplicate once more the amount (6 grams) of diet and mix. Repeat the process until reaching a volume of 2 cups.
4. Move the mix into a 10 Qt stan mixer and duplicate the amount of the diet using cups as units of volume (4 cups) and mix in level 1 for 10 min.
5. Add equal parts of the amount of powder diet (4 cups) and mix at level 1 for 5 min. Continue this process until the maximum volume in the mixing bowl is reached.
6. Transfer the contents of the mixing bowl into the 60 Qt mixing bowl and add equal parts of powder diet (10 Qt) and mix for 10 minutes. Continue adding the rest of the powder diet in equal increments and mix for 5 minutes each time until the last of the powder diet is added. Mix for another 10 minutes.
7. Pack the diet in 5 Kg batches using airtight containers and label accordingly.

Storage

- Maintain the powdered diet in an airtight container protected from light at -20 °C

APPENDIX E

IMMUNOHISTOCHEMISTRY OF T-CELL AND B-CELL MARKERS FOR PFA-FIXED COLON

Antibodies and reagents

B-cells

- Blocking agent: 5% donkey serum in PBS (S30-100mL, Millipore)
- Primary AB: Rat monoclonal anti- CD45R (B220) (clone: RA3-6B2), eBioscience/Thermo Fisher; Catalog # 14-0452-82
- Secondary AB: Donkey anti-Rat IgG – Alexa Fluor 647 (Cy5-Far Red) – Abcam: ab150155.

T-cells

- Blocking agent: 5% goat serum in PBS (ab7481, Abcam)
- Primary AB: Armenian hamster (IgG) monoclonal anti-CD3ε (clone: 145-2C11), eBioscience/Thermo Fisher; Catalog # 14-0031-82
- Secondary AB: Goat anti-Armenian hamster (IgG) H&L (Alexa Fluor 647) – Abcam: ab173004

Solutions

1. 10mM sodium citrate (Sigma, S4641)
2. Ethanol (KOPEC, V1001) 100%, 95%, 70%, and Xylene (Fisher, X2P-1GAL)
3. dH2O (Gibco, 15230-170) (Nanopure fine, but filter it)
4. 1X PBS
5. BSTt buffer (1x PBS with 0.2% Tween-20 (Sigma, P9416))

Other materials

1. Slide Holders
2. PAP Pen
3. Metal Pot
4. Dark moisture chamber
5. Coverslip
6. Nail Polish

Procedure:

___ Prepare 1.2 L of 10 mM sodium citrate, pH 6.0 (3.52 g sodium citrate trisodium ($C_6H_5Na_3O_7 \cdot 2H_20$) in 850 ml H_2O, adjust pH to 6.0 and then take final volume of 1.2 L). Preheat on hot plate by bringing to a boil at the level 10 on Thermolyne heat plate and once boiling, switch to level 5.9. **We want to make sure the solution is NOT bubbling at all once the tissues go in**

Deparaffinization/Rehydration

___ ___ ___ Xylene 3X 5 min

___ ___ ___ 100% ethanol 3X 4 min

___ ___ ___ 95% ethanol 3X 4 min

___ ___ 70% ethanol 2 x 4 min

___ ___ ___ dH_2O 3X 3 min

NOTE: Do not allow slides to dry at any time during this procedure.

Antigen retrieval

____ 20 min in sub-boiling (95-98 °C) citrate in metal pot.

____ Cool metal pot for 20 min in tub of tap water.

___ ___ ___ Cold PBS* 3x 5 min (shake)

___ Circle with PAP pen if needed **Make a thick circle and dry out completely**

Blocking

___ Block using 5% **normal serum** in PBS for 1 hr at RT (In Coplin Jars)

T cells	**B cells**
5% Goat serum in PBS 40 ml= 38 ml PBS + 2 ml goat serum	5% Donkey serum in PBS 40 ml= 38 ml PBS + 2 ml donkey serum

Primary Ab incubation

___ Dilute primary Ab (75 µl per slide) in 5% normal serum (PBS)

T cells	**B cells**
Anti-CD3e [1:50 dilution] in 5% Goat serum Negative: 75 µl 5% goat serum Positive (x6): 441 µl 5% goat serum + 9 µl Ab	**Anti-CD45R** [1:100] 5% donkey serum Negative: 75 µl 5% donkey serum Positive (x6): 445.5 µl 5% donkey serum + 4.5 µl Ab

___ Put slides in the immune stain moisture chamber and **add primary antibody**

___ Incubate overnight @ 4°C in a humidified chamber

___ Tap off the solution

___ ___ ___ Wash in PBS-T, 3X - 5 min each (rocking)

Secondary Ab incubation

___ Dilute secondary Abs in 5% normal serum *(100 µl per slide)*

T cells	**B cells**
Goat anti-ArmHamster – AF 647 [1:500] in 5% goat serum Positive (x6): 598.8 µl 5% goat serum + 1.2 µl Ab	**Donkey anti-Rat – AF 647** [1:500] in 5% donkey serum Positive (x6): 598.8 µl 5% goat serum + 1.2 µl Ab

___ Incubate for 1 hr @ RT in the dark

___ Tap off the solution

___ ___ ___ Wash in PBS-T, 3 times - 5 min each

___ ___ ___ Wash with Nanopure Water, 3 times – 5 min each

Coverslip slides

___ Coverslip with ProlongGold Antifade with DAPI overnight @RT (protect from light)

APPENDIX F

ASSESSMENT OF T-CELL AND B-CELL DENSITY AND B:T CELL RATIO

The assessment of **T and B cell density** was based in previously published methodologies targeted to assess T cell infiltration in primary tumors.[223–225] This analysis was performed in previously stained tissues from DSS-treated animals using ImageJ/Fiji (V. 2.1.0/1.53c). **T cell density**. Transform RBG images to binary (16 Bits) and adjust threshold using the Automatic Intermodes setting on Red (channel). Draw the three regions of interest (ROI) at 1) TLT, 2)1.5X the TLT size and 3) 2.0X the TLT size using the oval tool as indicated in **Figure F**. Apply threshold and run the following script (using the "analyze particles" tool, circularity=0.00-1.0) and save the area of each ROI. Calculate cell density (#cell/ area in pixels^2) on a calculation spreadsheet and conduct statistical analysis. Each TLT is considered as an individual sample in terms of analysis, n=5; 4 animals/ treatment group (n=8).

Script:

```
macro "tCount Action Tool - C059T3e16?"{
      numROIs = roiManager("Count");
      imgID = getImageID();
      fileDir = getDir("home")+"/fijiTemp/";
      for (i=0 ; i<numROIs; i++) {
          selectImage(imgID);
          roiManager("select", i);
          run("Duplicate...","  ");
          copyID = getImageID();
          run("Analyze Particles...", "size=0-Infinity
circularity=0.00-1.00 show=Nothing clear display summarize");
          selectImage(copyID);
          close();
      }
      if (isOpen("Results")) {
         selectWindow("Results");
         run("Close");
    }
```

```
}
```

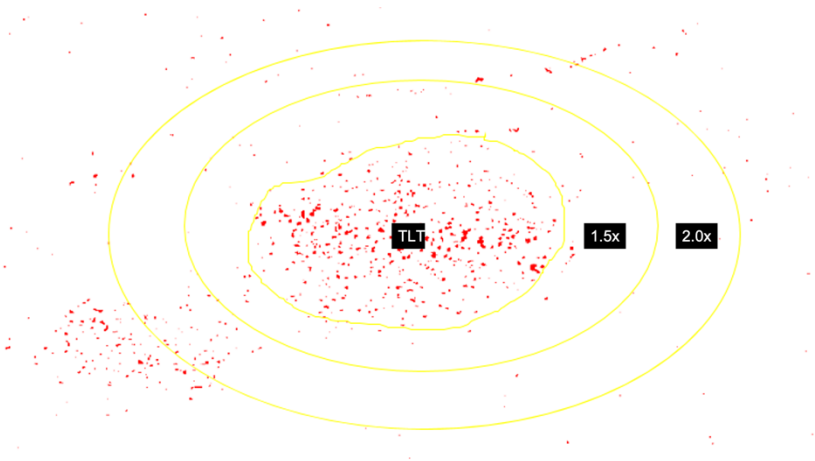

Figure F. ROI for T-cell distribution with respect to TLT location

B cell density. Transform RBG images to binary (16 Bits) and adjust threshold using the Automatic Intermodes setting on Red (channel). Draw the ROI at the TLT location using the oval tool. Apply threshold and run the following script (using the "analyze particles" tool, circularity=0.00-0.95) and save the area of each ROI. Calculate cell density (#cell/ area in pixels^2) on a calculation spreadsheet and conduct statistical analysis. Each TLT is considered as an individual sample in terms of analysis, n=5; 4 animals/ treatment group (n=8).

Script:

```
macro "bCount Action Tool - C059T3e16?"{
      copyID = getImageID();
      roiManager("Add");
      run("Analyze Particles...", "  circularity=0.00-0.95
      show=Ellipses display clear summarize");
      selectImage(copyID);
      roiManager("Select", 0);
      roiManager("Measure");
      close();
}
```

B:T ratio. B:T cell ratio (B cell density/ T cell density) was calculated per animal taking the average B cell density and the T cell density of the same mouse, not the same TLT since this calculation was not possible due to protocol restrictions (different tissue sections were used for T or B cell staining, hence determining the ratio in the same TLT was not feasible). Data was analyzed to determine mean differences between genotype, sex and diet.

APPENDIX G

ASSESSMENT OF MLN VOLUME AFTER DSS-INDUCED COLITIS

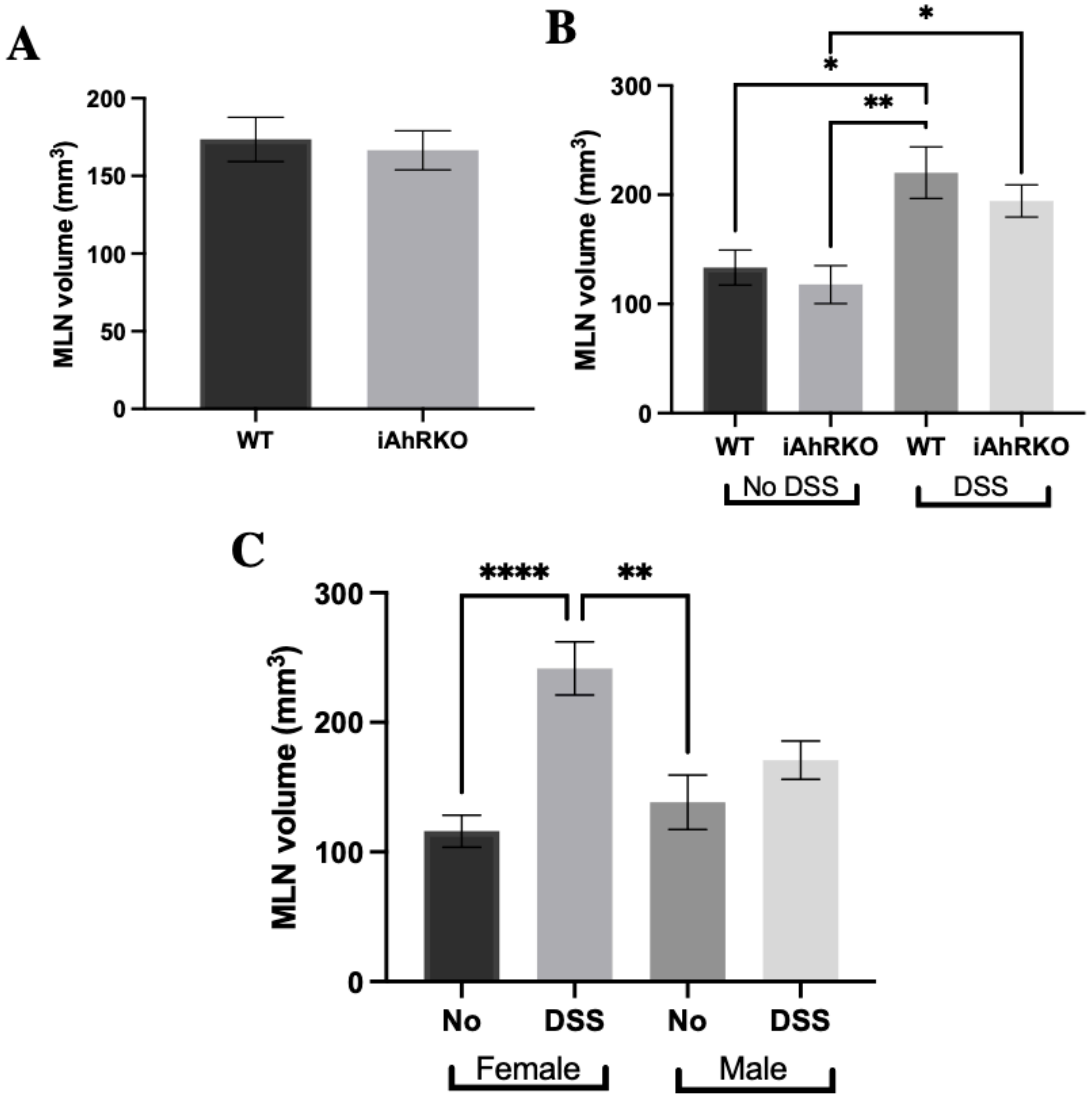

A. MLN volume (mm^3) by genotype***. B.*** MLN volume by genotype and treatment (DSS v. No DSS). ***C.*** Effect of DSS treatment and sex in MLN volume. Data presented indicate the mean ± SEM, n=84; *$p < 0.05$, **$p < 0.01$ and ***$p < 0.001$. Methods based on manuscript published by Ohya S (2014) https://doi.org/10.1152/ajpgi.00156.2013. Briefly, MLNs were collected and snapped frozen with LN_2 and stored at -80 °C until further assessment. While maintaining the tissues in ice to avoid MLN to thaw, MLN volume was assessed using a digital caliper record MLN width and length and calculated MLN volume using the formula (length × $width^2$) $\pi/6$.

APPENDIX H

EFFECT OF DIET AND GENOTYPE IN THE LOCATION OF T- AND B-CELLS

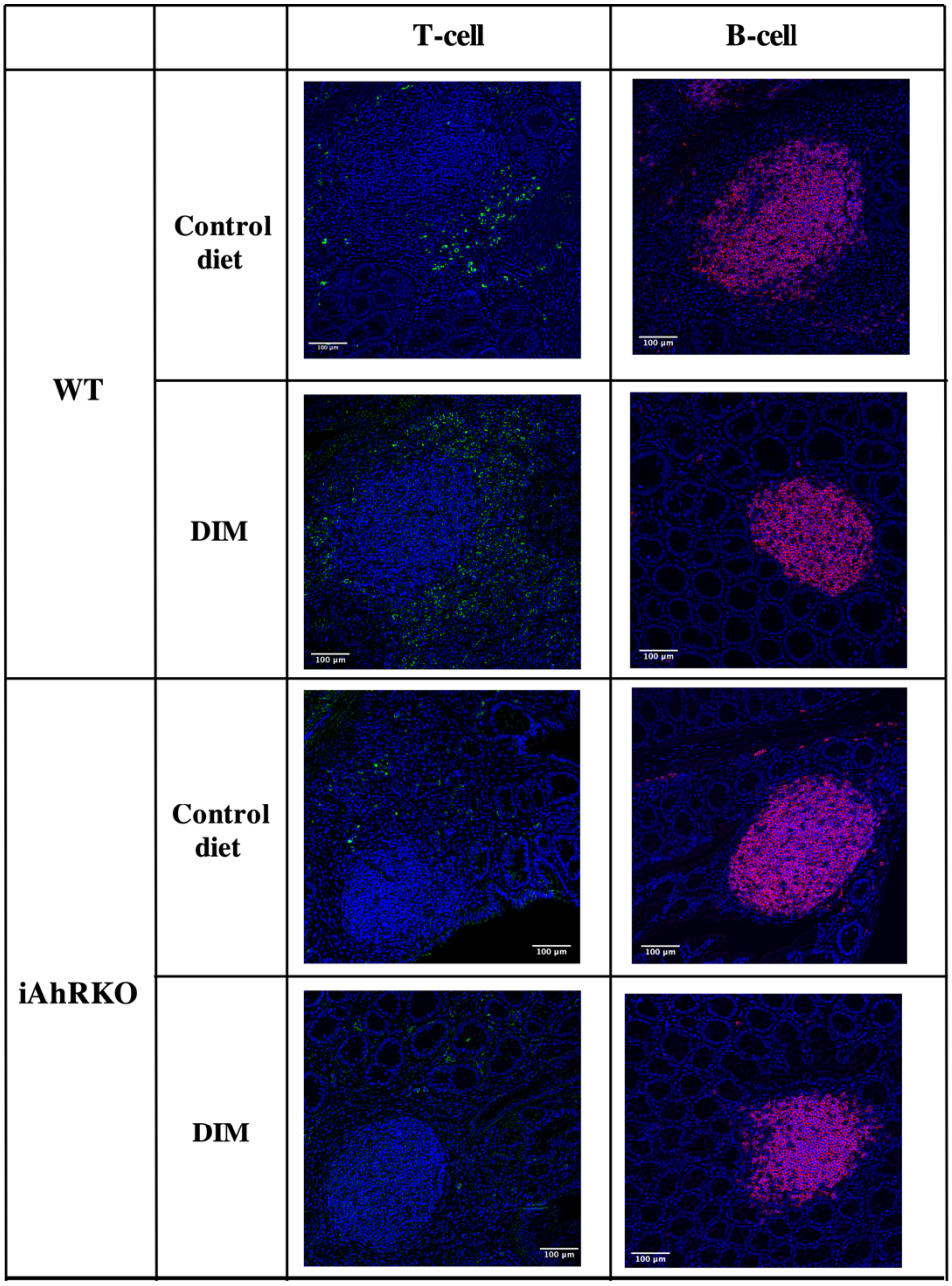

Representative images of immuno-fluorescence stained T-cell (CD3ε in green*), B-cells (CD45R in red) and nuclei (DAPI in blue) in the distal colon by genotype and diet in DSS-treated females. Scale bar=100 µm. 20X magnification. *'Green' false-color LUT.